Universidade de Aveiro Departamento de Biologia
Ano 2018

Ana Rita Barbosa Pinto

Neuregulin-1 effects in metabolic changes induced by Pulmonary Arterial Hypertension

Efeitos da Neuregulina-1 nas alterações metabólicas induzidas pela Hipertensão Arterial Pulmonar

DECLARAÇÃO

Declaro que este relatório é integralmente da minha autoria, estando devidamente referenciadas as fontes e obras consultadas, bem como identificadas de modo claro as citações dessas obras. Não contém, por isso, qualquer tipo de plágio quer de textos publicados, qualquer que seja o meio dessa publicação, incluindo meios eletrónicos, quer de trabalhos académicos.

Universidade de Aveiro Departamento de Biologia
Ano 2018

Ana Rita Barbosa Pinto

Neuregulin-1 effects in metabolic changes induced by Pulmonary Arterial Hypertension

Efeitos da Neuregulina-1 nas alterações metabólicas induzidas pela Hipertensão Arterial Pulmonar

Dissertação apresentada à Universidade de Aveiro para cumprimento dos requisitos necessários à obtenção do grau de Mestre em Biologia Molecular e Celular, realizada sob a orientação científica da Professora Doutora Maria Paula Polónia Gonçalves, professora associada do Departamento de Biologia da Universidade de Aveiro, sob a coorientação científica da Professora Doutora Carmen Dulce da Silveira Brás Silva Ribeiro, professora auxiliar da Faculdade de Medicina da Universidade do Porto e da Professora Doutora Isabel Alexandra Marcos Miranda, docente afiliada da Faculdade de Medicina da Universidade do Porto.

Fundação para a Ciência e a Tecnologia

COMPETE

QUADRO DE REFERÊNCIA ESTRATÉGICO NACIONAL

UNIÃO EUROPEIA
Fundo Europeu de Desenvolvimento Regional

Apoio financeiro da FCT e do FSE no âmbito do III Quadro Comunitário de Apoio (IMPAcT-PTDC/MED-FSL/31719/2017)

Aos meus Pais e ao Tiago, pelo incentivo e apoio incondicional.

O júri

Presidente	Professor Doutor Mário Guilherme Garcês Pacheco Professor Auxiliar com Agregação da Universidade de Aveiro
Vogal – Arguente principal	Professora Doutora Ana Patrícia Fontes de Sousa Professor Auxiliar do Instituto de Ciências Biomédicas de Abel Salazar da Universidade do Porto
Vogal – Coorientador	Professora Doutora Carmen Dulce da Silveira Brás Silva Ribeiro Professor Auxiliar da Faculdade de Medicina da Universidade do Porto

agradecimentos

Em primeiro lugar, agradeço à Professora Carmen Brás Silva, por me ter recebido (tão bem!) no seu grupo de investigação e me ter dado oportunidade de ingressar naquele que é apelidado do “melhor grupo do departamento”, mas também por toda a ajuda que me deu durante do desenvolvimento deste trabalho e pelas oportunidades de expandir horizontes que me foi proporcionando ao longo deste ano e meio.

Agradeço à Professora Isabel Miranda por todo o conhecimento que me transmitiu, pela confiança que depositou em mim e por todos os conselhos.

Não menos importante, agradeço ainda à Professora Paula Gonçalves por toda a preocupação e prestabilidade para com a realização deste trabalho.

Ao Professor Doutor Adelino Leite Moreira por ter disponibilizado todos meios necessários para o desenvolvimento deste trabalho.

Deixo também um agradecimento especial aos meus colegas de laboratório, à Mestre Carolina Rocha e ao Mestre Rui Adão, o “Boss”, por todo o conhecimento que me transmitiram, por toda a ajuda que me foram dando ao longo do desenvolvimento deste trabalho, mas também pelo companheirismo e amizade.

Agradeço ainda aos meus amigos, principalmente às Princesas da Disney e à Deia, pela amizade e pela compreensão face aos muitos convites recusados (prometo compensar-vos!), mas também por todo o suporte que me foram dando. Espero que um dia me perdoem por fazer experimentação em modelos animais.

À minha família, que desde sempre me apoiou, por toda a união e perseverança.

Ao Tiago, por não me ter deixado desistir e me fazer continuar a lutar pelos meus objetivos, pela compreensão da minha ausência e por toda a paciência.

Por último, o meu maior agradecimento aos meus Pais, por todas as oportunidades que me proporcionaram e por toda a confiança que depositaram em mim, mas mais ainda por me apoiarem sempre na realização dos meus sonhos.

palavras-chave

Hipertensão arterial pulmonar; neuregulina-1; ventrículo direito; efeito de Warburg; metabolismo.

resumo

A hipertensão arterial pulmonar (HAP) é uma doença crónica rara, caracterizada pelo aumento da resistência vascular pulmonar (RVP) com sobrecarga progressiva e remodelagem do ventrículo direito (VD), o que pode levar à insuficiência cardíaca do ventrículo direito (ICVD). Estas perturbações surgem na sequência de uma alteração metabólica na oxidação da glicose, um processo designado por efeito de Warburg, que afeta o metabolismo da glicose a nível sistémico. A neuregulina-1 (NRG1), uma proteína que demonstrou ter efeitos benéficos na hipertrofia do VD causada pela HAP, está também associada à regulação do metabolismo da glicose dado seu papel na modulação da expressão dos transportadores de glicose (GLUTs).

Neste estudo, o nosso objetivo tinha por base a avaliação do efeito do tratamento crónico com rhNRG1 na expressão de genes da via da glicólise no VD e em músculo esquelético num modelo animal de HAP induzida por monocrotalina (MCT) e num um modelo crónico de hipoxia/Sugen5416, que reproduz algumas das principais características fisiopatológicas da HAP humana.

Verificamos que a expressão de mRNA do GLUT1 e do GLUT4 no VD está alterada na HAP e que se demonstrou semelhante entre os modelos animais MCT e hipoxia/Sugen5416, estando relacionada com o desenvolvimento de hipertrofia do VD (HVD). No entanto, o tratamento com rhNRG1 apenas atenuou a expressão dos GLUTs para valores próximos aos normais no modelo de HAP induzida por MCT. Enquanto que a expressão do GLUT1 e do GLUT4 está correlacionada com marcadores cardíacos da doença, os genes da via glicolítica demonstraram estar correlacionados com as alterações morfofisiológicas resultantes do desenvolvimento da HAP no modelo MCT. A partir da análise de alguns genes da via glicolítica, concluímos que, para além dos GLUTs, alguns genes estão relacionados, não só com o efeito de Warburg, mas também com a progressão da doença. Verificamos também que o tratamento com rhNRG1 atenuou as alterações de expressão em alguns genes da via glicolítica, resultando numa melhoria do metabolismo da glicose. A avaliação da tolerância à glicose revelou que os animais com HAP de ambos os modelos são resistentes à insulina e que o tratamento com rhNRG1 regulou a concentração sistémica de glicose em ambos os modelos animais.

Em conclusão, os efeitos terapêuticos da NRG1 na HAP experimental podem dever-se, em parte, à regulação das alterações metabólicas que estão associadas à progressão da HAP e à disfunção do VD, e que se refletiram na reversão do fenótipo ventricular da doença.

keywords

Pulmonary arterial hypertension; right ventricle; neuregulin-1; Warburg effect; metabolism.

abstract

Pulmonary arterial hypertension (PAH) is a chronic rare disease, characterized by increased pulmonary vascular resistance (PVR) with progressive overload and remodelling of the right ventricle (RV), that eventually leads to right ventricular heart failure (RVHF). These derangements arise from a metabolic switch from glucose oxidation towards glycolysis, the Warburg effect, affecting glucose metabolism at the systemic level. The neuregulin-1 (NRG1), a protein that has been shown to play beneficial effects on PAH and RV hypertrophy, has also been associated with the regulation of glucose metabolism given its role in modulating the expression of glucose transporters (GLUTs).

In this study we aimed to evaluate the effect of rhNRG1 chronic treatment on glycolysis pathway genes expression in the RV and skeletal muscle in a monocrotaline (MCT)-induced PAH animal model and in chronic hypoxia/Sugen5416 model that also reproduces key pathophysiological features from human PAH.

We have found that RV GLUT1 and GLUT4 mRNA expression is altered in PAH and was similar between the MCT and hypoxia/Sugen5416 animal models, being this related with the development of RV hypertrophy (RVH). However, the treatment with rhNRG1 only attenuated GLUTs expression toward normal values in MCT-induced PAH model. The expression of GLUT1 and GLUT4 is correlated with cardiac markers of disease, while the glycolytic pathway genes are correlated with the morphophysiological changes resulting from the development of PAH in MCT model. From the analysis of some glycolytic pathway genes, we conclude that beyond GLUTs, several genes are related, not only with the Warburg effect, but also with the disease progression. We also found that the treatment with rhNRG1 attenuated the changes in some glycolytic pathway genes, resulting in an improvement of glucose metabolism. The glucose tolerance evaluation revealed that the animals with PAH from both models are insulin resistant and that the treatment with rhNRG1 regulated systemic glucose concentration in both animal models.

In conclusion, the therapeutic effects of NRG1 in experimental PAH may be due, in part, to the regulation of metabolic changes associated with PAH progression and RV dysfunction, which were reflected in the reversion of the ventricular phenotype of the disease.

Index

List of figures

List of tables

List of abbreviations

ACE Angiotensin converting enzyme
ACVRL1 Activin receptor-like type 1
acyl-CoA Acyl-Coenzyme A
Akt Protein kinase B

ApoE Apolipoprotein E
AR Adrenergic receptors
AT_1 Angiotensin type 1
ATP Adenosine triphosphate
AU Arbitrary Units
BMP Bone morphogenetic peptide
BMPRII Bone morphogenetic peptide receptor II
BNP Brain natriuretic peptide
BSA Bovine serum albumin
BW Body weight
Ca^{2+} Calcium ion
cAMP Cyclic adenosine monophosphate
CD36 Cluster of differentiation 36
cGMP Cyclic guanosine monophosphate
CI Cardiac index
cMyc MYC proto-oncogene
CO Cardiac output
CO_2 Carbon dioxide
CoA Coenzyme A
CPT1 Carnitine palmitoyl transferase 1
CRV Compensated right ventricular function
CTGF Connective tissue growth factor
CTRL Control group
DMSO Dimethyl sulfoxide
DRV Decompensated right ventricular function
EC Endothelial cells
EGF Epidermal growth factors
EndMT Endothelial to mesenchymal transition
eNOS Endothelial NO synthase
ErbB Erythroblastic leukaemia viral oncogene homolog
ET-1 Endothelin-1
FAO Fatty acid oxidation
FATP Fatty acid transport protein
FDG ^{18}F-fluorodeoxyglucose
FA Fatty acids
FFA Free fatty acids
FOXM1 Forkhead box protein M1
FoxO1 Forkhead box protein O1
GAPDH Glyceraldehyde 3-phosphate dehydrogenase
GLS1 Glutaminase
GLUT Glucose transporter
GMO Genetically modified organisms
GO Glucose oxidation
GTP Guanosine triphosphate
H_2O_2 Hydrogen peroxide
HF Heart failure

HIF Hypoxia inducible factor
HIF-1α Hypoxia inducible factor 1α
HK Hexokinase
HPAH Hereditary PAH
HS Hypoxia/Sugen group
IGF-I Insulin-like growth factor I
IL-6 Interlukin-6
IPAH Idiopathic PAH
IR Insulin receptor
IRS Insulin receptor substrate
LCFA Long-chain fatty acids
LDH Lactate dehydrogenase
LV Left ventricle
MAPK Mitogen activated protein kinase
MCP Monocyte chemoattractant protein
MCT Monocrotaline
MCTP Pyrrole metabolite dehydromonocrotaline
mDNA Mitochondrial DNA
Me Malic enzyme
Mef2 Myocyte enhancer factor 2
MET 13 Mediator of transcription 13
MHC Myosin heavy chain
miRNA MicroRNA
mPAP Mean pulmonary artery pressure
MPI Multiple pathological insult
MR mineralocorticoid receptor
mROS Mitochondria-derived reactive oxygen species
mTOR Mammalian target of rapamycin
NAD Nicotinamide adenine dinucleotide
NCoR1 Nuclear receptor corepressor 1
NFAT Nuclear factor of activated T cells
NO Nitric oxide
NRF1 Nuclear respiratory factor 1
NRG Neuregulin
OGTT Oral glucose tolerance test
OXPHOS Oxidative phosphorylation
PA Pulmonary artery
PAAT Pulmonary arterial acceleration time
PAB Pulmonary artery banding
PAEC Pulmonary artery endothelial cells
PAET Pulmonary arterial ejection time
PAH Pulmonary arterial hypertension
PASMC Pulmonary artery smooth muscle cells
PASP Pulmonary artery systolic pressure
PAVTI Pulmonary artery velocity-time integral
PCWP Pulmonary capillary wedge pressure

PDC Pyruvate dehydrogenase complex
PDE5 Phosphodiesterase type 5
PDGF Platelet-derived growth factor
PDGFR Platelet-derived growth factor receptor
PDH Pyruvate dehydrogenase
PDK Pyruvate dehydrogenase kinase
PECAM1/CD31 Platelet EC adhesion molecule 1
PET Positron emission tomography
PFK Phosphofructokinase
PFKm Muscle type posphofructokinase
PGC-1α Peroxisome proliferator-activated receptor gamma coactivator 1-alpha
PGI_2 Prostacyclin
PH Pulmonary hypertension
PI3K Phosphoinositide 3-kinase
PIK3R2 Phosphoinositide-3-kinase regulatory subunit 2
PK Pyruvate kinase
PKCζ Protein kinase C zeta
PKm muscle type pyruvate kinase
PPARα Peroxisome proliferator–activated receptor alpha
PPARδ Peroxisome proliferator-activated receptor delta
PPARγ Peroxisome proliferator-activated receptor gamma
PVR Pulmonary vascular resistance
RAAS Renin-angiotensin-aldosterone system
rhNRG1 Recombinant human neuregulin-1
RhoA Ras homolog family member A
ROCK Rho kinase
RTK Tyrosine kinase receptors
RV Right ventricular/ right ventricle
RVD Right ventricular dysfunction
RVEF Right ventricular ejection fraction
RVH Right ventricular hypertrophy
RVHF Right ventricular heart failure
RVIDd Right ventricular inner diameter in diastole
RVSP Right ventricular systolic pressure
SDF1 Stromal-derived factor 1
sGC Soluble guanylate cyclase
Sirt Sirtuins
SLUG/SNAI2 Snail Family Transcriptional Repressor 2
SMC Smooth muscle cells
SNAIL/SNAI1 Snail Family Transcriptional Repressor 1
SOD2 Superoxide dismutase 2
SPI Single pathological insult
SPRED-1 Sprouty-related protein-1
SU5416 Sugen 5416
TAG Triacylglycerol
TAPSE Tricuspid annular plane systolic excursion

TCA Tricarboxylic acid
Tfam Mitochondrial transcription factor A
TGF-ß Transforming growth factor-ß
TL Tibial length
TLR4 Toll-like receptor 4
TNFα Tumour necrosis factor α
TWIST1 Twist Basic Helix-Loop-Helix Transcription Factor 1
TXA2 Thromboxane A2
VE-cadherin/CD144 Vascular endothelial cadherin
VEGF Vascular endothelial growth factor
VEGFR Vascular endothelial growth factor receptor
VIP Vasoactive intestinal peptide
VSMC Vascular smooth muscle cells
WHO World Health Organization
α-SMA α-smooth muscle actin

Introduction

1. Cardiovascular diseases and Pulmonary Hypertension

Cardiovascular diseases are a group of disorders of the heart and blood vessels, and the first cause of death globally.[1] Pulmonary hypertension (PH) is a hemodynamic and pathophysiological abnormality that is found in many clinical conditions, most commonly cardiopulmonary diseases.[2,3] PH is characterised by pathologies on pulmonary vasculature with resulting elevations of pulmonary arterial pressure[4], defined as a mean pulmonary artery pressure (mPAP) of 25mmHg or more with a normal pulmonary capillary wedge pressure (PCWP) of 16mmHg (pre-capillary PH)[2,5], while the normal values for mPAP are 14 ± 3mmHg at rest.[5,6] According to World Health Organization (WHO), the current clinical PH classification can be subdivided into five groups based on the etiology of the disease (Table 1).[1,7] These five groups were defined in the fifth World Symposium on Pulmonary Hypertension (5th WSPH) which took place in Nice, France, in 2013, aggregating the multiple aspects of PH.[8]

1.1. Pulmonary arterial hypertension

Pulmonary arterial hypertension (PAH), that belongs to the Group 1 of PH subtypes[9], is very rare and could be more serious than systemic arterial hypertension.[10] As it is a rare disease, the globally reported incidence of PAH is about a 1.1 to 7.6 per million of adults for each year, while the prevalence of this pathophysiology varies between 6.6–26.0 per million of adults, affecting mostly women.[11–18] PAH is a progressive, fatal[5,19], complex and multifactorial cardiopulmonary disorder[3] that may progress to right ventricular (RV) heart failure (HF) and lead to death in 2.8 years if isn't correctly treated.[3,6,19] However, the prognosis depends on a variety of factors, such as the age of the patient or the severity of PAH, and the studies demonstrated a range of survival between 1 and 7 years with treatment.[18,20] The most common signs and primordial symptoms are dyspnoea (a shortness of breath during physical exertion), fatigue and syncope,[13,20,21] and as the condition progresses, the patients may also experience an increase in cardiac frequency, chest pain, oedema of the ankles or legs and dizziness.[20] The Registry to Evaluate Early and Long-term Pulmonary Arterial Hypertension Disease Management (REVEAL Registry), a multicentre

observational cohort study of WHO Group 1 PAH, also revealed that around 25% of the patients manifested depressive symptoms or even depression.[22,23] Although there are currently several treatments that contribute to the improvement of the symptoms of the disease and that allow the increase of the survival of patients with PAH, the cure for this disease has not yet been found.[24,25]

Based on diverse etiologies[26], PAH is a pulmonary vascular remodelling pathology that affects both the pulmonary vasculature and the heart.[27] It is characterized by pre-capillary PH[28] reflected by a continuous and notable elevation in mPAP, greater than 25 mmHg at rest or greater than 30 mmHg during exercise[2,3,29,30], PCWP inferior to 12 mm Hg and pulmonary vascular resistance (PVR) above or equal to 3 Wood units. [2,3,13,19] PAH is characterized by vascular remodelling, PVR, RV hypertrophy (RVH), progressive RV heart failure (RVHF) and, ultimately, death.[2,3,13,19,26,29–31] The clear increase in PVR is a limiting factor for the rate at which the RV can pump blood through the lungs, what causes a deficiency of breath and reduces the functional capacity.[32] Furthermore, although the underlying mechanisms of this syndrome in the RV are poorly understood[33], it is known that the RV function is an imperative determinant of survival in many cardiovascular diseases.[34–36] Indeed, the RV function is the most relevant prognosis determinant in PAH and the RV dysfunction (RVD) is characterized by abnormal energy metabolism.[37,38] The metabolic derangements originated evolve from the progress of this disease to the end-stages[4], encompassing not only the RV but several tissues of the organism, such as pulmonary artery (PA), left ventricle (LV) or skeletal muscle.[39]

In clinical terms, RVHF concerns to the inability of the RV to perfuse the lung circulation effectively to maintain LV filling at low venous/diastolic pressures.[40] The transition from RVH to RVHF involves a huge variability of RV adaptations among patients which are exposed to chronic PH according to the aetiology of the PH.[41,42] Due to the persistent increase on afterload caused by the progression of the disease, the RVH is usually accompanied by ischemia, myocardial apoptosis and excessive fibrosis, as well as by increased expression of non-contractile proteins that lead to diastolic dysfunction and inefficient coupling, triggering a decrease in RV systolic function followed by an acute RV dilatation and that can culminate in RVHF.[39,43–45] Once RV ischemia may lead to the generated metabolic switches in carbon utilization, that are associated with maladaptive

hypertrophy, it might potentiate the "hypoxia-like" program of gene expression[44] activating genes such as hypoxia inducible factor (HIF) and vascular endothelial growth factor (VEGF), who plays a central role in modulation of myocyte development and in myocardial angiogenesis.[43]

The Dana Point Clinical Classification, elaborated in association with WHO, categorized PH into five different subgroups with base on the etiologies of this pathophysiology, allowing the identification of the several forms of PH described in Table 1.[46,47] All of the subgroups of PAH share common changes not only in the signalling pathways but also in histological findings, as the solid remodelling of non-muscularised PA[48] and with regard to pathology, there is greater difference between the different WHO groups.[49] The actual classification groups patients with base in analogous pathological findings, hemodynamic profiles, and management strategies of the disease, emphasizing the different origins of the disease.[9,47]

Previously known as Primary PH[46], the Group 1 of PH comprises the several disorders that are responsible for the development of PAH. In a general way, this group is characterized by the hypertrophic PA remodelling with arteriolar muscularization[49,50], intimal fibrosis[49,51,52], *in situ* thrombosis with neovascularization[53–55], reduced pulmonary vascular compliance[52], and disorganized growth of endothelial cells (EC)[39,56], that in late stages evolves to angioproliferative plexiform lesions[56,57], morphologic hallmarks of severe PAH, that are complex and glomeruloid-like vascular structures which are originated from the pulmonary arteries[58], that lead to the characteristic increase in vascular resistance within the pulmonary system and eventually to maladaptive responses of the RV due the increased pressure load.[49,54]

2. Pathophysiological and Metabolic alterations in Pulmonary Arterial Hypertension

From foetal development to the birth, the RV suffers structural remodelling instigated by metabolic alterations: during the foetal development their walls are thick, as well as the pulmonary arteries; the pressure of ejection of blood is high, once the pulmonary circulation has a low-flow, and a high-resistance circuit results in a reduced venous flow to the left heart.[59,60] At birth, the remodelling starts, the walls get thinner, decreasing PVR and thus a

decrease in RV afterload, and the blood pressure becomes lower, which alters the metabolism in RV and leads to RVH regression.[43,59–61] During the foetal development, the glucose oxidation (GO) and glycolysis are the two major sources of cardiac ATP, and the circulating levels of fatty acids are low.[62] At child-birth occurs the transition to fatty acid oxidation (FAO) as the primary source of energy for the heart, promoted by an increase in the expression of genes that encode for the enzymes from the FAO pathway.[63] At this time, it also starts the increase in vasodilation through the enhanced release of vasodilators, as nitric oxide (NO), contributing for an increase in oxygen and ventilation, and prostacyclin (PGI2), that is responsible for the modulation of changes in pulmonary vascular tone at birth.[43] This process is accompanied by a decrease in the secretion of vasoconstrictors as endothelin-1 (ET-1)[41,43], leading to an increase in systemic vascular tone and a progressive decrease in RV wall thickness.[41] When a heart is hemodynamically or metabolically stressed, as it occurs in PAH, a regression to the foetal metabolism pattern usually occurs, reactivating the genetic packaging yore modified.[64]

All the types of PAH share pathological characteristics, such as the remodelling of the PA walls, as a consequence of the metabolic alterations inherent to the pathology, and activation of the foetal genetic package. These changes result in the proliferation of a myriad of cells, such as PA endothelial cells (PAEC), PA smooth muscle cells (PASMC), fibroblasts and myofibroblasts activation, differentiation and migration, that at the peak of the disease exhibit a proliferative and antiapoptotic phenotype similar to cancer cells, altering the contraction capacity of the vessels and increasing inflammatory conditions.[21,39,64,65] Furthermore, the existing imbalance between proliferation and apoptosis, that occurs among the three layers constituting of the vessels, play a crucial role in PAH development and progression[66], and it has been demonstrated that all of these cells acquire significant genetic characteristics that alter their normal cell course.[67] The metabolic derangements originated evolve from the beginning of this disease to the end-stages[4], encompassing not only the RV but several tissues of the organism, such as PA, LV or skeletal muscle.[39] Apart from the changes in LV, signs show that the RV of the patients with PAH is also hypertrophied, enlarged and subjected to ischemia[45], due to a compensatory mechanism for the alterations on LV[68], and this is the primary determinant of death for PAH.[69] The crosstalk between dysfunctional EC and the other cells that compose the pulmonary vascular wall are the key

feature of PAH pathogenesis[3,39], once the EC release a variety of vasoactive molecules that interact with blood elements but also with vascular smooth muscle.[70]

Recent studies on genetic and metabolism have generated important mechanistic insights into established disturbances of endothelial function and smooth muscle cell proliferation.[57] PASMC proliferation is also a pivotal part in the pathological vascular remodelling of PAH, whose mechanism is still a source of controversy.[31,39]

2.1. Alterations on endothelial cells

2.1.1. Vessels endothelium alterations

The EC compose the inner layer of the vessels, the intima[71,72], and are responsible for the paracrine and autocrine function, as well as vasomotion, thrombosis, platelet aggregation and inflammation inside de vessels.[71] The abnormalities in structure and function of the endothelium occur in conjunction with growth of neointimal, preceding the growth of medial layer, constituted by smooth muscle cells (SMC) (Figure 1) and adventitial layers, establishing regions of neovascularization.[46,228] Sometimes, those alterations may culminate in an occlusive arteriopathy, due to exacerbated proliferation of EC leading progressively to obliteration of the vessel lumen[39,61,73,74], and resulting in a progressive increase in vascular resistance.[74,75] The intimal modifications, that include endothelial injury or the invasion of this cell layer by fibroblasts and myofibroblasts and lead to fibrotic changes in the vessel walls[53,76], may prompt progressively the formation of atherosclerotic plates[77], vascular obliteration[21,39], hypertrophy of the medial layer and arteriolar muscularization (Figure 2).[9,50]

In most cases of PAH, the EC exhibit a disorganized growth[39,56] that in late stages evolves and gives rise to complex vascular lesions, the angioproliferative plexiform lesions.[56,57] The plexiform lesions, morphologic hallmarks of severe PAH, are composed by proliferating EC, matrix proteins and fibroblasts, constituting complex and glomeruloid-like vascular structures which are originated from the pulmonary arteries[58] and that can obliterate vascular lumen.[53] They are one of the causes of the pathogenicity of PAH[39,78,79] and may also induce the thickening of the walls of the RV and a responsible for the increase on his diameter.[69] Metabolic aberrations in EC also mediate vascular disturbances associated with

the pathogenesis of several disorders[80], and endothelial dysfunction, that occurs in early stages of PAH, may control the development of the disease.[81] Pulmonary vascular injuries origin endothelial dysfunction and apoptosis, thereby weakening endothelial-mediated suppression of quiescent SMCs[57], playing an integral role in mediating the structural changes in the pulmonary vasculature.[82]

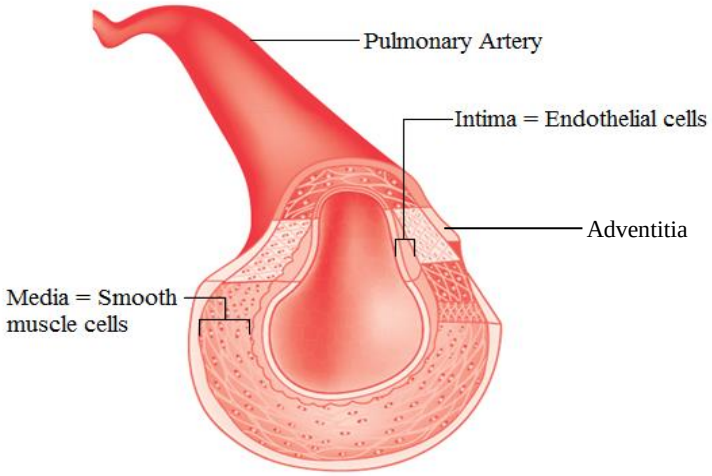

Figure 1 Cellular structure of the pulmonary artery. The pulmonary artery (PA) is composed by three layers: (i) the inner layer, designated by intima, which is composed by endothelial cells (EC); (ii) the media layer, composed by smooth muscle cells (SMC); (iii) the adventitial layer, constituted by connective tissue.

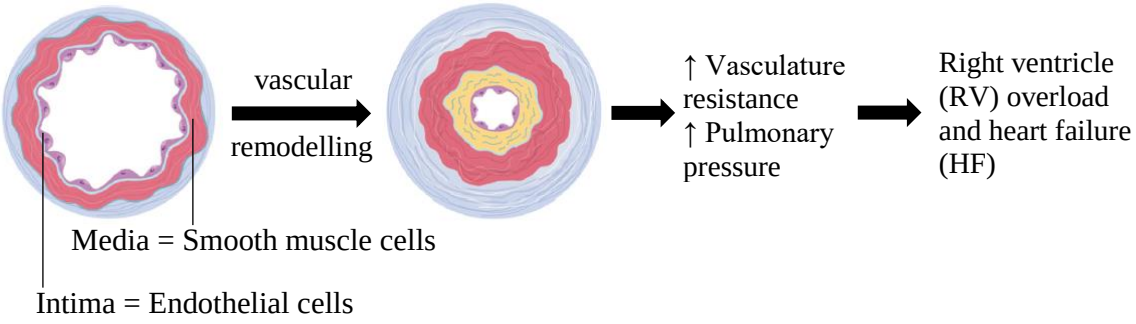

Figure 2 Vascular remodelling in pulmonary artery. The vascular remodelling in pulmonary artery (PA) can culminate in heart failure (HF). The abnormalities in structure and function of the endothelium occur in conjunction with growth of neointimal, preceding the growth of media layer. Due to vascular remodelling and intima growth is triggered progressively the obliteration of the vessel lumen. This remodelling will lead to an increase in mean pulmonary arterial pressure (mPAP) and pulmonary vascular resistance (PVR), that will drive to alterations on right ventricle (RV) that may culminate in HF and death. Adapted from McLaughlin, V. V., Shah, S. J., Souza, R. & Humbert, M. 2015. "*Management of pulmonary arterial hypertension*".

Pulmonary endothelium seems to underpin many of the cellular changes seen in PAH[53] and plays an important role in vascular homeostasis and in ventilation perfusion matching, enabling an efficient gas exchange in the lungs.[83] One of the features for endothelial dysfunction in PAH is reflected not only by reduced production of the vasodilators or growth inhibitors as NO and PGI2, but also by increased production of the vasoconstrictor/co-mitogens as ET-1 and thromboxane A2 (TXA2).[53,75,76,84] These mediators are responsible for the regulation of the diameter of the pulmonary vessel, inducing either vasodilatation (NO and PGI2) or vasoconstriction (ET-1)[70], being cyclic guanosine monophosphate (cGMP), a second messenger, also implicated in this mechanism.[85]

The deficit in NO in PAH can be triggered by the decreased expression of endothelial NO synthase (eNOS)[61,69] that produces NO endogenously from the amino-acid L-arginine[71,86], the inhibition of eNOS enzymatic activity or inactivation of NO by superoxide anion[53,75,84,87], or by the increased arginase activity, that competes with NOS for L-arginine substrate.[88,89] eNOS is responsible for synthesis of NO in vascular EC and plays an important role in the control of vasomotor tone[53,83], and PAH is undoubtedly related with a decrease in NO bioavailability.[49,75] The inactive eNOS bound to caveolin protein, and when receives a stimulus from increase in Ca^{2+}, eNOS detaches from caveolin and become activated, initiating the production of NO.[71] The increasing oxidant stress and the reactive oxygen species generation triggered by the decrease in bioavailability of NO may be due to the high levels of aldosterone, what relates this molecule with the endothelial dysfunction. Indeed, aldosterone also increases the activity of NADPH oxidase in the heart, which contributes to myocardial endothelial dysfunction[54], but some investigations on PAH patients found that the NO synthesis is more depleted or altered in the lungs.[89]

PGI2, who belongs to prostanoid family, is also synthesized by EC in response to vascular damage or stress, being released in a paracrine mode to exerts its action on nearby vascular SMCs, platelets, and other EC.[49] In normal situations, EC physiologically preclude platelet activation by producing NO and PGI2[66] and, since PGI2 analogues induce a rapid decrease in PVR and increase cardiac output, they have been used as treatment for PAH.[90]

2.1.2. Cardiac endothelium alterations

The adrenergic receptors (ARs) are the main regulators of the cardiovascular system and cardiac EC functioning.[91] Two classes of ARs have been identified: α and β, and the βAR are the ones present in the cardiac endothelium and involved in PAH.[92,93] The adrenergic system is responsible for several metabolic pathways, including the modulation of insulin production by pancreatic β-cells and the levels of fatty acids in plasma, being related with metabolic variations such as insulin resistance, altered glucose and mitochondrial dysfunction.[93]

In PAH, it has been demonstrated that occurs an overstimulation on βAR, which is related with maladaptive RV remodelling[92], cardiac hypertrophy[94] and HF.[93] Thus, some βAR antagonists are used as a treatment for chronic HF[94], since the chronic stimulation of βAR induces insulin resistance, as the β2AR modulates glucose metabolism and homeostasis, as well as fatty acid metabolism.[93] It is known that sustained β adrenergic stimulation induces insulin resistance, and the acute treatment with β2AR blockers increased glucose uptake in myocytes and skeletal muscle to similar values to those seen after de insulin stimulation.[95] Furthermore, βAR has the ability to affect insulin signalling by activating phosphoinositide 3-kinase (PI3K)/protein kinase B (Akt) (PI3K/Akt) and its downstream pathway in cardiomyocytes. βAR stimulation induces PI3K activity[94] and an increase in heart weight as well as contractile abnormalities and myocardial fibrosis[96], which are characteristics of PAH. Moreover, the β2AR appears to display a title-role in systemic glucose homeostasis through its action on pancreatic islet hormone secretion, liver and muscle glucose transport metabolism.[97]

In healthy heart, endothelium either produces neuregulin 1 (NRG1), that has been shown to diminish the myocardial inotropic response to adrenergic stimulation, playing effects on the reducing of cardiac output and blood pressure due the activation of NO production via eNOS stimulation[98], being the increased expression of the NRG1 in PAH documented by a study in an hypoxia animal model for PAH.[99] In disease state, cardiac endothelium also increases the production of molecules as ET-1, what is correlated with alterations and modulation of right atrial pressure, RV overload, increased inotropy, PVR and oxygen saturation.[100] The increased ET-1 production, verified in both human and rat hypertrophied RV, is also responsible to maintaining cardiomyocyte survival in situations of

a sustained increase in β-adrenergic stimulation as it occurs in PAH.[101] An in vitro study with genetically manipulated cardiomyocytes also revealed that NRG1 treatment is responsible for their protection by the activation of βAR through parasympathetic modulation, still relating the suppression of NRG1 gene with the increased risk of heart failure in human diseased hearts[102], highlighting the role of NRG1 in the regulation of AR.

2.2. Alterations on smooth muscle cells

In hypoxia conditions, as the ones that exist in PAH, the PASMC present a hyperproliferative behaviour[54], which is a significant feature of PAH[76], and the mutations on bone morphogenetic peptide receptor II (BMPRII) that may occur in idiopathic PAH (IPAH) and hereditary PAH (HPAH) may be in the basis of this behaviour.[51] The abnormal PASMC proliferation results from the dysregulation of cytokines activity, which are produced by several cells, including vascular cells.[103] Furthermore, the patients with IPAH are affected by significant morphological and functional skeletal muscle changes that affect their exercising capacity.[104–106] In experimental models[106] and patients with PAH[107], changes as muscle atrophy[106,107], a decrease in oxidative metabolism in muscle cells and mitochondrial alterations[106] have been described. The impairment of mitochondrial function in skeletal muscle precedes the RV pressure overload, however, the mechanisms behind these changes are not fully explained yet.[104]

Increased expression and accumulation of α-smooth muscle actin (α-SMA) by an enlarged number of cells usually occurs due to the remodelling of the pulmonary arteries and the occlusive lesions in patients with PAH[108,109] and this can be an indicator of endothelial to mesenchymal transition (EndMT) in PAH.[51] The cytokine interlukin-6 (IL-6) levels are also elevated in both patients and animal models with PAH in response to BMPRII gene disruptions, promoting pulmonary vascular remodelling and an elevation on right ventricular pressures under normoxic conditions, which causes a severe PH phenotype in hypoxic conditions.[55,110] In PAH, the increase in PVR is caused by remodelling of the distal pulmonary vasculature, not by the increase in vascular tone.[74]

According with the studies carried out, there are myriads of molecular origins for PH that promote remodelling of the pulmonary vasculature, with hyperproliferation of

vascular smooth muscle cells (VSMC) and increased cellular survival.[4,29,111] Disturbances in Ras homolog family member A (RhoA)-Rho kinase (ROCK) and in RhoA/ROCK pathway are one of the molecular origins for PAH due to their effects on vasoconstriction and vascular remodelling, once RhoA is evolved on growth and hypertrophy of PASMC induced by vasoconstrictors during vascular remodelling.[112] A recent study showed that in PAH, the RhoA/ROCK pathway along with Ca^{2+} and ET-1, are the main responsible for the hyperconstriction in PAH, what can be attenuated by RhoA/ROCK inhibitors.[113] Furthermore, the forkhead transcription factor (forkhead box protein O – FoxO) have also been implicated in vascular structural maintenance and the FoxO1 is involved in the hyperproliferative and apoptosis-resistant phenotype of PASMCs.[114]

In remodelled vessels, angiotensin signalling favours PASMC proliferation and vasoconstriction, existing evidences of angiotensin type 1 (AT_1) receptor upregulation.[54,115] To compensate the low cardiac output characteristic of patients with IPAH, the renin-angiotensin-aldosterone system (RAAS) is upregulated.[116] Via RAAS, aldosterone supports the blood pressure through its effects on the kidney, regulating sodium reabsorption and water balance, having effect on peripheral blood vessels to increase systemic vascular resistance, contributing as well to vascular stiffening.[54,117] Aldosterone elevated levels activate the mineralocorticoid receptors, which are cytoplasmic receptors that function as transcription factors that regulate gene and protein expression, which are expressed in EC, VSMC, cardiomyocytes and macrophages.[115] In vascular and cardiac cells, this binding of aldosterone to mineralocorticoid receptor (MR) will induce signalling pathways that promote vascular remodelling, an increase in RV systolic pressure (RVSP) and in PA systolic pressure (PASP), impairing vascular reactivity and contributing to RV cardiac dysfunction associated with the disease.[54,117] Furthermore, aldosterone induces vascular insulin resistance through desensitization of proteins involved in insulin pathways, such as insulin receptor substrate 1 (IRS1), PI3K, Akt and NOS.[115] Some studies proven that RAAS pathway is associated to cardiopulmonary vascular phenotype in PAH models and humans due to overexpression of aldosterone, designed by hyperaldosteronism, and this may occur due an increase in angiotensin converting enzyme (ACE)[54,118] owing to a polymorphisms on this protein gene and to increased adrenal production of aldosterone.[116,119] Due to vascular remodelling characteristic of the disease, the actual therapies mainly focus on dilating the

partially occluded vessels trough antiproliferative agents[3,55] as losartan, captopril or spironolactone, that act on RAAS.[54,118]

The NO produced in EC has vasodilatory, anti-proliferative and anti-thrombotic effects in SMC.[75] NO operates by activating soluble guanylate cyclase (sGC) in vascular SMCs as a catalyser for the conversion of guanosine triphosphate (GTP) into cGMP.[49,53,75,89] It diffuses to the VSMC to promote the relaxation of smooth muscle contractile filaments and vasodilation, through the decrease in calcium influx thus inhibiting proliferation of SMCs, and the reduction in NO bioavailability may contribute to vasoconstriction and to the increase on PAP.[49,75,86] It was also discovered that cGMP-specific phosphodiesterase type 5 (PDE5) activity is upregulated in pulmonary vascular smooth muscle in PAH, and the inhibition of PDE5, with PDE5 inhibitors as sildenafil which is used in the treatment of PAH, results in vasodilatory and antiproliferative effects.[86,120] Abnormalities in both K^+ channels and Ca^{2+} channels have been linked induction of fibroproliferative sequelae, particularly in SMCs.[76]

Despite being predominantly expressed on vascular EC, ET-1 is also expressed by arterial SMC and is a potent vasoconstrictor, stimulating Ca^{2+} entry to the cytoplasm, also performing duties in proliferation.[25,49] On the other hand, PGI2 is a vasodilator and anti-aggregating substance, whose effects are enhanced by the presence of NO[53], having the PGI2 signalling pathway effects on the attenuation of the smooth muscle proliferation and antithrombotic effects.[121] In SMCs, PGI2 triggers the decrease in cytosolic calcium and an increase in the breakdown of myosin light chains, leading to vasodilation.[49,75]

2.3. Intervention of platelets in pulmonary arterial hypertension

Due to their prothrombotic potential, platelets play a central role in pathophysiology of atherothrombotic cardiovascular diseases, and in diseases as PAH is documented the existence of an higher volume of platelets.[122] Platelets derive from megakaryocytes, and is proven that cytokines as IL-6 influence megakaryocytes[66] promoting the production of extra active and larger platelets[122]; once IL-6 is increased in patients with PAH[55,110], it can be a cause for the increased volume of platelets in this pathology[122], being this mechanism potentiated by the inflammatory environment of PAH.[66] Furthermore, the existence of larger

platelets and in hyperfunctioning, together with TXA2, enhances the platelet aggregation, what increases the possibility of thrombosis.[123]

The platelets release growth factors as platelet-derived growth factor (PDGF) and VEGF, which pathways are upregulated in PAH.[108,66] VEGF is a crucial regulator of vascular development, and the increase in this GF results in alterations in ligand VEGF-A and in VEGF receptor 2 (VEGFR) from the signalling cascade, potentiating endothelial proliferation, survival, motility, and angiogenesis, which was proved by histology of lung tissue with plexiform lesions.[108]

The shifts in the pathway of arachidonic acid towards an alternative product to cyclic adenosine monophosphate (cAMP), that induces vasodilatation, were also reported in cases of diabetes and atherosclerosis associated with PAH.[66,90] In those cases, the TXA2 produced will lead to platelet aggregation, vasoconstriction and cellular proliferation[121], due to a downregulation on PGI2, once the PGI2 synthase activity is diminished in the lungs of PAH subjects.[51,66] However, there are evidences who relate the possible communication between vascular cells and platelets in PAH by the activation of toll-like receptor 4 (TLR4), whose deletion will lead to an attenuation on the effects of PAH, like RV hypertrophy[66], being evidenced the inhibition of platelet aggregation through the inhibition of TXA2, what may ameliorate PAH symptoms.[49,75]

2.4. Inflammatory reaction in pulmonary arterial hypertension

Beyond the remodelling of the vessels, the vasoconstriction, the intimal proliferation, and medial hypertrophy, PAH is accompanied by illicit recruitment of inflammatory cells which release factors that enhance cell proliferation and elastin fibers degradation.[51] The maladaptation of the immune response is related with the accumulation of perivascular inflammatory cells and the overabundance of chemokines and cytokines[55] as IL-1β, IL-2, IL-4, IL-6 and IL-8.[124]

The hypoxia conditions resulting from PAH induce a specific inflammatory milieu in the PA, with lymphocytes accumulation in the lungs, which may also contribute to vascular remodelling[112] promoting neointimal formation, thrombosis, and luminal obliteration.[54,55] Thus, the inflammation is a common feature of PAH due to the presence of

mononuclear cells that infiltrate the vessels through the perivascular areas around them[74] and the proinflammatory state of the vessel walls suffer an increment along with the progression of PAH.[125] Furthermore, the generated hypoxic environment in PAH stimulates ET-1 expression[72], which is also involved in inflammatory process.[25,70] However, some cytokines may act as anti-inflammatory, such as IL-10, displaying compensatory mechanisms.[124]

Once PAH is related with metabolic disruptions, some studies report that this disease is associated with chronic inflammation due to the activation of proinflammatory cytokines, as the IL-6, which is associated with the permeation of adipose tissue to macrophages and lymphocytes potentiating inflammatory process.[50,126,127] A group of investigators also discovered that in individuals affected by IPAH, IL-6 is consistently increased in the lungs and serum, activating VEGF, the mitogen-activated protein kinase (MAPK) pathway with increase in MYC proto-oncogene (cMyc) transcription, along with downregulation of transforming growth factor-ß (TGF-β) and pro-apoptotic kinases, contributing the alteration on this gene to the development of pulmonary proliferative arteriopathy and the progress toward PAH[127], which is sustained by the same findings in animal models.[127,128]

PAH is characterized by fluctuating degrees of perivascular inflammatory infiltrates, encompassing T- and B-lymphocytes, macrophages, dendritic cells and mast cells, who are usually present in plexiform lesions.[55,124] Aldosterone increases endothelial cell adhesion molecule expression, facilitating the activation and vascular infiltration of monocytes, macrophages, and T- and B-lymphocytes that also induce inflammation.[54]

Medical reports from biopsies to organs of patients with PAH, such as lungs, account the existence of mononuclear cells in plexiform lesions, mainly T cells, macrophages, and a lesser extent of B cells[50], which is in accordance with the studies that refer to the existence of T helper 17 cells who play a key role in the development of PAH due to chronic hypoxia.[112] Moreover, the percentage of regulatory T cells expressing the leptin receptor, related with the promotion of pathogenesis of autoimmune diseases[129], was increased in PAH, with reduced function of these cells, which indicates a leptin-dependent immunomodulatory effect in PAH.[111] It occurs, in part, due the action of the nuclear factor of activated T cells (NFAT), a transcription factor that promotes cytokine gene transcription, which is upregulated in PAH, leading to increased levels of cytokines, a main feature of PAH. [29,39,68]

The numerous forms of bone morphogenetic peptide (BMP) are on the basis of several metabolic pathways, being essential on the correct functioning of cellular context and maintaining tissue homeostasis, and disturbances on BMP family may lead to inflammatory responses, vascular diseases and cancer.[51] The BMPRII is a transmembrane serine/threonine kinase receptor of BMP that is essential for maintaining the barrier function of the PAEC lining, displaying a vital role in the development of T cells from thymocytes.[51,55] Dysfunctions on his signalling pathway may be seen in all forms of PAH and can lead to unsuitable expression of growth factors and pro-inflammatory responses in vascular cells,[55] triggering an increase on endothelial inflammatory responses thereby contributing to adverse vascular remodelling.[51] Either the increased number of macrophages present in pulmonary lesions from patients with severe PAH induce the production of pro-inflammatory cytokines such as tumour necrosis factor α (TNFα) and interleukins (IL1β, IL6 and IL8)[50,51], monocyte chemoattractant protein (MCP)-1, and fractalkine[55], that will induce the expression of micro RNAs (miRNA) that inhibit BMPRII expression.[51] IL1β and TNFα function as biomarkers for the accumulation of extracellular matrix proteins such as fibronectin.[130]

2.5. Fibrosis development in pulmonary arterial hypertension

Fibroblasts, the main responsible for fibrosis, are mesenchymal cells that can be activated by several chemical stimulus that promote their proliferation and differentiation in myofibroblasts, who are involved in various cellular processes as inflammation, angiogenesis and pathological tissue fibrosis.[131,132] The fibroblasts deposit type I and III collagen fibrils as they move through the extracellular matrix to maintain their structural support in a balanced process of synthesis and degradation of fibrils[132], and in situations of disease, as PAH, their action is potentiated by the action of an array of autocrine and paracrine signals, as the TGF-ß produced by inflammatory cells, deregulating the process of renewal of collagen and assisting the fibrosis development.[131,133]

Fibroblasts are important cells for the structural support of the heart, constituting also a middle for interaction with cardiac myocytes.[132] The normal and fibrotic fibroblasts, fibrocytes, under instruction of TGF-ß, produce ET-1 that will generate matrix proteins

production and drive the contraction of extracellular matrix, conferring to fibroblasts also greater resistance to apoptosis.[134] The characteristic high levels of ET-1 in plasma of PAH patients are associated with the development of cardiac fibrosis, once they promote the undue deposition of extracellular matrix and fibroblast recruitment.[70,135] In situations of diabetes, there is a higher accumulation of collagen and the development of fibrosis[135,136], however, it was reported that the modulation of ET-1 levels on diabetic patients would be able to improve that condition, since the a lack of ET-1 attenuated the development of cardiac fibrosis through the reduction of the accumulation of fibroblasts and collagens in myocardium, controlling the development of the fibrotic areas.[137]

In situations of injury, the myocardium fibroblasts differentiate into myofibroblasts by action of inflammatory mediators, as TGF-ß and IL-1ß and by altered activation patterns, and are more susceptible to cytokines action, that themselves also secrete, maintaining the inflammatory response to injury.[132] The pathological myocardial remodelling is accompanied by an extreme deposition of extracellular matrix proteins by cardiac fibroblasts[138], what contributes to RV stiffness and to the progression of PAH, that can culminate in HF.[139]

As mentioned above, the aldosterone levels follow the increase in ET-1, which explains, in part, the increase in aldosterone levels[137], which is also involved not only on stimulation of perivascular fibrosis through the increase of the expression of profibrotic mediators as galectin-3, TGF-ß, connective tissue growth factor (CTGF), and type I and type III collagen, but also on decreasing the expression of two anti-fibrotic peptides, BMP4 and brain natriuretic peptide (BNP).[54]

Fibrosis not only affects myocardial area but also the lungs, what results in impaired air exchanges.[140,141] The pulmonary epithelium also releases TGF-ß in response to stress, that interact with fibroblasts and triggers an increase in their production and in profibrotic factors as fibronectin, collagen and α-SMA.[131,140] The lung vascular remodelling may still be associated to events of chronic inflammation.[76] The progression of fibrosis on respiratory organs and the successive structural and metabolic alterations on microvasculature tease diseases as systemic sclerosis, a systemic autoimmune disease associated to PAH.[142] The association of those diseases occurs due to the functional alterations and the structural

fibroproliferative character of this vasculopathy who affects the small and medium sized pulmonary arterioles.[143]

2.6. Endothelial to Mesenchymal transition

The EndMT is a process whereby a polarized epithelial cell suffers multiple biochemical changes that enable it to assume a mesenchymal cell phenotype[144], including enhanced migratory capacity, invasiveness and elevated resistance to apoptosis[142,144], being potentiated by hypoxia conditions.[145] The pulmonary arterial remodelling resulting from PAH and characterized by the activation of fibroblasts and smooth muscle-like cells in the walls of PA, is also associated to EndMT, being this mechanism a starting point for the arterial remodelling and PAH.[145]

EndMT, unleashed by Twist Basic Helix-Loop-Helix Transcription Factor 1 (TWIST1), Snail Family Transcriptional Repressor 1 (SNAIL or SNAI1), and Snail Family Transcriptional Repressor 2 (SLUG or SNAI2) transcription factors[108], corresponds to an aberrant vascular remodelling as consequence of the increased PVR, causing the concentric arterial wall thickening, the development of occlusive intimal lesions and neomuscularization of precapillary arterioles.[108] In this process, EC modify some of their molecular features, namely at genic level, occurring downregulation of EC-specific genes as platelet EC adhesion molecule 1 (PECAM1 or CD31) and vascular endothelial cadherin (VE-cadherin or CD144), but also the upregulation of SMC-specific genes, such as α-SMA and fibroblast-specific genes like vimentin.[58,108] During EndMT, EC lose their junctions to the endothelium and acquire migratory and proliferative abilities as they progressively switch from endothelial to a mesenchymal phenotype.[108] As EC progress to mesenchymal cells, there is an acquisition of the characteristic fibroblastic markers of these cells, as α-SMA.[135] The interaction between ET-1 and TGF-ß pathway also contributes to EndMT.[142]

3. Metabolism

PAH is also associated to a heterogeneity of systemic metabolic derangements such as the metabolic syndrome[111], the insulin resistance[77], hyperglycemia (diabetes) and dyslipidemia[146], glucose intolerance and alterations in the aerobic glycolysis, also known as

Warburg effect[147,148], which also implies alterations in tricarboxylic acid (TCA) cycle[147,149], but also in the FAO.[146] Usually, when associated to chronic hypoxia, PH occurs due an imbalance among GO, glycolysis, and FAO.[150] Besides, the metabolic disruptions may trigger the progression of severity for PAH and the resultant metabolites may be used as biomarkers to the disease.[151]

To preserve its correct functioning, the heart requires an uninterrupted supply of energy and oxygen to keep its intracellular adenosine triphosphate (ATP) standardized, which is mandatory for the maintenance of myocardial systolic and diastolic activity[152,153], what involves the metabolization of a wide range of energy substrates to fill its energy requirements beyond fatty acids and glucose, as ketones and branched chain amino acids.[154] The elements of cardiac energy metabolism comprise the substrate use, the oxidative phosphorylation (OXPHOS), and also ATP transfer and utilization.[155] Ohira, H. *et al.*, describe that the metabolic reprograming that characterizes PAH relates not only with the increased glucose utilization along with progressive PH, but also with the increase in fatty acid utilization accompanying severe RVD[155], which is in part refuted by a previous study from Nagaya, N. *et al.*, who described an impaired fatty acid uptake in the failing hypertrophied RV.[156]

An adult healthy heart hold very high energy utilization rates; the ATP produced is derived not only from GO, but also from other oxidizable energy sources like fatty acids, lactate, ketones, and amino acids.[69,157] In cardiomyocytes 60 to 90% of the energy comes from FAO[69,158,159], whereas glucose metabolism is considered a secondary source of energy production[160], even consuming 12% more oxygen per mole of ATP produced than GO.[42,69,155] Nevertheless, the rate of glucose utilization is higher than in other tissues, and the reduction of glucose uptake and oxidation could be the major pathophysiologic factor that contributes for contractile dysfunction in cases of HF[161] being this condition an hyperadrenergic state, who leads to an increase in plasma levels of free fatty acids (FFA), which is implicated in a wide variety of metabolic dysfunctions as impaired fatty acid (FA) uptake and oxidation in the myocardium.[162]

The substrate preference for FAO occurs due the inhibition of GO by FAO after the child-birth, via Randle cycle, once the long chain FAs oxidation inhibits glucose uptake, directing the metabolism toward aerobic glycolysis that has as consequence the lactate

accumulation[59,62,152], requiring an additional effort from various energy-dependent pumps to maintain pH balance.[42] However, in the late stages of HF occurs downregulation of myocardial FAO while the GO is fomented[52,157] and usually when associated to chronic hypoxia, PAH usually occurs due an imbalance among GO, glycolysis, and FAO.[150]

3.1. Fatty acid metabolism

Cardiac FAO starts when the FAs are taken up from bloodstream to cytoplasm as FFA and bound to albumin, or as FAs released from triacylglycerol (TAG)[163], that can diffuse through the membrane or be translocated into the cell by cluster of differentiation 36 (CD36) molecules, the FA transport protein-1 (FATP-1) and -6 (FATP-6).[78] In the classical pathway of mitochondrial FAO, the metabolism of free long-chain FAs (LCFA) starts in the cytosol of cardiomyocytes with their activation by Coenzyme A (CoA) and their conversion into fatty acyl-Coenzyme A by acyl-CoA synthetase, an activated FA constituted by a long-chain molecule.[69,164,165] In this step, acyl-CoA may be either esterified to triglyceride.[165] Then, in the outer mitochondrial membrane, carnitine palmitoyl transferase 1 (CPT1), the enzyme responsible for mitochondrial FA uptake, converts fatty acyl-CoA into a long-chain acylcarnitine, that will move through the porins of mitochondrial membrane to the mitochondrial matrix by the action of acylcarnitine translocase, where it will undergo β-oxidation.[69,78,166,167] At mitochondria matrix, fatty acylcarnitine is converted into fatty acyl-CoA in a reaction catalysed by CPT2, located on the inner mitochondrial membrane, where acyl-CoA undergoes β-oxidation, generating acetyl-CoA, that enters to the Krebs cycle[69,164,166,167] A complete cycle of FAO, with β-oxidation, of a FA containing 6 carbons may yield 48 ATPs.[62] In the end, fatty acyl-CoA, particularly palmitoyl-CoA, might be used for afresh synthesis of ceramides, which plays pleiotropic effects on cellular function.[165]

Myocardial steatosis, an ectopic accumulation of lipids within the cardiomyocytes[33,166,168], can be related with the impairment of mitochondrial FAO and may be a cause and not only a consequence of RVHF[33], due to the permanent relocation of CD36, a transporter of LCFA, to the sarcolemma.[166,169] The increase in CD36 expression is not only related with an increase in cardiac FA uptake, once this molecules are one of the responsible for inducing cardiac hypertrophy and contractile dysfunction[69,166,170] but also the increased accumulation of triglycerides in human RV of PAH patients with BMPRII mutation.[166,168]

An increased content of ceramide in RV tissues from those patients was reported too, and that, according with the literature, is lipotoxic, an pro-apoptotic mediator, and is also involved in the development of insulin resistance, cardiac dysfunction, and HF.[33,69,163,168] Furthermore, the overexpression of peroxisome proliferator–activated receptor alpha (PPARα) is associated to a lipid overload due the increase in enzymes involved on FAO[163], once occurs an increase in FA utilization along the severe RVD[155], but also with the regulation of glucose transporters (GLUTs), as the GLUT4.[153] FAO can also be inhibited by GO pathway once the CPT1 is the rate-limiting step in acylcarnitine formation.[33]

The Randle cycle is responsible for the production of citrate during FAO, that is the prompter for phosphofructokinase (PFK) inhibition and accumulation of glucose-6-phosphate.[59,69,160] This molecule , in its turn, will inhibit hexokinases (HK) and decrease GO and the production of pyruvate. [59,160] Then, the acetyl-CoA generated from FAO has the ability to inhibits pyruvate dehydrogenase (PDH), interrupting the cycle of production of PDH, leading to the decrease of their concentration and, subsequently, to the inhibition of the production of acetyl-CoA and the production of substrates by the Krebs cycle, what generates an imbalance on cellular energy[59,69,171] through the inhibition of the electron transport chain, increasing the reliance on aerobic glycolysis.[62]

In situations of cardiac hypertrophy and HF, downregulation of genes involved in mitochondria biogenesis and oxidative metabolism, such as PPARα, peroxisome proliferator-activated receptor gamma coactivator 1-alpha (PGC-1α), which is a transcriptional coregulator and a master regulator of mitochondria and their targets, has been observed and proposed as an important causal mechanism for decrease in FAO under those conditions.[153,163] It is also mostly expressed in tissues with high energy demands, such as skeletal muscle, heart or brain, being its expression increased under conditions of higher energy requirements.[172] On the other hand, during the development of cardiac hypertrophy, upregulation of hypoxia inducible factor 1α (HIF-1α) gene occurs due the development of hypoxia conditions.[173]

3.2. Glucose metabolism and the Warburg effect

The metabolic perturbation most reported and studied in PAH is a process designated by Warburg effect[147], that triggers numerous adaptive and maladaptive downstream effects

as a stress response, especially in EC[49], supporting the metabolic requirements for proliferation characteristic of the disease, what turns PAH into a consequence of this process.[174] The Warburg effect was firstly described in 1920 by Otto Warburg[147], and concerns the cessation of mitochondrial OXPHOS, consequently leading to aerobic glycolysis[29,147,175] akin to what is observed in cancer cells[35,68,147], pointing the glycolysis as the main source for catabolic needs of hyperproliferative cells.[176] This process can be considered an aerobic pathway to small amounts of ATP production, indicating that this can progress in the absence of molecular oxygen, giving continuity to the production of ATP.[147,177] Indeed, the suppression of GO and the subsequent increase in glycolysis, once the presence of oxygen is compromised in cases of PAH due to hypoxia conditions, causes the cells to metabolize glucose into carbon dioxide (CO_2) by oxidation of glycolytic pyruvate[177] in mitochondrial TCA cycle.[17,23] The accelerated glycolysis evidenced in PAH constitutes an hallmark of the increased glucose metabolism in cardiac hypertrophy and in remodelled RV.[68,147,177,178]

The regulation of intracellular and extracellular levels of glucose depends on levels of control of expression of the genes that encode the different isoforms of GLUT proteins.[153,179] Once the rate of glucose utilization in the heart is higher than in other tissues, to respond to the high demand of glucose of the myocardium, this process is mediated by GLUTs[180], who work as uniporter[181] and allow the facilitated diffusion of glucose through the plasma membrane of the cells[179], and its regulation may also be dependent on stimuli associated with pathologies.[153] The GLUT4 is the major isoform of GLUTs in human heart, representing about 70% of the GLUTs.[182] The pressure overload inherent to PAH leads to the increase in GLUT1 expression, but to a decrease in the GLUT4 expression, and those alterations will reflect on their distribution into the plasma membrane, what will reflect in alterations on glucose transport and its metabolism.[153,183] Therefore, under conditions of myocardial disease, ischemia or pressure overload hypertrophy, as the ones that occur in PAH, the heart shows an increased dependence on glucose[4,180], and a study from Ohira *et al.*, demonstrated, in left heart failure, an increase in glycolysis rate to afford an anaerobic source of ATP to challenge the decrease in OXPHOS. The same study demonstrated that the degree of glucose uptake is related with the degree of overload and dysfunction.[155] So, the increase in dependence on glucose metabolism in situations of cardiac hypertrophy can be,

in part, attributed to impaired FAO due to effect of Randle mechanism on management of glucose.[153]

In cases of overload of the RV and myocardial hypertrophy, frequent in PAH, while the myocardial glucose uptake and the glycolytic rate are increased, the FFA metabolism decreases.[155,184] This metabolic increase in glucose uptake has been proved and verified by several investigations using ^{18}F-fluorodeoxyglucose (FDG) in combination with positron emission tomography (PET), by an increased uptake of PDF in patients with PAH.[184–186] The glucose may be metabolized in multiple pathways, providing not only energy but also other metabolites important for cell functioning.[187]

The glucose metabolism, represented in Figure 3, starts with the import of glucose into the cells by GLUT1, an insulin-independent transporter, and GLUT4, an insulin-sensitive transporter, that is activated and recruited to cellular membrane by insulin molecules[69,187], but also by stimulus as ischemia or catecholamines.[182] Since glucose is in the intracellular medium, this molecule is phosphorylated and converted into glucose-6-phosphate by HKs (1,2 and 3) in a critical step for glucose utilization.[69,188] The HK1, HK2 and HK3 isoforms are located in the outer membrane of mitochondria and inhibited by its product glucose-6-phosphate, being the HK1 and HK2 the major cardiac isoforms.[189] HK2 is mainly found in cardiac and skeletal muscle, an insulin-sensitive tissue, whose position varies between the mitochondria and cytoplasm in response to changes in intracellular glucose-6-phosphate, pH and cardioprotective signalling from Akt pathway.[190] HK2 is also responsible for glucose phosphorylation after its entrance to the cell.[191] The HK3 is located in the cytoplasmic and is mainly responsible for anabolic functions.[190] Then, a succession of reactions mediated by PFK and pyruvate kinase (PK) turns glucose-6-phosphate in pyruvate that can be subsequently converted in lactate, with a yield of 2 ATP molecules.[42,69,192] However, pyruvate may also be transported to the mitochondrial matrix via a monocarboxylate acid or pyruvate carrier, it may undergone mitochondrial oxidation passing by mitochondrial pyruvate carrier to TCA cycle[69,153] or carboxylation to form oxaloacetate or malate via ATP-dependent pyruvate carboxylase.[165,193]

The glycolysis provides pyruvate to the mitochondria matrix for GO, where the PDH breaks down pyruvate to produce acetyl-CoA, releasing CO_2 and NADH, however, it only happens if the PDH is active, producing 36 molecules of ATP.[69,78,192,194] The generated

NADH is translocated to mitochondria where it regenerates cytosolic NAD^+ necessary for glycolysis to continue, once it is the electrons acceptor.[153] In PAH, there is increased aerobic glycolysis due to normoxic upregulation of the transcription factor HIF-1α, which upregulates pyruvate dehydrogenase kinase (PDK) to inhibit pyruvate dehydrogenase, and epigenetic regulation of the superoxide dismutase 2 (SOD2) gene.[78]

The generated pyruvate may go through different pathways: it may be oxidized producing acetyl-CoA, who induces histone modifications, functioning as an epigenetic control of gene expression, or inhibit PDK.[153] Though, if pyruvate cannot be used by mitochondrial PDH to the processing of OXPHOS, lactate is the end product of glycolysis, resulting in acidosis of the milieu.[192] This may occur due the interaction of PDK and PDH in the mitochondria, responsible for GO[42], where the first will phosphorylate the second one, leading to the constrain of GO, since PDK activation [17,35,195] and FAO activation inhibit PDH.[39,155] The inhibition of PDH will lead to the suppression of mitochondrial function[196], to a decrease in the influence of GO in acetyl-CoA production by the TCA cycle and leads to the development of a bioenergetically disadvantageous increase in glycolysis in relation to GO, the Warburg effect.[63,197–199] This will generate an uncoupling between glycolysis and GO, altering pyruvate influx into the mitochondria and its metabolism and constitute an antiapoptotic environment.[196] The suppression of GO and the election of glycolysis as an alternative metabolism, reflects the acceptance by the cell of the reduced efficiency for ATP generation in PAH[62], and the increase in glucose utilization occurs during the progression of the disease[155], as well as a decrease in mitochondria-derived reactive oxygen species (mROS).[196]

Furthermore, mitochondrial OXPHOS defects that impair mitochondrial oxidation may occur due to changes in mitochondrial pyruvate dehydrogenase complex (PDC), an oxidoreductase that contains PDH who catalyses the irrevocable conversion of pyruvate into acetyl-CoA and CO_2, which establishes the bridge of communication between glycolysis and TCA cycle.[200,201] Thus, a disturbance in PDH will result in inappropriate removal of pyruvate and lactate from blood and tissues[200], causing an increase in glycolysis in relation to GO.[202] Once the impaired PDH is implicated in errors in mitochondrial metabolism[200], the derangement may be in anyone of the enzymes of PDC, as in the most important enzyme of the complex, the PDH (E1)[201], which is composed by two α and two β subunits.[203–205] The

PDHα1 subunit, the most affected by mutations, plays a key role in PDH functioning once it contains the binding site for pyruvate[203], and the phosphorylation of this subunit by PDK is enough to preclude the pyruvate binding to PDH.[201] In models of RVHF, the mRNA levels of PDHα1 and PDHα2 are decreased in RV of PAH animal model, being this accompanied by an increase in PDK.[202] The PDHβ subunit is mostly expressed in the heart and is related with lactic acidosis, once an mutation in its gene leads to lactic acid accumulation and disturbances in cell proliferation.[205]

In hypoxia conditions, where the oxygen supply becomes inadequate, nicotinamide adenine dinucleotide (NAD^+) is regenerated into NADH by lactate dehydrogenase a (LDHa) in order to maintain glycolysis, generating lactate as sub-product, in a process known as anaerobic glycolysis.[206] LDH is an enzyme whose function is the increase of the rate of the concomitant inter-conversion of pyruvate to lactate and NADH to NAD+, which is usually used by cells during anaerobic respiration.[206,207] LDH, which favours Warburg Effect[207], is a tetrameric complex composed by four isoforms:

-LDHa, also known as M subunit and predominant in skeletal muscle[206,207], is regulated by transcription factors as the HIF-1, that promotes the transcription of LDHa, cMyc, which regulates cell growth, proliferation and apoptosis, and forkhead box protein M1 (FOXM1), involved in angiogenesis[206], favouring lactate production without being inhibited by it;[207]

-LDHb, known as the H subunit and found predominantly in the heart[206], also favours lactate production, but unlike LDHa, it is inhibited by high lactate concentrations.[207]

-LDHc forms a homotetrameric complex, that despite being testis specific is expressed in tissues from heart, lungs and skeletal muscle, and catalyses the lactate production in anaerobic glycolysis;[206,207]

-LDHd, whose sequence is homologous to the one from yeast d-lactate dehydrogenases, have uncharacterized function in human metabolism.[207]

The expression of some genes as the TNFα has been shown to also inhibit myocardial PDH, resulting in a metabolic disruption that may contribute to the myocardial dysfunction that characterizes sepsis, once the body's response to this metabolic shift may promote injures on tissues and organs.[196] In patients with PAH was also reported an increased expression of PDGF and PDGF receptor (PDGFR) on lung tissue, that interact and activate a downstream signalling pathway promoting PASMC proliferation and migration.[31] The

PI3K/Akt/mammalian target of rapamycin (mTOR) (PI3K/Akt/mTOR) signalling pathway, crucial to prevent cell damage and apoptosis[208], is downstream of PDGFR, playing an essential role in Warburg effect due to inhibition of mitochondrial respiration by upregulating HIF-1α, provoked by the hypoxia conditions characteristics of PAH[29,62], activating transcription factors such as cMyc that induces ischaemia[198], also inhibiting the mitochondrial electron transport chain.[186] In hypoxic environments, HIF-1 promotes the transcription of certain target genes for metabolism, cancer and apoptosis, supporting cell survival in these conditions, as it occurs in PAH.[206]

The PI3K signalling pathway is linked to both growth control and glucose metabolism, regulating the glucose uptake and his use, requiring high levels of glucose flux.[177] When the metabolism occurs in a normal way by OXPHOS, even in non–insulin-dependent tissues, PI3K signalling regulates the GLUT expression through the family of kinases Akt, enhancing glucose capture by HK, and stimulating PFK activity.[147,177,181] Due to downstream of the PI3K/Akt/mTOR signalling pathway and upregulation of HIF-1α are unleashed alterations in the enzymes essential for the TCA cycle, which lead to the interruption of OXPHOS[31,209], as the levels of HK and PFK who are higher in in the failing RV compared with the hypertrophied RV.[38] The regulation of intracellular and extracellular glucose also depends on levels of control of gene expression of the genes who encode different isoforms of GLUTs[179]. The upregulation of nuclear FoxO1 that regulates cell cycle progression, is also caused by the hypoxia conditions and the upregulation in HIF-1α[114,199,210], which triggers the increase of PDK1 expression[198], contributes to PDH activity inhibition and prompts shifts of metabolism to aerobic glycolysis.[31,62,208]

While the GLUT4 only expresses in after the birth and to the adulthood[153], GLUT1 is the major GLUT expressed in the foetal heart and his expression is re-induced and increased in the adult heart in some pathophysiological states, as in response to myocardial damage or stress, including pressure overload and hypertrophy.[153,180,211] This insulin-independent GLUT is the mainly responsible for basal cardiac glucose uptake in quiescent myocytes[211] and its expression has been increased when it is in the plasmalemma, indicating that it is active.[212] Some researchers had described the existence of adaptative mechanisms to the maintenance of glucose concentration homeostasis, based on the recruitment of GLUT4, one of the most abundant GLUTs in myocardium, for the plasma membrane of the

cells.[183] This mechanism may be controlled by insulin that acts through two intracellular signalling transduction pathways, MAPK and the PI3K/Akt, controlling the GLUT4 translocation to cell membrane[213,214], consequently, modulating glucose uptake by the cells.[179] The knockout of GLUT4 gene triggered cardiac hypertrophy in LV[180] and this may be one of the reasons for the existence of a high concentration of GLUT4 in animal models with PAH during the compensatory state (which precedes cardiac hypertrophy) and the variation of GLUT4 according with the disease state and his severity.[215] It has also been reported that, as cardiac hypertrophy progresses to heart failure, GLUT1 mRNA expression is reduced in human healthy hearts, suggesting that decreased GLUT1-mediated glucose uptake and utilization could play a role in the transition to heart failure.[211,212]

The SOD2 gene has also been reported and related with PAH due the existence of a polymorphism that alters the SOD2 protein[24,147], playing a pivotal role on oxidative stress system, which is one of the basis of this disease.[24] This antioxidant enzyme, that participates in several cellular processes, among which glucose metabolism, has decreased expression in PAH[24,216] being related with the development of plexiform lesions characteristic of PAH.[216] In PAH, the downregulation of the mitochondrial hydrogen peroxide (H_2O_2), the generating enzyme of SOD2, triggers the decrease on production of the redox signalling molecule H_2O_2, contributing to the generation of an hypoxia-like redox environment that stimulates HIF-1α.[62]

Sirtuins (Sirt) are enzymes responsible for deacetylate histones and other transcriptional regulators[217–220], through the regulation mitochondrial functions.[220] However, in order to exercise its activity, they require NAD^+ as substrate, which is also used in glycolysis, reducing NAD^+ availability for Sirts.[219] A study found that Sirt1 exerts a antiproliferative role in vascular remodelling in hypoxia conditions in rats and humans, and a deficit in Sirt1 can induce an imbalance which favours glycolysis at the expense of oxidation, potentiating the vascular remodelling as it occurs in PAH, that is why its activation can have beneficial effects in this disease.[217] Furthermore, it intervenes in glucose metabolism and respond to physiological fluctuations in energy, contributing to the maintenance of energetic homeostasis and health[219] improving mitochondrial activity through the activation of stress signalling pathways.[217] Sirt1 has the ability to control glycolysis by deacetylating PGC-1α, who directs mitochondrial biogenesis and activity[219],

resulting in the repression of glycolysis[218], increased glucose output[220], and downstream of pathways that control mitochondrial gene expression.[219] This enzyme also suppresses HIF-1α by deacetylation, causing a repression on GO through TCA cycle[219], what trigger the prevention of inhibition of the cMyc, the activator of the transcription of mitochondrial transcription factor A (Tfam) mediated by HIF-1α, that usually are overexpressed in PAH[104,217,221], improving the expression of mitochondrial-encoded respiratory genes and GO.[217]

Investigations also discovered numerous similarities between PAH metabolic phenotype and cancer that reflect a shift from oxidative to glycolytic metabolism, such as the high expression of cellular growth factors, dysregulated angiogenesis and enhancement of antiapoptotic activity.[29,38] Despite the similarities, differences between PAH and cancer, as the lack of invasion and metastasis, along with genetic causes and degrees of angiogenesis impairment, are evident.[222,223]

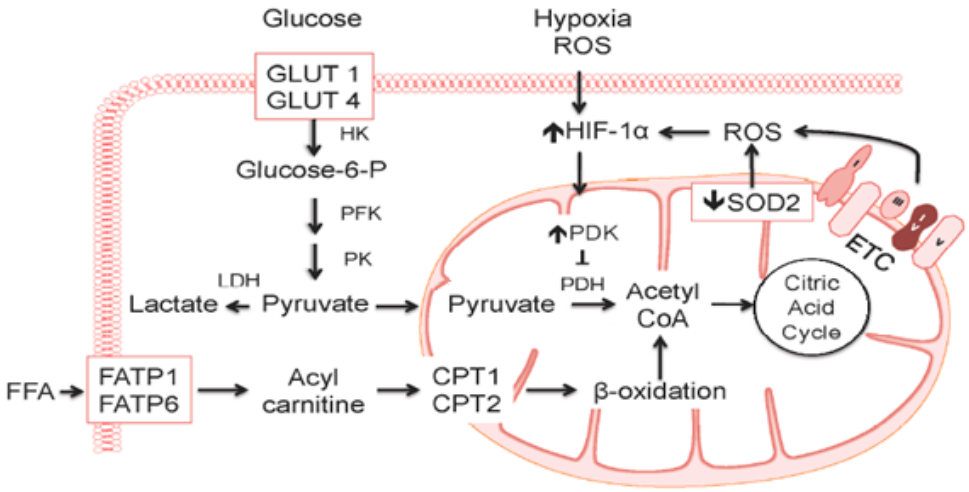

Figure 3 Cellular metabolism characteristic of PAH. In PAH, cells acquire a metabolic pattern similar to what is observed in cancer cells. Glycolysis starts when glucose is taken up by the glucose transporters 1 (GLUT1) and 4 (GLUT4), is posteriorly phosphorylated by hexokinase (HK), and then suffers a series of reactions until pyruvate is produced. Pyruvate is the substrate for pyruvate dehydrogenase (PDH) in the mitochondria, supporting glucose oxidation. Free fatty acids (FFA) are taken up by fatty acid transport protein-1 (FATP-1) and -6 (FATP-6) and then transformed into acyl carnitines that are transported across the mitochondrial membrane by carnitine palmitoyltransferase-1 (CPT1) and transformed to acyl CoA by carnitine palmitoyltransferase-2 (CPT2). Into the mitochondria, acyl CoA is converted to acetyl CoA during β-oxidation. In PAH occurs an intensification of aerobic glycolysis due to normoxic upregulation of HIF-1α, which upregulates pyruvate dehydrogenase kinase (PDK) to inhibit PDH, and epigenetic regulation of the superoxide dismutase 2 (SOD2) gene. PFK, phosphofructokinase; PK, pyruvate kinase; LDH, lactate dehydrogenase; ROS, reactive oxygen species; ETC, electron transport chain. Adapted from Leopold, J. A. and Maron, B. A. 2016. '*Molecular mechanisms of pulmonary vascular remodelling in pulmonary arterial hypertension*'.

3.2.1. Glutaminolysis

The glutaminolysis induced by the GO[224], which is a type of metabolism characteristic of cancer cells, has recently been found that is selectively induced in the RV during RVH.[42,44,62] The continued action of the TCA cycle requires the replenishment of carbon intermediates[193], which is achieved by anaplerosis through glutaminolysis, resulting in a net flow of carbon for the TCA cycle, being this process linked to animal models of PAH.[42,44,62]

Glutamine is an additional source of cellular energy, as well as carbon, and nitrogen, that is used particularly in rapidly cell-growth and proliferating cells[44,224], where occurs deamidation of glutamine through the action of the enzyme glutaminase (GLS1).[193] During the hyperproliferative state, cells go through aerobic glycolysis and glutaminolysis instead of the standard OXPHOS pathway, potentiating an extra rapid, although inefficient, management of glucose and glutamine for energy and nutrient synthesis.[4,225] The resulting changes from metabolism in PAH lungs may trigger the use of these glutamine stores and increase the glutaminolysis, alike to what occurs in cancer cells.[225]

Glutaminolysis occurs when glutamine transporters, the solute carrier proteins SLC1A5 and SLC7A5, transport glutamine into the cytosol, and then the mitochondria by hydrolyzation converts glutamine into α-ketoglutarate, that enters to TCA cycle to restore the metabolic intermediates that support rapid cell growth without apoptosis.[42,62,198] This process has some similarities with glycolysis: when mitochondria faces an impaired PDH, occurs an increase in malic acid from the glutamine-fed TCA cycle that is oxidized into pyruvate by malic enzyme (Me), increasing lactate levels.[44,224]

This process appears to be induced by an ischemic activation of the cMyc transcriptional pathway[62,224], that triggers the reactivation of components of the foetal gene package, as it is characteristic of RV remodelling[42], being also associated with an increase in the expression of mitochondrial malic enzyme and the glutamine transporters as SLC1A5 and SLC7A5, analogous to GLUTs in glicolysis.[62,224] Moreover, an impairment with increase in cardiac glutaminolysis has been documented in myocytes from maladaptive RVH animals in a MCT-induced PAH model, along with an increase in the expression of cMyc. The same study demonstrated that the inhibition of glutaminolysis improves GO, however,

the importance of glutamine metabolism in the pathogenicity of PAH has not been well defined.[193]

3.3. Pulmonary arterial hypertension and insulin resistance

As result of the deficiency on glucose uptake caused by alterations on GLUTs due the metabolic shifts in PAH, the body will need higher levels of insulin to help glucose enter cells and keep the homeostasis[226] which may lead to changes in GLUTs.[179,180] Likewise, several studies report that in patients with PAH there is reduced pulmonary mRNA expression of peroxisome proliferator-activated receptor γ (PPARγ) and apolipoprotein E (apoE), that regulates adipogenesis and glucose metabolism, and circulating levels of low-density lipoprotein and atherogenesis in the vessel wall, respectively.[50,51,196] Other circulating factors associated with insulin resistance, and that are normally repressed by PPARγ expression, display elevated levels in PAH, such as the inflammatory cytokine IL-6[77,110,127] and ET-1.[77,84,227] Furthermore, once the FA modulate the expression of GLUT4, the increase in cardiac FAO, due to the overexpression of PPARγ, triggers the inhibition of GLUT4 protein and mRNA, what causes a deficit in glucose transport.[153] In cases of insulin resistance, the cells do not assume the signals that the hormone tries to send out to grab glucose out of the bloodstream, for example to activate GLUT4 for glucose transport, and place it into cells, leading to a deficit in glucose transport and also in glucose, affecting cell bioenergetic availability.[181,226]

The insulin resistance is characterized by the insulin disability in stimulate glucose uptake from body peripheral tissues[228] due to the inability of the tissue to respond to insulin stimulus.[115] In this cases, there is an inappropriate response of muscle, fat, and liver cells to insulin[226], which has to be transported to skeletal muscle to guarantee a provision of insulin to myocytes[229], and, consequently, the absorbance of glucose from the bloodstream is faulty.[226] The activated insulin receptor (IR), that plays a crucial role in the regulation of glucose homeostasis, creates docking sites with the ability to bind and phosphorylate several substrates, as the IRS family proteins (IRS1 to IRS4).[182] The IRS are insulin receptors who mediate not only insulin signaling[230], but also the signals from insulin-like growth factor I (IGF-I) to metabolic pathways as the PI3K/Akt and RAS mitogen activated protein kinase (RAS/ MAPK) after its phosphorylation.[229] However, it is hard to define the role played by

each of the IRS, but through knockout models was discovered that IRS1 plays a role in cellular growth, mediation of insulin action in peripheral tissues[230], and that derangements on this gene also induce glucose intolerance and dyslipidaemia.[231] In relation to IRS2, it was concluded that it is involved in compensatory cellular mechanisms, insulin resistance[230] and defects on this receptor trigger defects on insulin signalling in EC and impairs glucose uptake.[229] The IRS1 and IRS2 are also very important in EC, and the pathways activation by these receptors culminates in the production of NO and vasodilatation by PI3K/Akt pathway, and in RAS/MAPK pathway as it induces endothelial secretion of ET-1, that activates protein kinase C in vascular SMC inducing their contraction.[229] Furthermore, IRS1 deficient mice demonstrated higher blood pressure than IRS2 deficient mice, which allows to infer that IRS1 influences blood pressure and may be impaired in PAH.[231]

As mitochondria are crucial to cellular metabolism, several studies mention that the typical conditions of insulin resistance may be caused or promoted by mitochondrial suppression, that in the case of PAH will inhibit the GO on pulmonary vascular cells.[39,68,111] Indeed, the suppression of GO and the subsequent increase in glycolysis, since in the presence of oxygen is usually compromised in PAH due to hypoxia conditions, causes the cells to metabolize glucose to CO_2 by oxidation of glycolytic pyruvate in mitochondrial TCA cycle.[147,177] This is one of the hits of PAH, being evidenced in all PA layers and in the remodelled RV.[68,147,177]

Some evidences show that vascular cells from individuals with PAH and cancer cells share some features in terms of morphology and mitochondrial phenotype, such as the increased mitochondrial fragmentation, caused by a fission or fusion imbalance which alters the mitochondrial network in cytoplasm.[39,62,68,84] Moreover, the mitochondrial fragmentation contributes to the pro-proliferative and apoptosis-resistant phenotype of both diseases.[62] Furthermore, some genes may be disrupted and contribute to mitochondrial imbalance. There are genes that express proteins who regulate mitochondrial biogenesis and mediate several metabolic functions.[105,232] The PGC-1α gene, mainly induced by hypoxia conditions, is one of those master genes that regulates, interacts and induces the activation of several transcription factors, as the nuclear respiratory factor 1 (NRF1) and Tfam, and each of them has different characteristics.[104,105,232] The NRF1 factor gene encodes mitochondrial proteins[105] who play a key role on activation of some metabolic target genes who regulate

cellular growth, genes who are required for mitochondrial respiration[233], and mediates mitochondrial DNA (mDNA) transcription and replication through the Tfam.[232,233] The Tfam is the main responsible for mDNA replication, regulating the expression of 13 gene products, including the components of the mitochondrial cytochrome C oxidase complex from the electron transport chain.[105]

Even knowing that the RV is the main prompter of death by PAH due to RVHF, and RVD is characterized by abnormal energy metabolism[37,38], there are evidences that RVH has impact on metabolism.[69]

4. Right ventricular dysfunction in pulmonary arterial hypertension

In PAH, the metabolic derangements and the resulting cellular alterations culminate in HF, mostly due to RVHF. However, this process is not so linear and there are several steps from the first symptoms of the disease until the HF is reached.

In clinical terms, RVHF concerns to the inability of the RV to perfuse the lung circulation effectively to maintain LV filling at low venous/diastolic pressures.[40] The transition from RVH to RVHF involves a huge variability of RV adaptations among patients which are exposed to chronic PH according to the aetiology of the PH.[41,42] Due to the persistent increase on afterload caused by the progression of the disease, the RVH is usually accompanied by ischemia, myocardial apoptosis and excessive fibrosis, as well as the increased expression of noncontractile proteins that lead to diastolic dysfunction and inefficient coupling, triggering a decrease in RV systolic function followed by an acute RV dilatation that can culminate in the failure of RV.[39,43–45] The response also includes β-receptor downregulation, an increase in glycolysis, and a decrease in capillary density.[198] It also occurs an increase in RV glucose uptake in patients and animals with RVH.[155,192] Once RV ischemia may lead to the generated metabolic switches in carbon utilization that are associated with maladaptive hypertrophy, it may potentiate the "hypoxia-like" program of gene expression[44] activating genes such as HIF-1α and VEGF, who play a central role in modulation of myocyte development and in myocardial angiogenesis.[43]

The increase in RV oxidative metabolism is usually associated to several prognostic markers such as mean mPAP, PVR, and BNP.[234] BNP, from natriuretic peptide family

hormone, is the most sensitive marker myocardial stress and injury, more specifically for ventricular disorders and HF.[86] It is mainly released in response to cardiomyocyte stretch, as it occurs in RVH, and high levels of this biomarker reflect right atrial/ventricular volume and pressure overload and hypertrophy, as it is characteristic of PAH.[25,32,75,235] BNP is initially secreted by the cardiac ventricles and is continually cleaved, generating the N-terminal fragments (NT-proBNP) and the active hormone BNP[25,86,235], being involved in processes such as natriuresis, vasodilatation and downregulation of RAAS.[75] Another advantage of this biomarker is that we can relate it with hemodynamic parameters and stablish a direct proportional relationship between BNP levels and RV overload, PAP and diastolic pressure.[25,75]

Once RV oxidative metabolism may be a prognostic marker[234], several studies found out that some metabolic characteristics of the RVHF related to PAH are essentially based on the decreased level of FAO[37,69], increased GO[158,183] and intracellular lipid deposition.[69,163]

In PAH, a premature response to increased RV afterload occurs through the adaptive RVH.[39,41,69] The investigations carried out allowed the identification of two clinical patterns of RVH with base on the rate of progression to RVHF and hemodynamic parameters: the compensated (or adaptive) (cRVH) and the decompensated (or maladaptive) (dRVH) states.[41,44] In cRVH, the patients develop RVH but keep RV function, preserving the cardiac output (CO) and RV ejection fraction (RVEF), while in dRVH they rapidly develop RVHF, the CO diminishes, the RVEF and the RVSP are reduced, but the mPAP remains elevated, being sometimes associated to RV fibrosis and dilatation.[35,42,44,192,236] However, once the RV compensatory mechanisms reach the saturation point, the RV will transit from adaptive to maladaptive RVH, developing RV failure with decreased CO and diminished oxygen delivery.[44,236]

The metabolic switch from mitochondrial OXPHOS, to glycolysis that characterizes PAH is defined in the compensated phase of RVH[35,39], which is shorter than dRVH phase, and leads to a rapid alterations on RV, as functional deterioration and dilatation.[111] In this adaptive stage, mitochondria become more hyperpolarized, what drives to the suppression of mitochondria-dependent apoptosis, a decreased production of mROS, which inhibit p53 protein expression[41], and an increase in HIF-1α activity, what will trigger an increase in GLUT1 levels and, consequently, in glucose uptake.[35,39,42] The decrease in mROS may also

be a response to minimize additional sources of stress in myocardium who strives to maintain cardiac output[39], nevertheless, in RVH, an increase in mROS is enough to inhibits HIF-1α, suppressing angiogenesis[42] and the activation of ROS-dependent signalling pathways acts as a suppressor of myocardial function.[237] Along with the activation of HIF-1α during the cRVH phase, the NFAT is also activated[39], contributing to the proliferation and resistance to apoptosis characteristic of the phenotype of this disease.[238] Also the VEGF and stromal-derived factor 1 (SDF1) are activated in cRVH, contributing to the promotion of glucose uptake and angiogenesis.[35,41] An upregulation of myocyte enhancer factor 2 (Mef2) was also documented in this phase, maybe due the enhancement in its transcriptional activity during cRVH.[42] It has been verified that Mef2 gene is implicated in the regulation of several genes involved on metabolic genes of PAH, such as PDK4, GLUT4, PPARγ, PGC-1α, but also genes involved on contractility, for example α- and β-myosin heavy chain (MHC)[35,42], and angiogenic genes like VEGF[239], besides playing a role in the transition from compensated to decompensated RVH.[42] Moreover, Mef2 has been associated to miRNAS that arose as determinants of gene regulation in cardiac development and hypertrophy, as miR-208, specific from myocardium.[42,239] Once Mef2 is a target gene for GLUT4, this followed a similar pattern of expression and there has been an increase in translocation of GLUT4 to plasma membrane in cRVH, contributing to glucose uptake.[35,239] The transcription complex formed by the mediator of transcription 13 (MET13) and nuclear receptor corepressor 1 (NCoR1), MET13/NCoR1, is critical for the regulation of metabolic and angiogenic genes, but also for the regulation of Mef2 function via negative feedback loops.[239]

According with a study from Sutendra *et. al* (2014) that used an animal model of monocrotaline (MCT) for PAH, the transition from cRVH to dRVH is marked by an exponential increase in mROS, that in association with mitochondrial dysfunction drives to an increase in intracellular Ca^{2+} and Ca^{2+}- dependent signalling, as the NFAT activation pathway, inducing hypertrophy and failure.[237] The decrease of levels of VEGF, SDF1 and HIF-1α, along with the activation of p53, a protein responsible for HIF-1α signalling pathway inhibition[41], occurs a decrease on the expression of PDK, what triggrs effects on GO, mitochondrial function and angiogenesis.[35] In this phase, arterial stiffness also increases due to the increment of circulating vasoconstrictors, such as ET-1 and serotonin, what contributes to the HF state[237], being that the transition from cRVH to dRVH is also accompanied by a loss in capillary density.[195] Throughout the decompensated phase, the

Mef2 expression values start declining until they are inhibited, what contrast with the levels of TNF- that increase as the disease progresses toward RVHF.[239]

Another study documented that the miR-126 also plays a role in the pathogenicity of this disease, since it plays a regulatory role in the angiogenesis and acts by suppressing the sprouty-related protein-1 (SPRED-1) and the phosphoinositide-3-kinase regulatory subunit 2 (PIK3R2), which are two inhibitors of the VEGF signalling pathway, activating MAPK and PI3K signalling, promoting angiogenesis.[240] The expression of this miR is significantly decreased in dRVH comparatively to normal and cRVH in human samples of PAH patients, and this downregulation promotes the transition from cRVH to dRVH.[240] Moreover, the occurrence of an elevated FAO in RVH is demonstrated to be maladaptive mechanism by a study in animal models of PAH with PA banding (PAB), since the inhibition of FAO increased the ATP concentrations on RV and improved the RV function *in vivo*.[160]

5. Neuregulin-1

NRGs are a subclass of transmembrane polypeptide epidermal growth factors (EGF) expressed in several systems, that mediate cell-cell interactions in several tissues from breast to cardiovascular and nervous system.[241–243] From the four forms of NRG (NRG1, NRG2, NRG3, and NRG4), the NRG1 is the one that is known to perform cardiovascular functions and is produced by cardiac endothelium.[242,244,245] The NRG1 mRNA expression and protein synthesis is dependent of neurohormones: while ET-1 stimulates NRG1 mRNA expression, the angiotensin II and phenylephrine are responsible for NRG1 inhibition, as they are released by EC in conditions of low blood pressure, to improve cardiac output and rise peripheral resistance.[246]

NRG1 is a paracrine factor whose functioning depends on its binding to erythroblastic leukaemia viral oncogene homolog (ErbB), a family of tyrosine kinase receptors (RTK) (ErbB2, ErbB3, and ErbB4).[243] When NRG1 binds to ErbB3 or to ErbB4 induces a conformational change, allowing the dimerization with ErbB2 or ligand-activated ErbB3/ErbB4 receptors, wherein the intracellular kinase domains phosphorylate the intracellular C-terminal domain of the dimerization set.[242,244] From the receptor dimerization results homodimers or heterodimers with docking sites for several proteins, designated as

NRG1/ErbB system. The NRG1/ErbB system acts as an initiation bridge for several signalling cascades as the MAPK or PI3K/Akt pathways, whose downstream signalling mediates numerous cellular processes[241,242,244] as survival, migration, proliferation, cellular adhesion or differentiation.[242,245,247,248] NRG1 is also involved in oxidative stress reduction, in mitochondrial activity and in recovering mitochondrial function.[245]

5.1. Neuregulin-1 and signalling in regulation of glucose metabolism

Regarding to the metabolic actions of NRG1 in rat skeletal muscle cells, the chronic treatment with NRG1 improved not only oxidative metabolism through the regulation of GLUTs expression, but also mitochondrial activity through the stimulation of the expression of PGC-1α and peroxisome proliferator-activated receptor delta (PPARδ).[241] Furthermore, NRG1 is responsible for inducing the activation of Ras/Raf/MEK/MAPK cascade[241], being also accountable for the modulation of muscle metabolism through the induction of glucose uptake by the modulation of the PI3K-PDK1- protein kinase C zeta (PKCζ) pathway, in an independent manner of insulin.[172] Beyond insulin, NRGs are also responsible for inducing the translocation of GLUTs to plasma membrane in muscle cells, potentiating glucose transport and myogenesis.[241,242] In a model of breast cancer on L6E9 muscle cells from rats, the treatment with NRG1 induced the translocation of GLUT4 to the plasma membrane in a manner similar to the effect of insulin, increasing the glucose uptake.[249] Another study in L6E9 muscle cells is consistent with these findings, having further disclosed that the treatment with NRG increased GO and decreased lactate release[172], what suggests that the chronic treatment with NRG1 could regulate glucose metabolism and homeostasis by modulation of glycolysis and control of Warburg effect.

In cardiac muscle, NRG/ErbB signalling have been related with the pathophysiology of HF[250] and a deficiency in NRG1 signalling increases the likelihood for cardiac injury.[251] NRG1 prevents cardiomyocytes apoptosis through the activation of the ErbB4/PI3K/Akt pathway[242,251], what may also occur as a repair mechanism after cardiac injury[252], and also by inhibiting cytochrome c release and caspase-3 activation.[242] This effects of NRG1 on glucose uptake were assessed in an *in vitro* study, were the glucose uptake was completely abolished in situations of PI3K inhibition.[253] PI3K/Akt pathway seems to be involved in the

protection of cardiomyocytes against apoptosis, as well as regulation of metabolism and growth[98,247], and this a reason why PI3K inhibition may also trigger insulin resistance and glucose intolerance.[254]

However, NRG1 also displays effects in liver through glucose metabolism regulation. Insulin seems to inhibit the effects of NRG1 action in rat hepatocytes due to downregulation of ErbB[255] by the impairing in NRG1 to the receptor through a PI3K-dependent pathway.[256] In two animal models of insulin deficiency, type I diabetes and fasting, the liver ErbB3 expression was inhibited by insulin treatment, what suggests that insulin regulates the ErbB expression and that exists an interaction between insulin and NRG1/ErbB pathway.[257]

5.2. Role of neuregulin-1 in Pulmonary Arterial Hypertension

NRG1 is expressed and released by cardiac endothelium, whereas ErbB2 and ErbB4 receptors are expressed in cardiomyocytes[242], and once NRG1 binds to ErbB4, induces conformational changes in this receptor, that allow its dimerization with ErbB2 or with ligand-activated ErbB4.[258] Apart from their cardioprotective effects[242,245,247], via PI3K/Akt-dependent mechanism[244] and the maintenance of structural and functional integrity in the adult heart[242], NRG1/ErbB signalling is also determinant for the proper formation of the heart and cardiac conduction system[245,248], being the main responsible for the correct formation of the ventricular trabeculae.[249] Furthermore, cardiac NRG-1ß/ErbB signalling foment cardiomyocyte survival and proliferation, supporting normal cellular functions.[247]

Consistent with this notion, NRG1 administration significantly attenuated neointimal formation and vascular injury in a model of atherosclerosis.[259] In an MCT model for PAH was reported the beneficial effects of NRG1 administration in rats in conditions of myocardial stress, since it attenuates some hallmarks of PAH as neointimal hyperplasia and vascular remodelling, protecting both smooth muscle and EC but also cardiac dysfunction and ventricular dysfunction. However, the highlighted effects were the reduction of the severity of PAH and RVH, as well as the expression of genes associated with overload and hypertrophy, as ET-1 and BNP, respectively.[99]

The RVD is also correlated with a decrease in the expression of intermediaries of FAO, while RVH is related with an increase in intermediaries of FAO and in FAO itself.[160,260] Some studies showed that there is an increase in RV glucose uptake in patients and animals with RVH[192], given the switch to glycolysis that is a less energetically efficient process.[42] Furthermore, in mouse models, the NRG receptors ErbB2 and ErbB4 are expressed in response to pressure overload during compensated RVH phase, and reduce its expression in the transition to HF.[247] However, a study with in humans detected that in cases of advanced HF defined at dRVH phase, while NRG1 increases, the receptors ErbB2 and ErbB4 expression and activity is maintained reduced, enhancing the apoptotic susceptibility and death.[261]

6. Experimental models to study pulmonary hypertension

The existence of animal experimentation on living animal remounts to third and fourth centuries as described in manuscripts of Greek philosopher physicians[262] and despite not being well accepted by all clinicians in the actual times, the animal experiments provided, and still provide, a lot of important biological knowledge to our understanding of mechanisms of diseases.[263] The need for new therapeutic approaches in numerous pathophysiologies intensified research using animal models.[264] The animal model used should be selected taking into account several criteria requires background knowledge of their biological properties once they may affect the study.[265]

The different experimental approaches can be subdivided into four groups: single pathological-insult (SPI), multiple-pathological insult (MPI), knockout, and overexpression.[266] Despite numerous animal models are available to study PAH, the most performed experimental approaches are from SPI and MPI groups.[266–269] Some alternative experimental approaches are also performed and involve genetic manipulation of the animal models, commonly referred as genetically modified organisms (GMO). Some examples are the use of animals with overexpressed genes as the calcium binding proteins, as (S100A4/Mts1) or the IL-6, but also knockout animals for BMPRII[267,268] or the vasoactive intestinal peptide (VIP) that regulates the pulmonary circulation.[268] Those alternative models are also represented in the Table 2.[26]

However, even though they are very representative, the animal models still do not completely mimic the human PAH.[267] A big part of PH animal studies targeted the chronic hypoxic exposure model or the MCT PAH-induced rat model, which are SPI models.[26]

6.1. The monocrotaline model

MCT, an anti-mitotic agent[270], is an 11-membered macrocyclic pyrrolizidine alkaloid extracted from the seeds of the plant *Crotalaria spectabilis*, who is used to induce PAH in rats (Figure 4).[268,270,271] This substance requires prior activation for the reactive form of pyrrole metabolite dehydromonocrotaline (MCTP), that occurs in the liver, and whose reaction is dependent on cytochrome *P*-450 (Figure 5).[267,268,270,271] This model is one of the most accomplished models due to its technical simplicity, high reproducibility and because it has lower costs associated.[268,271]

Figure 4 ***Crotalaria spectabilis.*** Plant that produces the seeds from which the monocrotaline (MCT) compound is extracted.

MCT can be administered by a single subcutaneous or intraperitoneal injection, that induces maladaptive RVH[224], causes vascular injuries[267] associated to severe ischemia, PH[224], and widespread pneumotoxicity.[272] This model recapitulates many other features of human IPAH in 3–4 weeks after MCT injection[270,271], such as the EC apoptosis and disruption, oxidative stress[271], and genetic modulation of the BMPRII, Smad3,4, TGF-β receptors and activin receptor-like type 1 (ACVRL1) genes.[266,271] MCT induces pulmonary arterial medial hypertrophy through the proliferation of PASMC ant their resistance to apoptsis[266,271], adventitial thickening, caused mainly by accumulation of inflammatory cells in adventitial in the early stages of the development[266,267], and obstructive pulmonary vascular remodelling[224,266,271] which are accompanied by changes in PA pressures (Figure 5).[267,270] Despite causing RVH and RVD as a consequence of pressure overload[224,268,270],

what helps the scientific community to understand better the mechanisms of pulmonary vascular remodelling and its pathophysiology[266], this model has some side effects once it induces pathological changes in lungs, as interstitial pulmonary fibrosis in mice[270] and pulmonary oedema[273], triggers the development of myocarditis in both RV and LV[267,268], fails in the induction of plexiform lesions[270] and is also involved in hepatotoxicity development[266,267], what difficult the study of RVH and RVHF.[267]

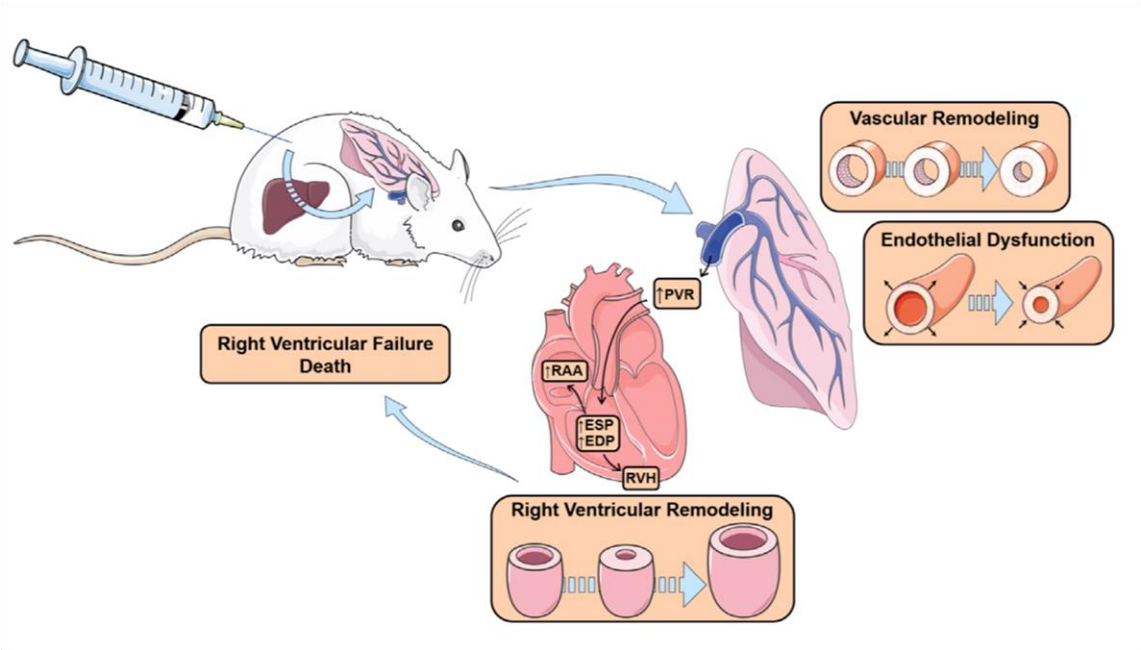

Figure 5 Effects of monocrotaline (MCT)-induced pulmonary arterial hypertension (PAH) in rat. The MCT reproduces the effects of PAH in cardiorespiratory system, as the increase in pulmonary vascular resistance (PVR) provoked by the vascular remodelling of pulmonary artery (PA), the increase in right atrial area (RAA) due the right ventricle remodelling, what may culminate in right ventricular hypertrophy (RVH) and right heart failure and death. ESP: end-systolic pressure; EDP: end-diastolic pressure. Adapted from Santos-Ribeiro, D. *et al.* 2016. *"Pulmonary arterial hypertension: Basic knowledge for clinicians"*.

6.2. The hypoxia model

The chronic hypoxia is frequently used to induce PH through the exposition of the animals to hypoxic conditions in hyperbaric chambers.[268] The hypoxic model in rats is only performed to study less severe PH, not for PAH, but this does not make it unfeasible for its value, once this method is very predictable and reproducible within a selected animal strain.[267,268] Nevertheless, while the vascular remodelling observed is smooth[267,268], the PH developed is associated with de muscularization of small arterioles and the increase in the

expression of α-SMA in non-muscularized arterioles[268,272] due to hypertrophy and/or moderate hyperplasia SMC.[272] It also results in EndMT[268], RV hypertension and hypertrophy, not reaching HF[267,268], what leads to an increase in mPAP and in structural changes in pulmonary vasculature, which are followed by an influx of inflammatory cells.[268,272] However, the developed condition may return to the normal phenotype if the animal is subjected to an environment of normoxia.[269]

The shortcomings that come from this model are the fact that it does not represent the pulmonary vascular damage as it is observed in human PH[266] and it fails in the generation of non-reversible intimal fibrosis or plexiform lesions as those that occur in human PH.[267]

6.3. The hypoxia/Sugen model

Another animal models which combines more than one procedure, designated by MPI, can be performed.[267] One example of this type of experimental approach is the Hypoxia/Sugen5416 model, a model for severe PAH[268], that combines Sugen5416, a VEGF inhibitor, and exposure to chronic hypoxia.[274] This model allows a better understanding not only on etiologic mechanisms that cause EC hyperproliferation and plexiform lesions formation in human PAH[268] but also the study the angioproliferative characteristics of PH and hemodynamic changes.[266] SU5416 by himself causes smooth PH and pulmonary vascular remodelling, but when associated to chronic hypoxia, their effects are irreversible PH associated with precapillary arterial endothelial proliferation, SMC proliferation[268], and the animals develop sustained and progressive PH.[269] Due the progressive nature of this model and its ability to reproduce key pathophysiological features from human PAH, it is used to evaluate new treatments for PAH.[268]

7. Aims of the study

Based on the published findings described in the previous sections, this study aimed to contribute to the study of the impact of chronic treatment with NRG1 on the metabolic changes that occur in the development of PAH. We believe that the beneficial effects of chronic treatment with NRG1 in PAH could be associated with the modulation of glycolytic metabolism.

According to the results obtained in our previous studies in this area, in this thesis we aimed to explore the potential involvement of NRG1 in systemic and cellular glucose homeostasis as well as in the regulation of the effect of Warburg at the cellular level.

Our specific goals are:

- To determine the expression of GLUT1 and 4 in different PAH animal models and establish correlations between their expression with parameters of cardiac function and disease markers;
- To evaluate the effects of chronic exposure to NRG1 on GLUT1 and GLUT4 expression in animal models of PAH;
- To determine whether chronic NRG1 administration affects blood glucose homoeostasis and regulates insulin receptors in animal models of PAH;
- To evaluate and correlate the expression of glycolysis genes in RV with parameters of cardiac function in PAH;
- To evaluate the effects of chronic exposure to NRG1 and determine the changes induced by rhNRG1 treatment in glycolysis genes in two animal models for PAH.

Materials and Methods

All the procedures in this work followed the recommendations of the Guide for the Care and Use of Laboratory Animals, published by the US National Institutes of Health (NIH Publication No. 85-23, Revised 1996), and are accredited by the Portuguese Direção Geral de Alimentação e Veterinária (DGAV) and approved by Fundação para a Ciência e a Tecnologia (FCT PTDC/SAU-FCT/100442/2008; IMPAcT-PTDC/MED-FSL/31719/2017).

1.Animal models

1.1.MCT model

Male Wistar rats (Rattus Norvegicus Albinus, Rodentia, Mammalia) (Charles River Laboratories, Barcelona, Spain), weighting 180-200g and seven- to eight-week-old, were randomly assigned to receive either a subcutaneous injection of 60mg/kg of body weight (BW) of MCT (Sigma Aldrich, Missouri, EUA) or an equivalent volume of vehicle (0.9% NaCl). Fourteen days after the first injection, when the animals that received MCT have developed PAH, they were again randomly assigned into four subgroups according to pharmacological treatment that consisted on a daily intraperitoneal injection of 40μg/kg of BW of recombinant human NRG1 (rhNRG1) (Peprotech, Hamburg, Germany) for 7 days, while the vehicle treatment consisted of 0.1% bovine serum albumin (BSA) (Sigma Aldrich, Missouri, EUA) intraperitoneal injection for 7 days. Were defined four groups of animals: control (CTRL) (animals without PAH and without pharmacological treatment, n=10); MCT (animals with PAH and without pharmacological treatment, n=20); MCT+rhNRG1 (animals with PAH and with pharmacological treatment, n=15); CTRL+rhNRG1 (animals without PAH and with pharmacological treatment, n=4). Animals were grouped three per box, in a controlled environment, with a light-darkness cycle of 12:12h, controlled temperature at 22ºC, and water and food *ad libitum*.

1.2. Sugen/hypoxia model

Male Wistar rats (Rattus Norvegicus Albinus, Rodentia, Mammalia) (Charles River Laboratories, Barcelona, Spain), weighting 200-230g were placed in a ventilated chamber

(Biospherix, Lacona, USA) for up to 21 days and maintained in either normoxic conditions (21% O_2) or exposed to normobaric hypoxia (10% O_2) for three weeks. Sugen 5416 (SU5416), a VEGF inhibitor, was diluted in dimethyl sulfoxide (DMSO) and administered (20mg/kg, s.c.) by injection on the first day prior to hypoxia exposure. Three weeks after hypoxia, animals were placed in normoxia conditions for 2 weeks. The three groups of animals defined were normoxia (N) (animals in normoxic condition with vehicle (DMSO), n=2); normoxia/Sugen5416 (N/S) (animals in normoxic condition with Sugen5416, n=2) hypoxia (H) (animals in hypoxia condition with vehicle, n=3); and hypoxia/Sugen5416 (H/S) (animals in hypoxia condition with Sugen5416, n=4).

Another different work was performed, following the same model, hypoxia/Sugen5416, but with an additional treatment with rhNRG1, that begun on week 6, after hypoxia and normoxia exposition and that lasts for 2 weeks. The treatment consisted on a daily intraperitoneal injection of 40µg/kg of BW of rhNRG1 (Peprotech, Hamburg, Germany) for 2 weeks, while the vehicle treatment consisted of 0.1% BSA (Sigma Aldrich, Missouri, EUA) intraperitoneal injection for 2 weeks. From this work resulted two groups of animals: the hypoxia/Sugen5416 H/S) (animals in hypoxia condition with Sugen5416, n=5) and the hypoxia/Sugen5416 treated with rhNRG1 (H/S+rhNRG1) (animals in hypoxia condition with pharmacological treatment, n=5).

In both works, animals were grouped three per box, in a controlled environment, with a light-darkness cycle of 12:12h, controlled temperature at 22ºC, and water and food *ad libitum*.

2. Echocardiographic evaluation

Before starting the protocols, a transthoracic echocardiographic evaluation was performed to allow a basal evaluation to compare experimental groups and to prevent the inclusion of potential ill animals (cardiac pathology or other). At the end of the protocols, the animals were submitted again to transthoracic echocardiographic evaluation to confirm and define the degree of disease development.

Before the echocardiography the BW of each animal was checked, and posteriorly, rats were anaesthetized by inhalation of sevoflurane (8%) SevoFlo® lot 6055792 (Abbott,

Berkshire, United Kingdom) in O_2. Then, animals were orotracheally intubated and mechanically ventilated. Anaesthesia was maintained with sevoflurane (1-2.5%) titrated according to the toe-pinch reflex. Rats were placed in left lateral decubitus on the heating pad (temperature maintained at 38ºC) and the skin was shaved and depilated. After applying warm echocardiography gel, a 15MHz sensorial probe Sequoia 15L8W (Siemens, Erlangen, Germany) was gently placed on the thorax. The echocardiographic evaluation was performed with an Acuson Sequoia C512 ultrasound system (Siemens, Erlangen, Germany) and acquisitions were averaged from three consecutive heart beats.

Bi-dimensional and M-mode images were obtained, in short axis of LV at the papillary muscle level. In apical projection of 4 and 5 cavities, after previous acquisition of bi-dimensional image, tricuspid valve flow and pulmonary valve flow, were evaluated by conventional Doppler. Right atria area was evaluated in the 4-chamber view and tricuspid annular plane systolic excursion (TAPSE) in M-mode following alignment of the gate to the tricuspid valve. The right ventricular inner diameter in diastole (RVIDd) was assessed in 4-chamber view projection on tricuspid valve and measured as the distance from the right ventricular free wall to the interventricular septum.

The PA flow was measured with pulsed-wave Doppler positioned within the main PA at a distal plan from the pulmonary valve and parallel to the flow, allowing the acquisition of pulmonary arterial acceleration time (PAAT), the interval of blood flow time from the start to the peak velocity, pulmonary arterial ejection time (PAET), from the start to the cessation of flow[275] to determine the PAAT/PAET ratio, and PA velocity-time integral (PAVTI). CO and cardiac index (CI) were also calculated.[276]

3. Morphometric analysis and sample collection

After the echocardiographic evaluation, the animals were euthanized with overdose of the anesthetizing substance and immediately exsanguinated. Posteriorly, heart and lungs were excised and was performed a morphometric evaluation of the organs, were it was assessed the weights of the lungs, heart, LV + septum (LV+S), RV, soleus and gastrocnemius muscles. Tibial length (TL) was also achieved and used for normalization, once tibia is not affected by the presence or absence of the pathological lesions resulting from MCT during the lifetime of the rat, being this parameter independent of the other changes that occur in

body weight.[277] Tissue samples from different organs were collected, snap frozen in liquid nitrogen and stored at -80ºC. The samples collected to molecular biology studies, as gene expression studies by mRNA quantification, were obtained from organ fragments, such as lung, RV, soleus muscle and gastrocnemius muscle and stored with RNA stabilizing reagent RNA*later* (Qiagen, Hilden, Germany) to prevent tissue and genetic material degradation.

4. Oral glucose tolerance tests

Oral glucose tolerance tests (OGTT) were performed to evaluate whole-body glucose tolerance *in vivo*. Rats were fasted overnight (12 hours) and OGTTs was performed through glucose loading by gastric gavage (2g/kg BW). Blood glucose levels were determined using a FreeStyle Precision system glucometer (Abbott, Berkshire, United Kingdom) at the time of glucose loading (0), and then at 15, 30, 60, 90 and 120 minutes after loading.

5. Gene expression studies

5.1. Total RNA extraction

The total RNA was isolated from the different tissues through the phenol–chloroform extraction method with NZYol® ref MB18501, lot 14031 (Nzytech, Lisboa, Portugal) and TripleXtractor ref GB23.0050, lot 7E20109A (GRiSP, Porto, Portugal) with 1.4mm zirconium oxide beads ref KT03961-1-103.BK, lot160811-890 (Precellys, Montigny-le-Bretonneux, France) following the Protocol 1 in Appendix section.

5.2. Total RNA quantification and quality assessment

Concentration and purity of RNA were evaluated using the NanoDrop® ND-2000 spectrophotometer (Thermo Fisher Scientific, Wilmington, DE, USA). The purity of the mRNA was evaluated by the A260/A280 ratio obtained from spectrophotometry analysis. Only the samples with ratio between 1.8 and 2.1 were considered suitable for molecular studies.

5.3. Total RNA electrophoresis

To verify the presence of genomic DNA, samples were loaded in a 1% agarose gel and run at 70V for 1 hour. The gel was scanned with ChemiDoc™ XRS$^+$ Imaging System (Bio-Rad Laboratories Inc., Hercules, California, USA) and analysed with equipment software, Image Lab™ (Bio-Rad Laboratories Inc., Hercules, California, USA).

5.4. mRNA reverse transcriptase

The mRNA relative expression quantification was performed by two-step RT-qPCR. The first step, the reverse transcription, was performed in a conventional thermocycler (Biometra, Göttingen, Germany) with the SensiFast™ cDNA synthesis kit lot RA653-B051360 (Bioline, London, United Kingdom) following the protocol and PCR program recommended by the kit manufacturer, that consisted in denaturation for 10 minutes at 25ºC, annealing for 15 minutes at 42ºC, and extension for 5 minutes at 85ºC.

5.5. RT-qPCR

From each sample obtained from reverse transcription, 1µl (50ng) was amplified and detected by RT-qPCR equipment StepOne™ (Applied Biosystems, California, USA) in MicroAmp® Fast 96-Well Reaction Plates (0.1mL) ref 4346907 (Applied Biosystems, California, USA), using the probe SYBR Green SensiFast™ Hi-ROX Kit lotSF576-B048530 (Bioline, London, United Kingdom) according with the manufacturer instructions. Gene analysis expression to understand the metabolic alterations observed in PAH was divided into three categories according to gene function: biomarkers for PAH (HIF-1α, ET-1 and BNP), genes who intervein on glucose metabolism (GLUT1, GLUT4, HK1, HK2, muscle type PFK (PFKm), muscle type PK (PKm), LDHa, LDHb, LHDc, LDHd, PDHa1a and PDHb), insulin receptors (IRS1 and IRS2) genes involved in mitochondrial function (PGC-1α, NRF1, Sirt1 and Tfam).

Using RV, skeletal muscle, lung and soleus muscle samples from the CTRL groups, standard curves were built to each target gene, correlating the initial total cDNA quantity and the threshold cycle with the values of each sample. To perform the standard curves for

each gene, we have prepared 7 dilutions with different concentrations of cDNA template (400, 200, 100, 50, 25, 12.5 and 6.25 ng) from a control sample, that we know to express the gene of interest and the we determined their threshold cycle values. Amplification curves were analysed with StepOne™ software version 2.3 (Applied Biosystems, California, USA), through absolute quantification. Melting curves of each PCR reaction were used to exclude the formation of primer-dimers and unspecific products, confirming the purity of the amplified product. Glyceraldehyde 3-phosphate dehydrogenase (GAPDH), a housekeeping gene, was chosen as reference gene, since no significant changes were observed between the different groups. Gene expression results were presented in Arbitrary Units (AU), being the CTRL group means values after GAPDH normalization correspondent to 1AU. The primers used in the molecular analysis (see Table 3) were designed in-house with the appropriated software, Oligo Analyzer 3.1 (Integrated DNA Technologies, Inc., California, USA).

6. Statistical analysis

Statistical analysis was performed using *GraphPad Prism 7* (GraphPad Software, San Diego, CA). Two-way ANOVA with Tukey's post-test was used to statistically analyse echocardiographic and molecular parameters, which followed a normal distribution. One-way ANOVA nonparametric analysis of variance with Tukey's post-test was used for mRNA analysis in hypoxia model. Correlations were determined using Pearson correlation tests. Group data are presented as means ± SEM. Only differences with $p<0.05$ were considered statistically significant.

Results

1. Metabolic changes in the development of pulmonary arterial hypertension in MCT model - Effects of the treatment with Neuregulin-1

1.1. Characterization of the MCT model

a. Evaluation of disease markers

The MCT animal group was divided into two subgroups according to their RVEF and ventricular functioning (Figure 6A): (i) compensated right ventricular function (CRV), that displayed an EF above of 35% with preserved ejection fraction despite the RVH, and (ii) with decompensated right ventricular function (DRV) characterized by exhibiting EF values below 35%, being the decrease in EF a characteristic of HF.[278] The transition point between compensated and decompensated animals defined as 35% was determined with base in the hemodynamic, morphological and clinical analysis performed. A significant difference on EF was found between the CTRL group (C) and both with CRV and DRV, reflecting the disease state as being more evolved in the DRV group.

The evaluation of mRNA expression in the RV showed a significant increase in mRNA expression of the main cardiac disease markers in DRV groups comparing to both CTRL and CRV groups: HIF-1α, an indicator for hypoxia[122] (Figure 6B); ET-1, an indicator for overload and hypertrophy[279] (Figure 6C); and BNP, an indicator for myocardial stress, overload , injury and hypertrophy[86] (Figure 6D).

b. Evaluation of GLUT1 and GLUT4 expression

In both MCT groups has occurred a significant increase in GLUT1 mRNA expression, being this increase incremented in DRV group when compared with CTRL and CRV groups (Figure 7A). Conversely, GLUT4 mRNA expression was significantly decreased in DRV group in comparison with CTRL group (Figure 7B).

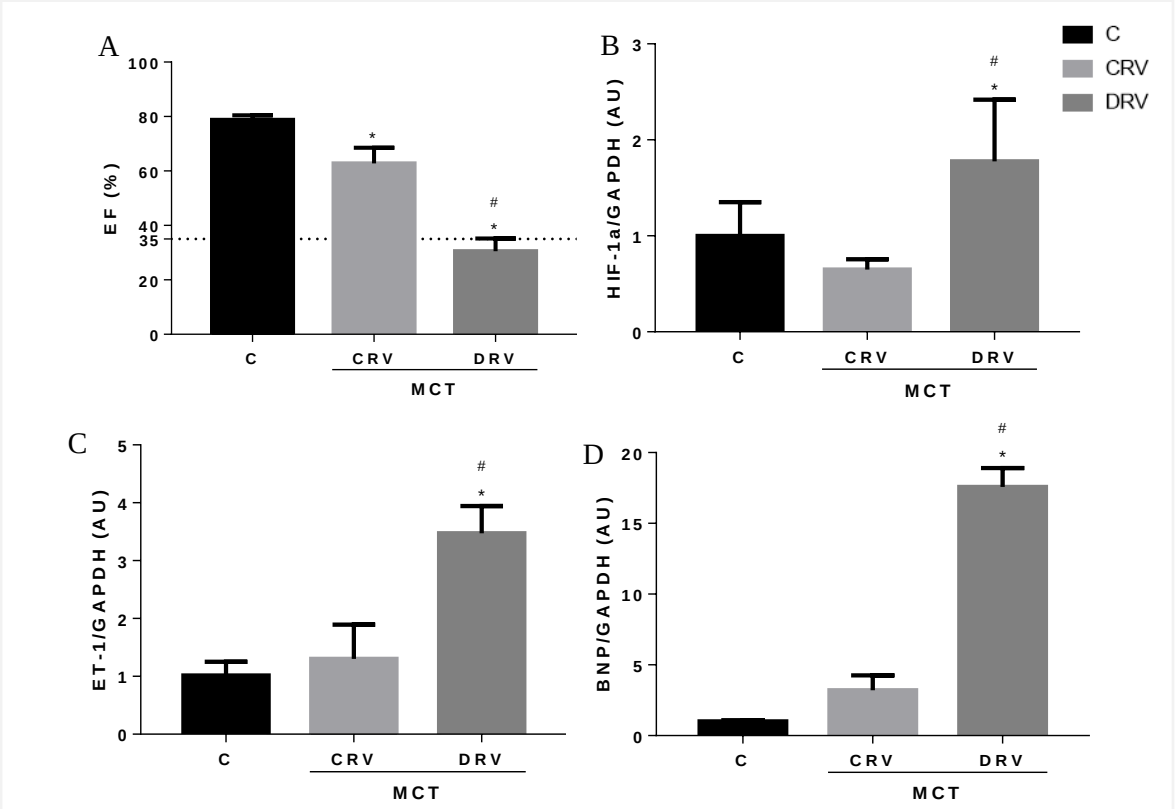

Figure 6 Alterations on ejection fraction (EF) and in the gene expression of disease markers are clearly evidenced in the RV from MCT model of PAH. C: control group; CRV: compensated right ventricular function group; DRV: decompensated right ventricular function group; GAPDH: glyceraldehyde 3-phosphate dehydrogenase; HIF-1α: hypoxia inducible factor 1α; ET-1: endothelin-1; BNP: brain natriuretic peptide.
Bars represent mean ± SEM of 10 rats per control group and 20 rats per MCT group. *P<0.05 vs. C; #P<0.05 vs. CRV. Two-way ANOVA analysis of variance with Tukey's posttest was used for all the parameters presented.

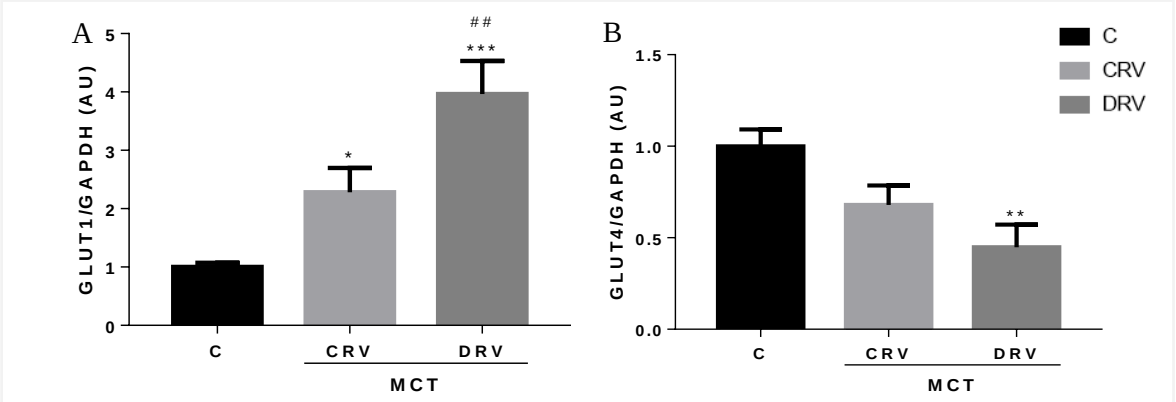

Figure 7 RV alterations on glucose transporters (GLUTs) 1 and 4 gene expression are evidenced in MCT model of PAH. C: control group; CRV: compensated right ventricular function group; DRV: decompensated right ventricular function group; GAPDH: glyceraldehyde 3-phosphate dehydrogenase.
Bars represent mean ± SEM of 10 rats per control group and 20 rats per MCT group. *P<0.05 vs C; **P<0.01 vs C; *** P<0.001 vs C; ## P<0.01 vs CRV. Two-way ANOVA analysis of variance with Tukey's posttest was used for all the parameters presented.

c. GLUT1 and GLUT 4 correlation with markers of disease

The correlation between the GLUT1 and GLUT 4 expression in DRV group and markers of cardiac disease was also determined. The ejection fraction values correlate negatively with mRNA levels of GLUT1 ($r = -0.8465$, $p<0.001$) (Figure 8A). We also found a positive correlation between RV GLUT1 and HIF-1α mRNA expression ($r = 0.7622$, $p<0.001$) (Figure 8B).

Unlike GLUT1, the GLUT4 mRNA expression was positively correlated with EF ($r = 0.5043$, $p<0.05$), once both decrease as the disease progresses (Figure 8C). GLUT4 mRNA expression is also related with the expression of BNP ($r = -0.6832$, $p<0.001$) (Figure 8D) and ET-1 ($r = -0.6127$, $p<0.01$) (Figure 7E).

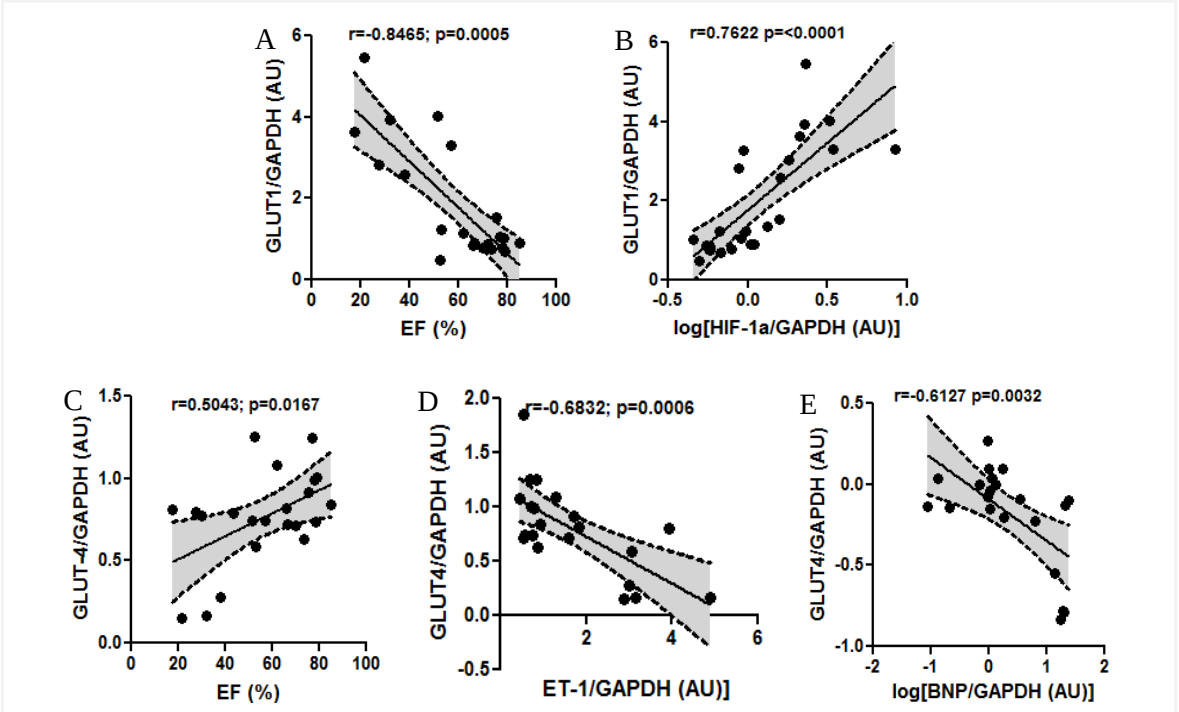

Figure 8 The gene expression of RV glucose transporters 1 and 4 (GLUT1 and GLUT4) in MCT-induced PAH animals is correlated with markers of cardiac disease. GAPDH: glyceraldehyde 3-phosphate dehydrogenase; EF: ejection fraction; HIF-1α: hypoxia inducible factor 1α; ET-1: endothelin-1; BNP: brain natriuretic peptide.
Data used for the correlation analysis were obtained from animals that had both echocardiographic and mRNA analysis. Correlations were determined using Pearson correlation test.

1.2. Effects of the chronic treatment with Neuregulin-1

a. Morphometric characterization of MCT model

MCT-induced PAH resulted in a decrease of BW of the diseased animals in comparison with CTRL animals (CTRL-BSA: 272.4±28.89g; MCT-BSA: 240.24±13.86g) (Figure 9A), however, the treatment with rhNRG1 did not attenuated the weight loss significantly (MCT-rhNRG1: 241.88±14.77g). Furthermore, Fulton index calculated trough morphological parameters evaluated (RV/LV+S) and which is an indicator for RVH[280,281], was significantly increased in PAH-induced group, having been markedly attenuated by the treatment with rhNRG1 (Figure 9B). The Lung/TL ratio (Figure 9C), allows to verify the existence of pulmonary oedema[99], was also reduced by the rhNRG1 treatment when comparing with MCT group. The MCT animals also presented greater values of RV/TL ratio, which is also an indicator of RVH[277], being this increase attenuated in MCT-treated animals (Figure 9D).

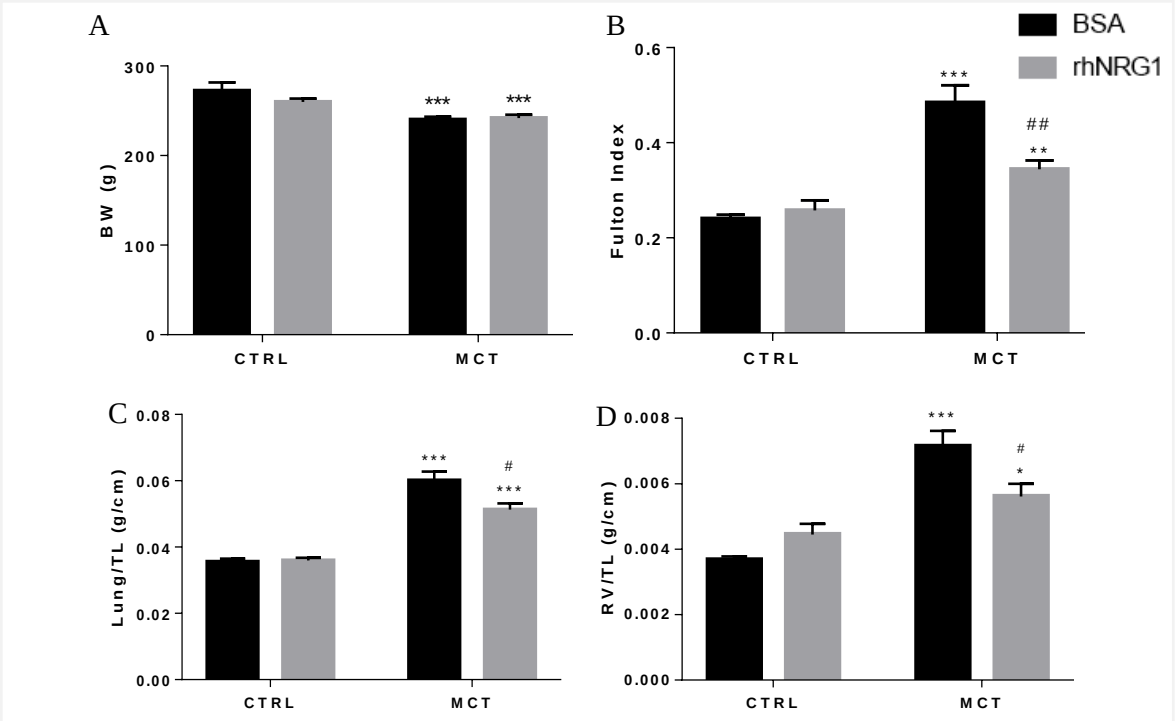

Figure 9 rhNRG1 treatment attenuated right ventricle (RV) and lung remodelling in MCT-induced PAH. BW: body weight; TL: tibial length.
Bars represent mean ± SEM of 10 rats per CTRL+BSA group, 20 rats per MCT group and 15 rats per MCT+rhNRG1 group for the morphometric data. *P<0.05 vs. CTRL-BSA; **P<0.01 vs CTRL-BSA; ***P<0.001 vs. CTRL-BSA; #P<0.05 vs. MCT-BSA; ##P<0.01 vs. MCT-BSA. Two-way ANOVA analysis of variance with Tukey's posttest was used for all the parameters presented.

b. Echocardiographic characterization of MCT model

MCT-induced PAH resulted in a significant decrease in PAVTI in MCT animals (Figure 10A), that represents a decrease in velocity-time integral of blood flow in PA, almost normalized by rhNRG1 to control values, indicting a restoring on pulmonary circulation on rhNRG1 treated animals. PAAT/PAET ratio varies with RV dilatation and RVH, and since PAH animals presented altered PA flow, the PAAT/PAET ratio significantly decreased in MCT animals in comparison to CTRL animals (Figure 10B), being this decrease also attenuated by rhNRG1 treatment. The assessment of RVIDd revealed the existence of dilatation in RV of MCT-induced PAH animals, as it is characteristic of this pathology[34], with rhNRG1 treatment reverting the dilatation (Figure 10C). MCT animals presented a significant decrease on TAPSE, an indicator of RVD[281] related with the RV contractility capacity[249] (Figure 10D).

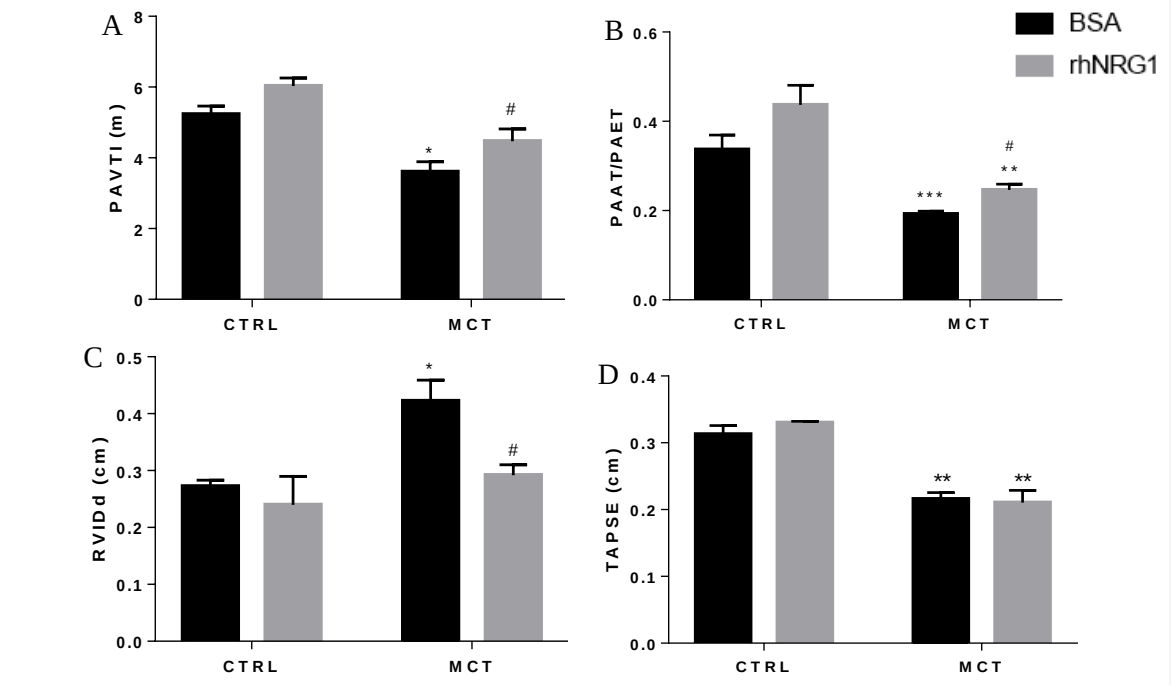

Figure 10 rhNRG1 treatment improves pulmonary flow and right ventricle (RV) structural changes in MCT-induced PAH. CTRL: control group; MCT: monocrotaline group; PAVTI: pulmonary artery velocity time integral; PAAT: pulmonary artery acceleration time; PAET: pulmonary artery ejection time; RVIDd: right ventricle inner diameter during diastole; TAPSE: tricuspid annular plane systolic excursion.
Bars represent mean ± SEM of 10 rats per CTRL+BSA group, 20 rats per MCT group and 15 rats per MCT+rhNRG1 group for the morphometric data. *P<0.05 vs. CTRL-BSA; **P<0.01 vs. CTRL-BSA; ***P<0.001 vs. CTRL-BSA; #P<0.05 vs. MCT-BSA. Two-way ANOVA analysis of variance with Tukey's posttest was used for all the parameters presented.

1.3. Evaluation of the effects of the administration of Neuregulin-1 on systemic glucose metabolism

a. Oral glucose tolerance test

There were no significant differences in fasting plasma glucose when comparing MCT with CTRL group (Figure 11A). When compared with CTRL animals, MCT animals presented a tendency to higher blood glucose concentrations for the time points between 60 and 120 min, but this increase was not significant (Figure 11B). There is also a tendency for higher postprandial glucose concentrations in MCT animal group when compared with CTRL animals, as we can see by the area under the curve (AUC) (Figures 11B and 11C).

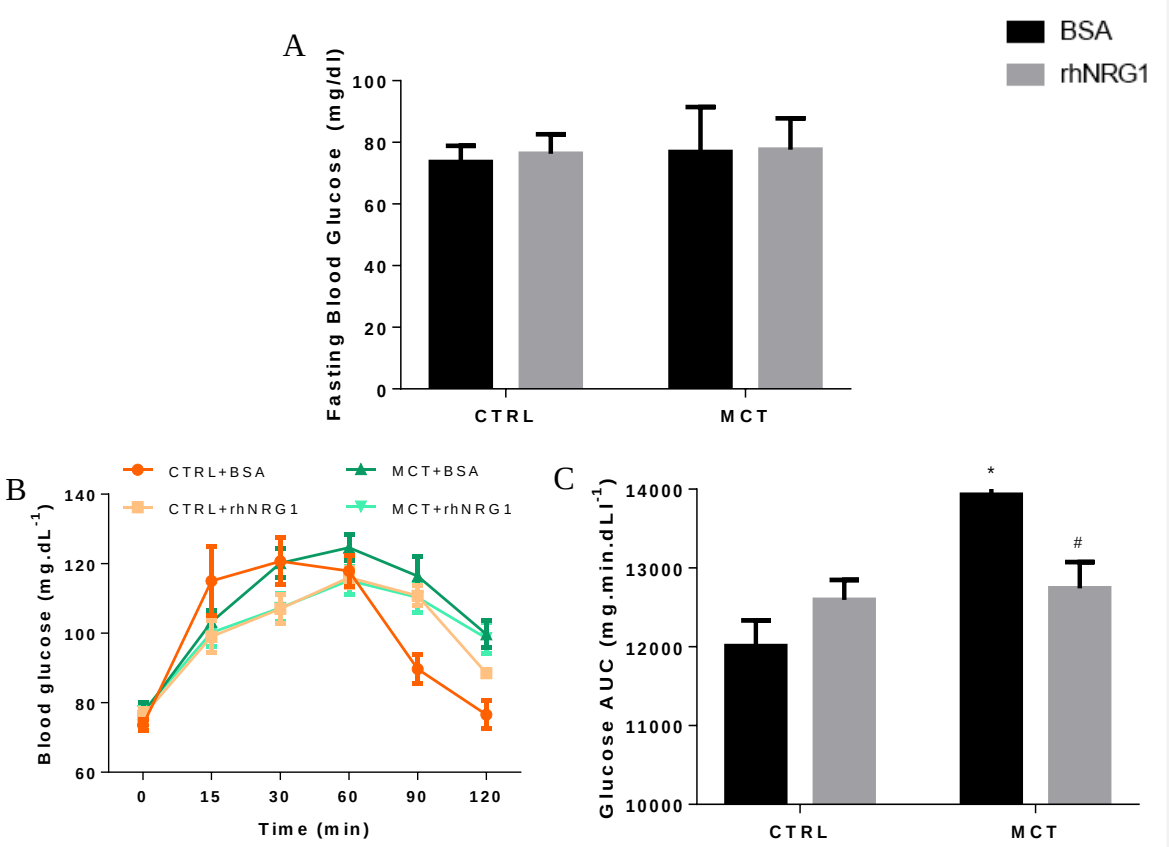

Figure 11 rhNRG1 attenuated whole-body glucose tolerance in MCT-induced PAH animals. CTRL: control group; MCT: monocrotaline group; AUC: area under the curve.
Bars represent mean ± SEM of 10 rats per CTRL+BSA group, 20 rats per MCT group and 15 rats per MCT+rhNRG1 group for the OGTT. *p<0.05 vs CTRL+BSA; #p<0.05 vs MCT+BSA. Two-way ANOVA analysis of variance with Tukey's posttest were used for all the parameters presented.

b. Evaluation of IRS1 and IRS2 expression

1. Insulin receptor substrate mRNA expression in soleus muscle

The IRS, mediators of insulin signalling[230] and glucose uptake[229], presented variations on the expression in soleus muscle. MCT-induced PAH group presented a significant decrease in IRS1 mRNA expression when compared with CTRL-BSA group, as well as the rhNRG1 treated MCT group (Figure 12A). A significant decrease in IRS2 mRNA expression also occurred in MCT-BSA group when compared with CTRL-BSA group of animals (Figure 12B).

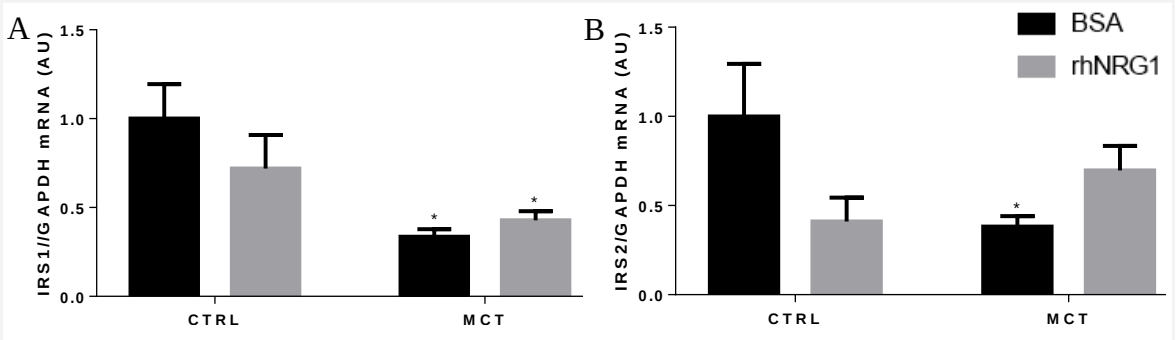

Figure 12 Alterations on insulin receptors substrate (IRS) 1 and 2 are evidenced in soleus muscle from animals in MCT model of PAH. CTRL: control group; MCT: monocrotaline group; GAPDH: glyceraldehyde 3-phosphate dehydrogenase. Bars represent mean ± SEM of 10 rats per CTRL+BSA group, 20 rats per MCT group and 15 rats per MCT+rhNRG1 group. *P<0.05 vs CTRL-BSA. Two-way ANOVA was used for all the parameters presented.

2. Insulin receptors substrate mRNA expression in RV

No significant changes were observed in both IRS1 (Figure 13A) and IRS2 (Figure 13B) expression in the RV from the different experimental groups.

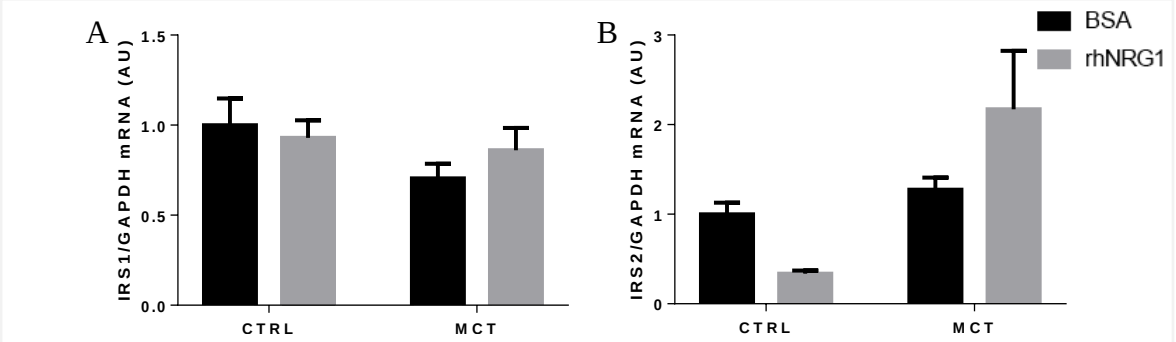

Figure 13 Alterations on insulin receptors 1 and 2 (IRS 1 and 2) were not evident in right ventricle (RV) from animals in MCT model of PAH. CTRL: control group; MCT: monocrotaline group; GAPDH: glyceraldehyde 3-phosphate dehydrogenase. Bars represent mean ± SEM of 10 rats per CTRL+BSA group, 20 rats per MCT group and 15 rats per MCT+rhNRG1 group. Two-way ANOVA was used for all the parameters presented.

1.4. Study of gene expression from the glycolytic pathway

a. mRNA expression on soleus muscle

In this tissue, no significant changes were observed in the expression of GLUT1 (Figure 14A), GLUT4 (Figure 14B) or HIF-1α (Figure 14C) of the four different experimental groups.

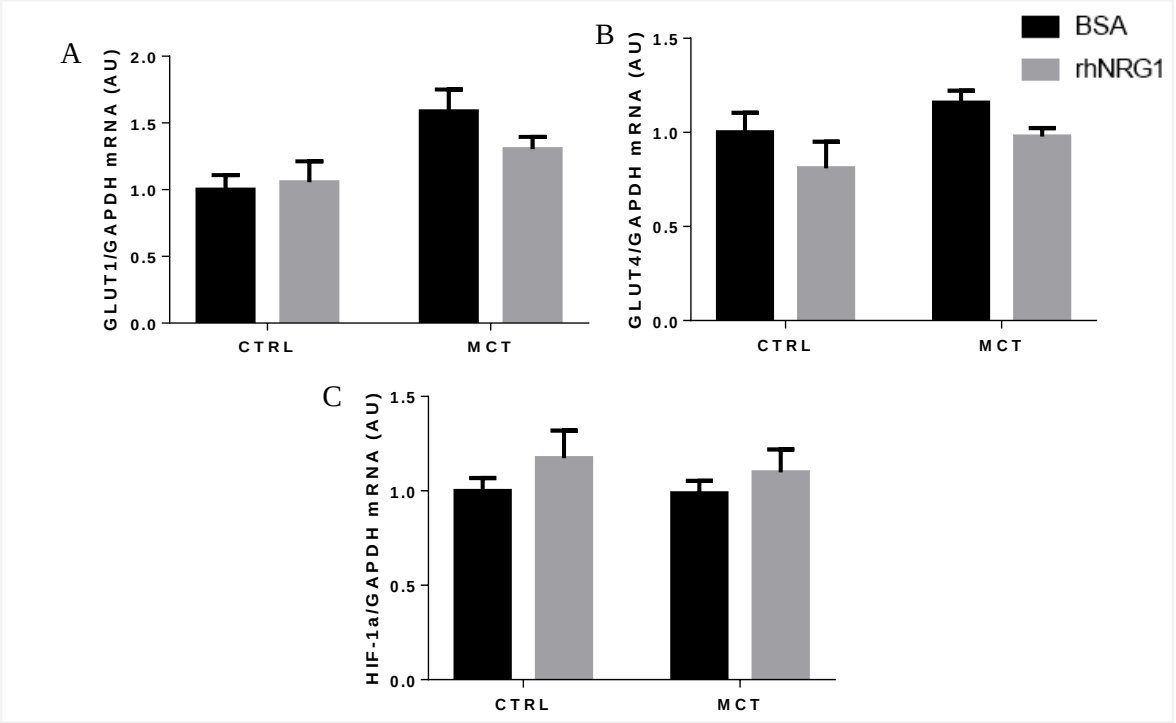

Figure 14 No alterations on glucose transporters (GLUT) 1 and 4 and hypoxia inducible factor 1α (HIF-1α) have been evidenced in soleus muscle of MCT-induced PAH animals. CTRL: control group; MCT: monocrotaline group; GAPDH: glyceraldehyde 3-phosphate dehydrogenase.
Bars represent mean ± SEM of 10 rats per CTRL+BSA group, 20 rats per MCT group and 15 rats per MCT+rhNRG1 group. Two-way ANOVA was used for all the parameters presented.

The first enzymes to act during glycolysis are HKs; the mRNA from HK1 did not presented expression alterations between the groups in this tissue (Figure 15A). However, the treatment with rhNRG1 attenuated the expression of HK2 mRNA and significantly reduced its gene expression in comparison with the MCT-induced PAH non-treated animals (Figure 15B). No differences were noticed in mRNA expression of PFKm, involved in the production of fructose 1,6-phosphate an allosteric activator of PK, between CTRL and MCT-induced PAH groups (Figure 15C). The PKm, which is involved in the formation of pyruvate

when activated by PFK, followed the same pattern of expression of PFKm, with no expression alterations between the experimental groups studied (Figure 15D).

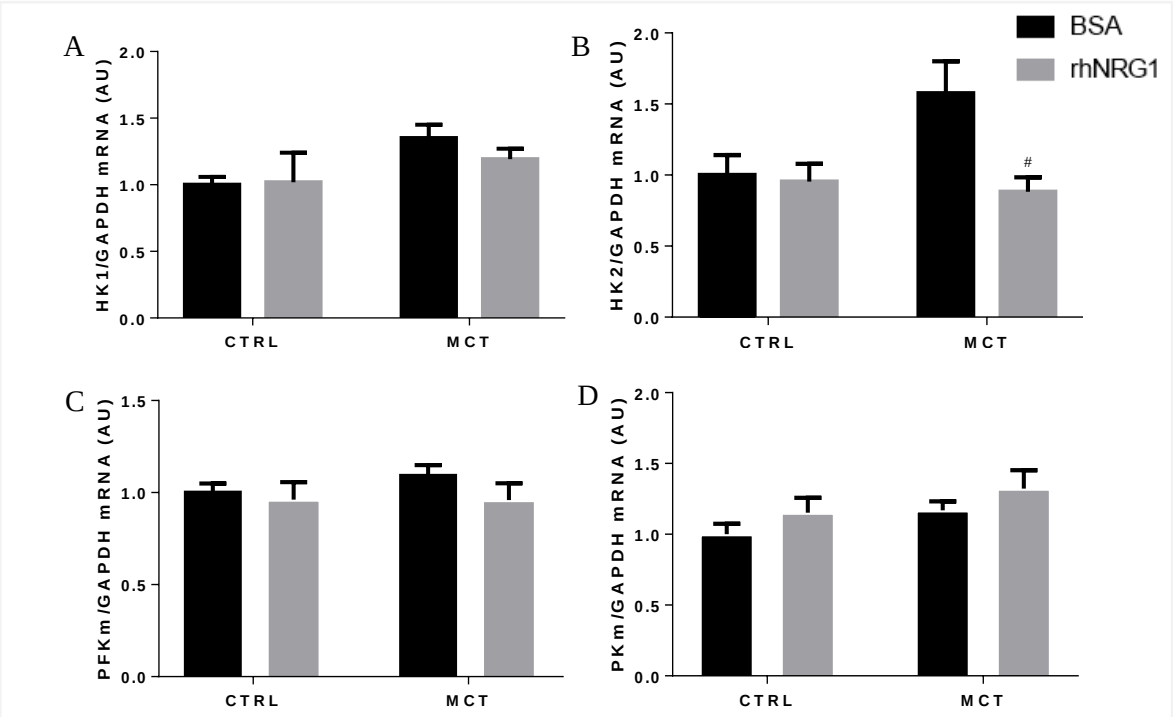

Figure 15 rhNRG1 attenuated the overexpression of hexokinase 2 (HK2) in soleus muscle of MCT-induced PAH animals. CTRL: control group; MCT: monocrotaline group; PFKm: muscle type phosphofructokinase; GAPDH: glyceraldehyde 3-phosphate dehydrogenase; PKm: muscle type pyruvate kinase.
Bars represent mean ± SEM of 10 rats per CTRL+BSA group, 20 rats per MCT group and 15 rats per MCT+rhNRG1 group. Two-way ANOVA was used for all the parameters presented.

mRNA expression of each subunit of LDH complex, which is involved in lactate production, was evaluated. No significant changes were found in the expression of mRNA from LDHa (Figure 16A), LDHc (Figure 16C) or LDHd (Figure 16D) subunits. However, the treatment with rhNRG1 significantly decreased LDHb mRNA expression (Figure 16B) in soleus muscle from MCT-induced PAH animals.

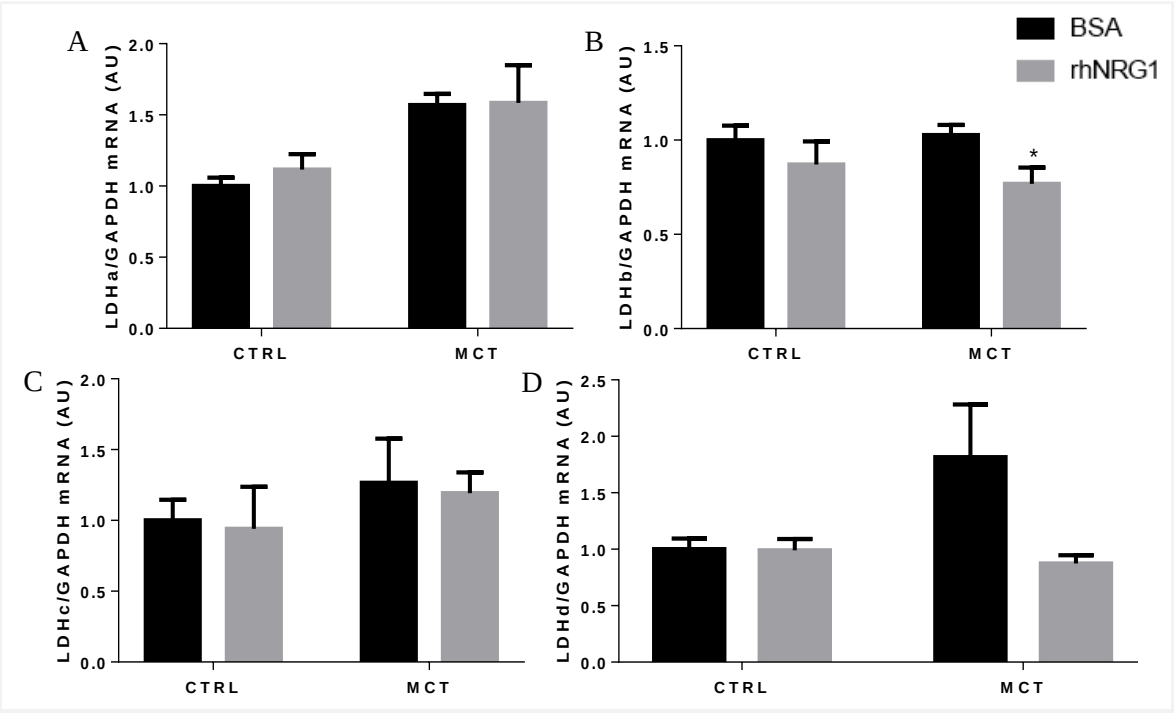

Figure 16 rhNRG1 reduced the expression of lactate dehydrogenase b (LDHb) in soleus muscle from MCT-induced PAH animals. CTRL: control group; MCT: monocrotaline group; GAPDH: glyceraldehyde 3-phosphate dehydrogenase.
Bars represent mean ± SEM of 10 rats per CTRL+BSA group, 20 rats per MCT group and 15 rats per MCT+rhNRG1 group. *P<0.05 vs. CTRL-BSA. Two-way ANOVA was used for all the parameters presented.

From the analysis of PDH in soleus muscle, who is responsible for catalyse pyruvate into acetyl-CoA and CO_2[200,201], no expression changes were found in both subunits PDHa1 (Figure 17A) or PDHβ (Figure 17B).

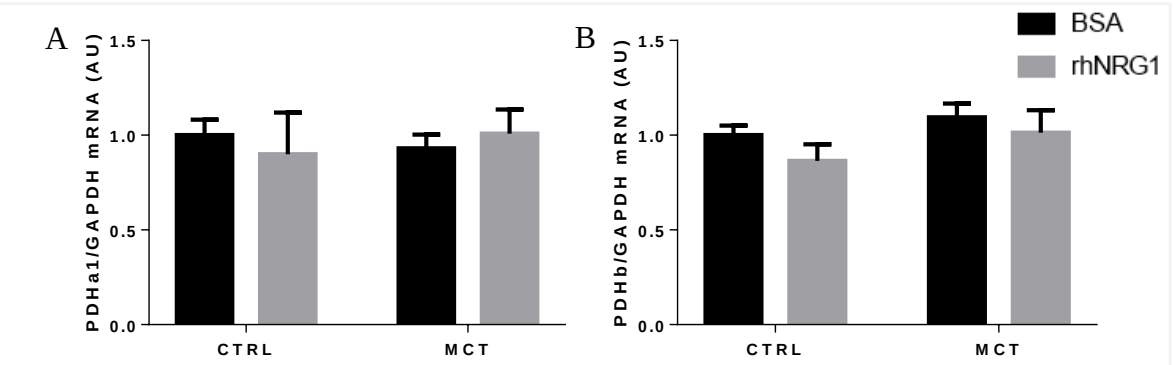

Figure 17 No alterations on pyruvate dehydrogenase complex (PDH) have been identified in soleus muscle of MCT-induced PAH animals. CTRL: control group; MCT: monocrotaline group; GAPDH: glyceraldehyde 3-phosphate dehydrogenase.
Bars represent mean ± SEM of 10 rats per CTRL+BSA group, 20 rats per MCT group and 15 rats per MCT+rhNRG1 group. Two-way ANOVA was used for all the parameters presented.

Relatively to mitochondrial function genes that were analysed, no changes were observed in the expression of PGC-1α in the soleus muscle of the four different experimental groups (Figure 18A). Neither NRF1 that regulates mitochondrial respiration[233] (Figure 18B) or Sirt1 that controls PGC-1α[219] (Figure 18C) presented variations between the MCT-induced PAH or control groups in this tissue.

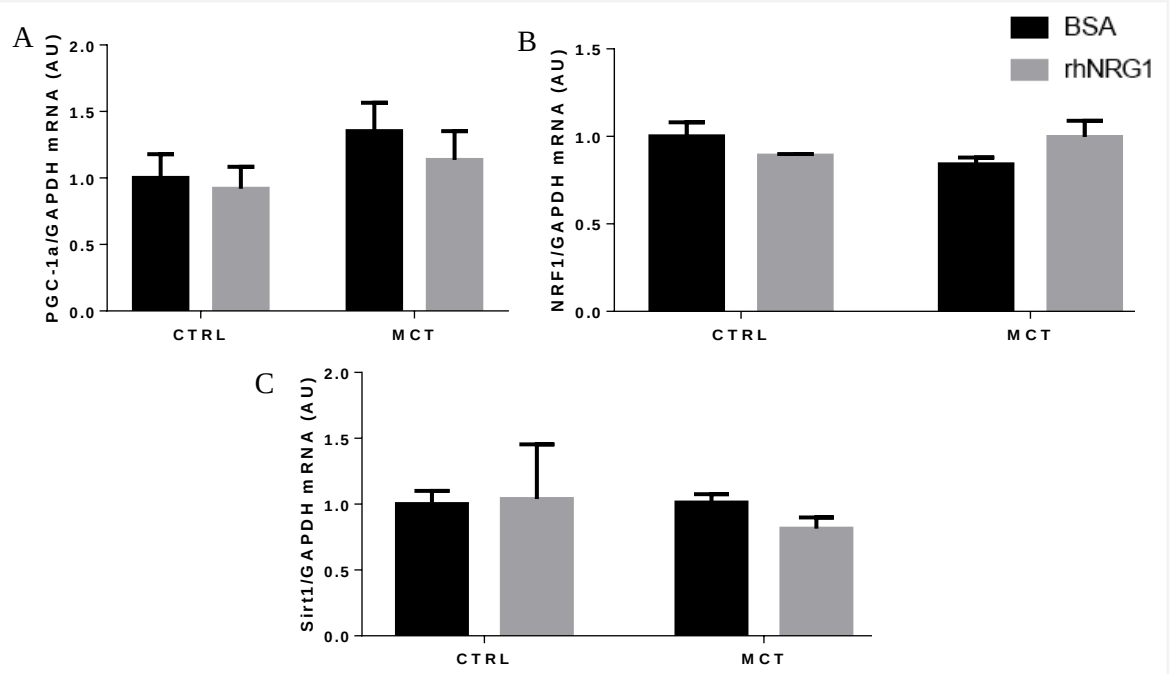

Figure 18 There were no changes in mitochondrial function genes in soleus muscle of MCT-induced PAH animals. CTRL: control group; MCT: monocrotaline group; PGC-1α: peroxisome proliferator-activated receptor gamma coactivator 1α; GAPDH: glyceraldehyde 3-phosphate dehydrogenase; NRF1: nuclear respiratory factor 1; Sirt1: sirtuin 1.
Bars represent mean ± SEM of 10 rats per CTRL+BSA group, 20 rats per MCT group and 15 rats per MCT+rhNRG1 group. Two-way ANOVA was used for all the parameters presented.

b. mRNA expression on RV

Most of significant variations in gene expression were detected in RV tissue.

As expected, MCT-induced PAH resulted in a significant increase in mRNA expression of GLUT1 in MCT-BSA group, which has been attenuated by rhNRG1 in MCT-treated animals (Figure 19A). There was also a significant decrease in GLUT4 mRNA expression in MCT-BSA group when compared with CTRL-BSA, which was significantly reversed by the treatment with rhNRG1 in MCT animals (Figure 19B). The HIF-1α mRNA expression significantly increased in MCT-BSA animals (Figure 19C). MCT-BSA animals

demonstrated significantly increased levels of BNP mRNA expression (Figure 19D). In relation to ET-1 mRNA expression, a vasoconstrictor, there were no significant changes between the CTRL and MCT-induced PAH groups (Figure 19E).

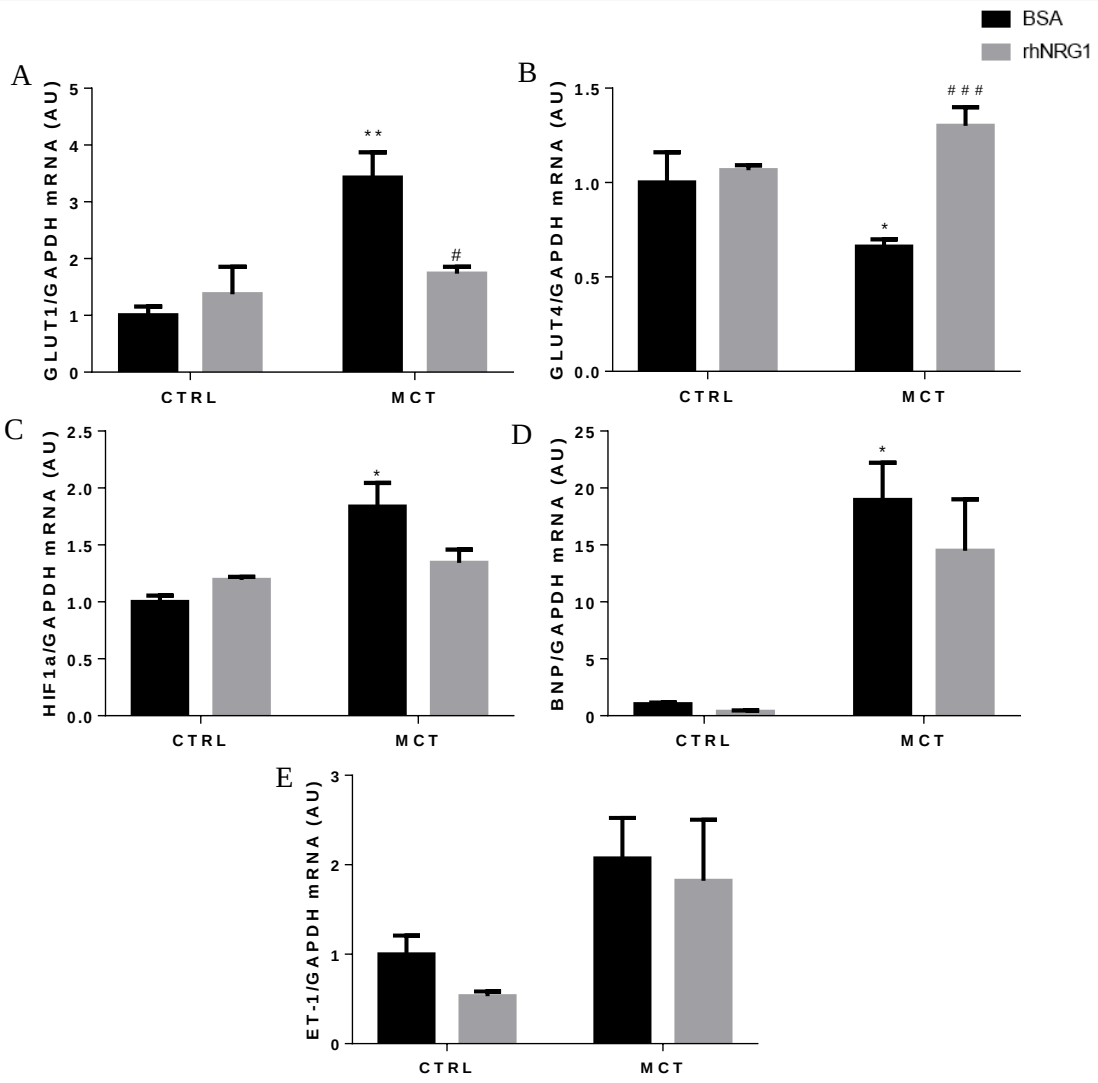

Figure 19 rhNRG1 treatment induced significant alterations on glucose transporters (GLUT) 1 and 4, hypoxia inducible factor 1α (HIF-1α) and brain natriuretic peptide (BNP) mRNA expression in right ventricle (RV) of MCT-induced PAH animals. CTRL: control group; MCT: monocrotaline group; GAPDH: glyceraldehyde 3-phosphate dehydrogenase; ET-1: endothelin-1.
Bars represent mean ± SEM of 10 rats per CTRL+BSA group, 20 rats per MCT group and 15 rats per MCT+rhNRG1 group. *P<0.05 vs. CTRL-BSA; **P<0.01 vs. CTRL-BSA; #P<0.05 vs. MCT-BSA; ###P<0.001 vs. MCT-BSA. Two-way ANOVA was used for all the parameters presented.

The mRNA levels of HK1 presented greater expression in both MCT groups when compared with CTRL-BSA group (Figure 20A). MCT-induced PAH animals displayed an increased mRNA expression of HK2 when comparing with CTRL-BSA group, and the

treatment with rhNRG1 increased the expression of HK2 mRNA in MCT-induced PAH treated animals in comparison with CTRL-treated group (Figure 20B).

In MCT-BSA group a significant decrease in PFKm mRNA expression was found when compared with CTRL-BSA group (Figure 20C). The PKm mRNA expression significantly increased in MCT-induced PAH animals, being the most marked increase in the group of PAH animals treated with rhNRG1 (Figure 20D).

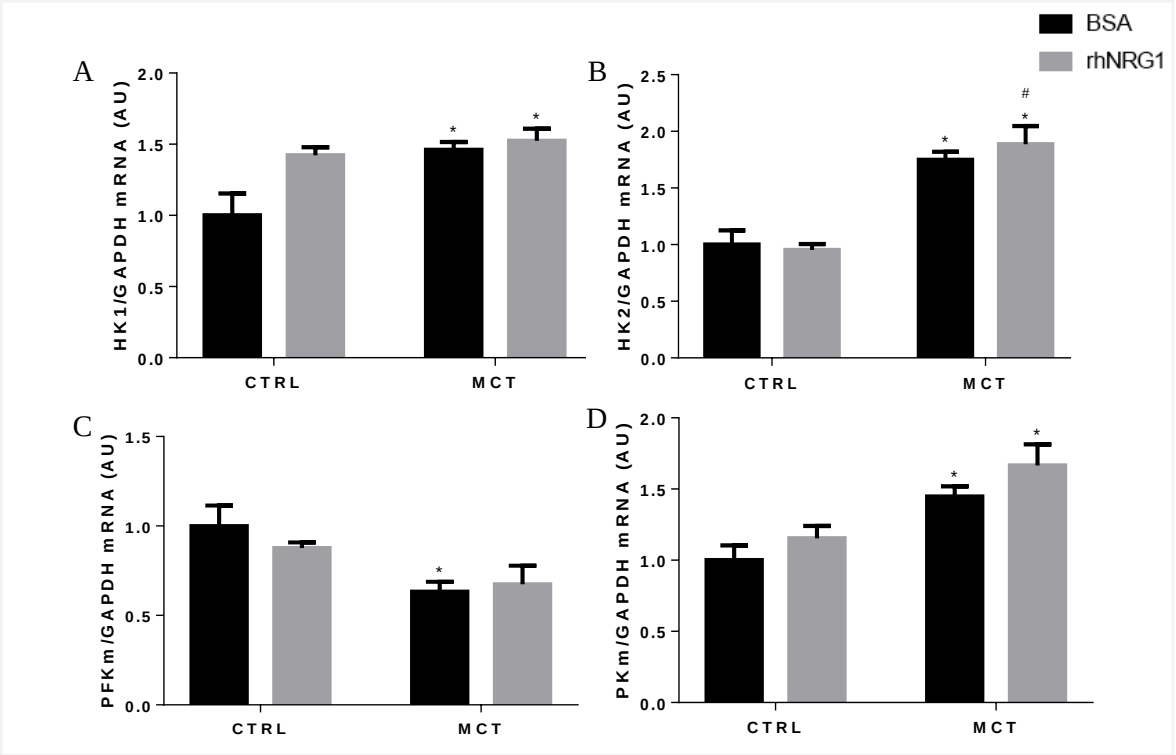

Figure 20 rhNRG1 modulated the expression of glycolysis rate-limiting enzymes in right ventricle (RV) of MCT-induced PAH animals. CTRL: control group; MCT: monocrotaline group; GAPDH: glyceraldehyde 3-phosphate dehydrogenase; HK: hexokinase; PFKm: muscle type phosphofructokinase; PKm: muscle type pyruvate kinase. Bars represent mean ± SEM of 10 rats per CTRL+BSA group, 20 rats per MCT group and 15 rats per MCT+rhNRG1 group. *P<0.05 vs. CTRL-BSA; #P<0.05 vs. MCT-BSA. Two-way ANOVA was used for all the parameters presented.

No significant changes were detected in the expression of mRNA from LDHb (Figure 21A) or LDHd (Figure 21B).

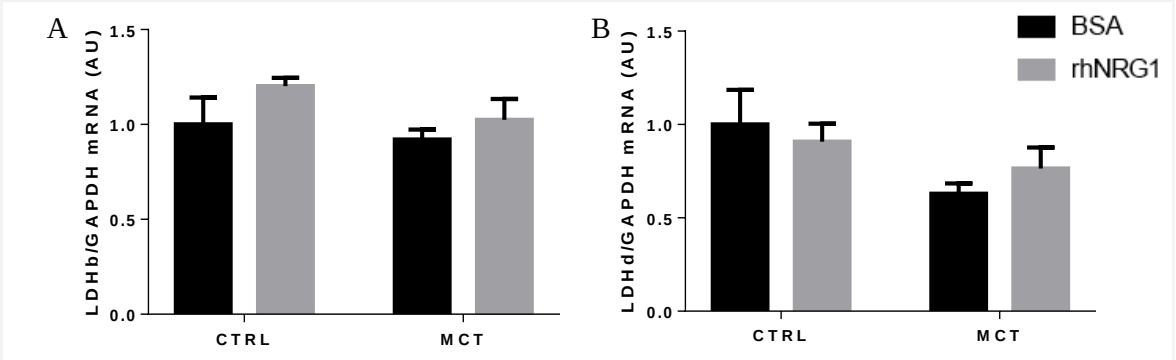

Figure 21 No significant changes on mRNA expression of lactate dehydrogenase (LDH) in right ventricle (RV) from MCT animals were found. CTRL: control group; MCT: monocrotaline group; GAPDH: glyceraldehyde 3-phosphate dehydrogenase.
Bars represent mean ± SEM of 10 rats per CTRL+BSA group, 20 rats per MCT group and 15 rats per MCT+rhNRG1 group. *P<0.05 vs. CTRL-BSA. Two-way ANOVA was used for all the parameters presented.

In the RV tissue, as in the soleus muscle, no significant changes were reported in the expression of both PDHa1 (Figure 22A) and PDHβ (Figure 22B).

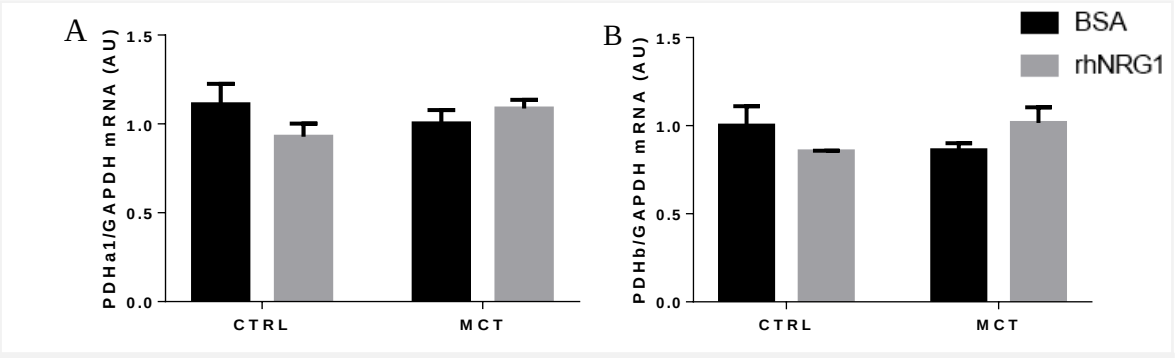

Figure 22 No significant alterations on pyruvate dehydrogenase complex (PDH) have been identified in right ventricle (RV) of MCT-induced PAH animals. CTRL: control group; MCT: monocrotaline group; GAPDH: glyceraldehyde 3-phosphate dehydrogenase.
Bars represent mean ± SEM of 10 rats per CTRL+BSA group, 20 rats per MCT group and 15 rats per MCT+rhNRG1 group. Two-way ANOVA was used for all the parameters presented.

From the gene analysis in RV, no significant changes were observed in the gene expression of the mitochondrial function genes analysed, namely PGC-1α (Figure 23A), NRF1 (Figure 23B) or Sirt1 (Figure 23C) between the MCT-induced PAH or control groups.

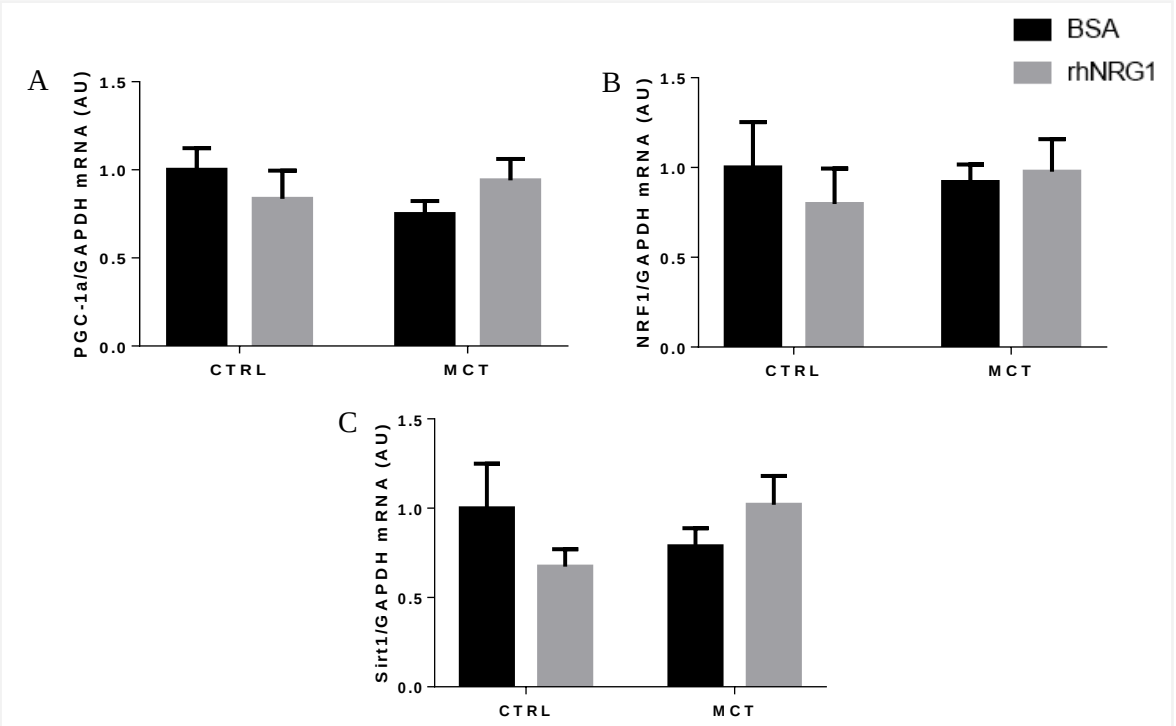

Figure 23 There were no changes in mitochondrial function genes mRNA expression in right ventricle (RV) of MCT-induced PAH animals. CTRL: control group; MCT: monocrotaline group; PGC-1α: peroxisome proliferator-activated receptor gamma coactivator 1α; GAPDH: glyceraldehyde 3-phosphate dehydrogenase; NRF1: nuclear respiratory factor 1; Sirt1: sirtuin 1.
Bars represent mean ± SEM of 10 rats per CTRL+BSA group, 20 rats per MCT group and 15 rats per MCT+rhNRG1 group. Two-way ANOVA was used for all the parameters presented.

c. Correlation of RV gene expression from glycolytic pathway genes with morphometric and echocardiographic parameters

The correlation between the genes with significant changes in RV and morphometric and echocardiographic parameters was also performed. The results presented refer only to the variables that presented significant correlations with each other.

GLUT1 expression is correlated with morphometric and echocardiographic parameters. It was verified that there is a positive and strong correlation between GLUT1 and Fulton index ($r = 0.618$, $p<0.001$) (Figure 24A), once both are increased in MCT-induced rhNRG1 non-treated animals, associating this gene to the increase in the RV area and RVH.[281] The GLUT1 and TAPSE displayed a negative correlation ($r = -0.5284$, $p<0.05$) (Figure 24B), also reflecting RV dysfunction. The correlation between GLUT1 and CO is negative and strong ($r = -0.7322$, $p<0.001$), once as the disease progresses the GLUT1 increases and the CO decreases (Figure 24C).

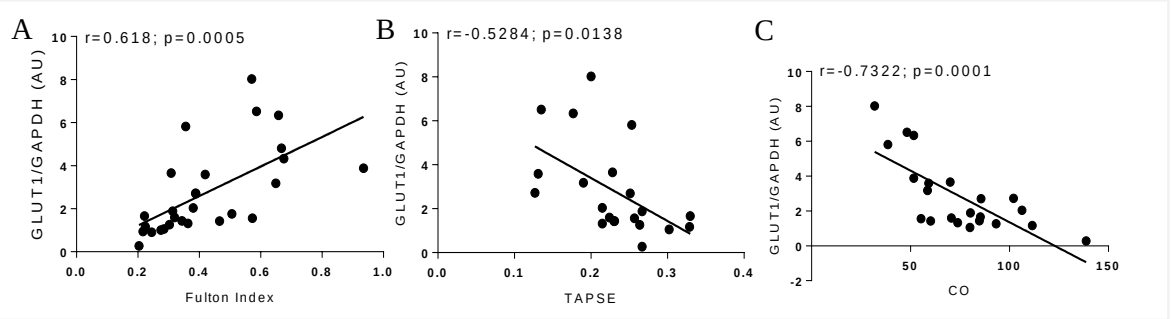

Figure 24 Glucose transporter 1 (GLUT1) mRNA expression is corelated with Fulton index, tricuspid annular plane systolic excursion (TAPSE) and cardiac output (CO).
Data used for the correlation analysis were obtained from animals that had both echocardiographic and mRNA analysis. Correlations were determined using Pearson correlation test.

GLUT4 gene expression correlated negatively with Fulton index since they have opposite behaviours in PAH, but without statistical significance (r = -0.2414, p ns) (Figure 25A). The correlation between GLUT4 and TAPSE was positive and significant (r = 0.6528, p<0.05) (Figure 25B). Regarding to the correlation between GLUT4 and CO, it was no significant (r = 0.1964, p ns) (Figure 25C).

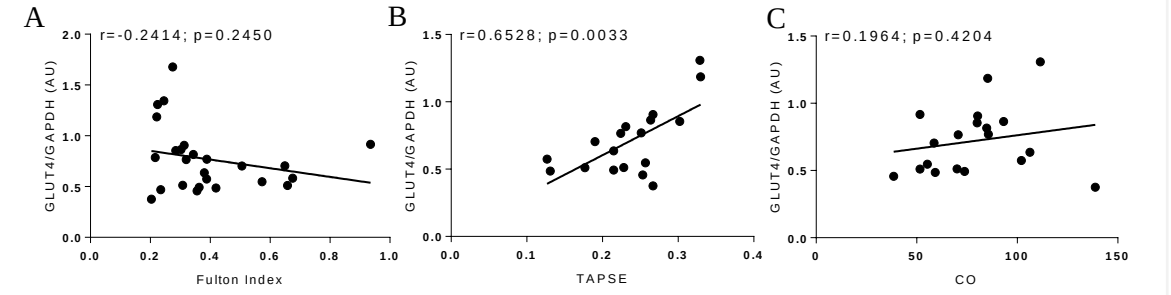

Figure 25 Glucose transporter 4 (GLUT4) mRNA expression is corelated with Fulton index, tricuspid annular plane systolic excursion (TAPSE) and cardiac output (CO).
Data used for the correlation analysis were obtained from animals that had both echocardiographic and mRNA analysis. Correlations were determined using Pearson correlation test.

HIF-1α gene expression is positively correlated with Fulton index (r = 0.4840, p<0.05), what relates HIF-1α with the presence RVH (Figure 26A). There was no significant correlation between HIF-1α and TAPSE (r = -0.3991, p ns) (Figure 26B). Relatively to the correlation between HIF-1α and CO, this is negative (r = -0.5324, p<0.05) (Figure 26C).

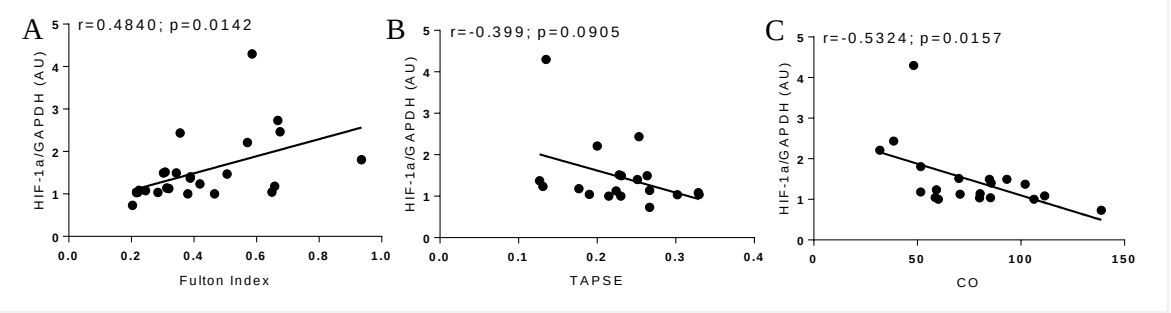

Figure 26 The increased mRNA expression of hypoxia inducible factor (HIF-1α) is correlated with Fulton index, tricuspid annular plane systolic excursion (TAPSE) and cardiac output (CO).
Data used for the correlation analysis were obtained from animals that had both echocardiographic and mRNA analysis. Correlations were determined using Pearson correlation test.

The existence of correlation between GLUTs and HIF-1α was also assessed. GLUT1 gene expression is negatively correlated with GLUT4 expression, as expected (r = -0.4326, p<0.05), what reveals a potential compensation mechanism in PAH (Figure 27A). On the other hand, the correlation between GLUT1 and HIF-1α is positive and strong (r = 0.7264, p<0.001) (Figure 27B). Relatively to the correlation between GLUT4 and HIF-1α, it has no statistical significance (r = -0.262, p ns) (Figure 27C).

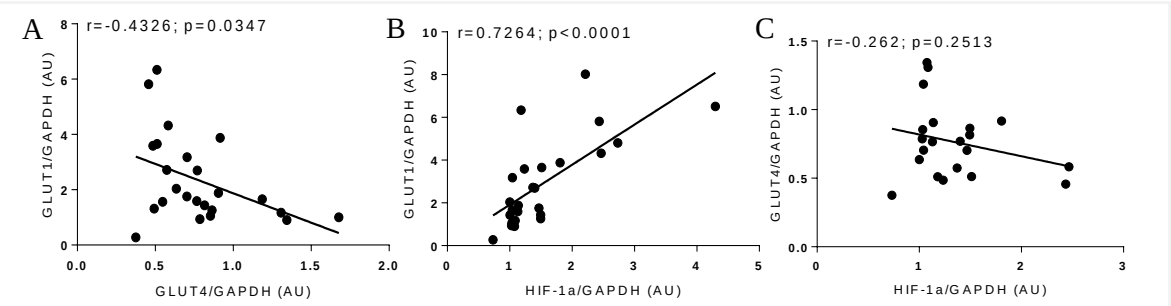

Figure 27 Glucose transporter 1 (GLUT1) mRNA expression is correlated with GLUT4 and with hypoxia inducible factor (HIF-1α).
Data used for the correlation analysis were obtained from animals that had both echocardiographic and mRNA analysis. Correlations were determined using Pearson correlation test.

HKs demonstrated to be only correlated with TAPSE. HK1 gene expression is negatively correlated with TAPSE (r = -0.6318, p<0.01) (Figure 28A). The correlation between HK2 and TAPSE is also negative (r = -0.5222, p<0.05) (Figure 28B).

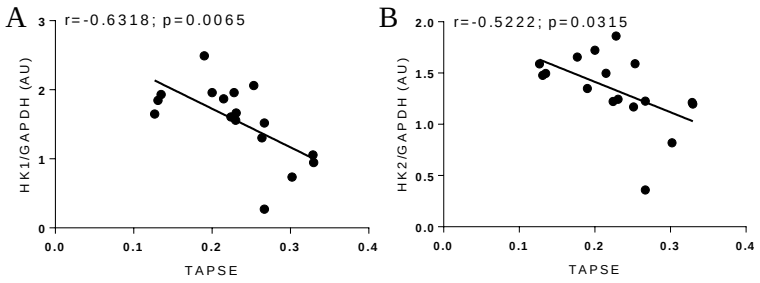

Figure 28 Both hexokinase 1 and 2 (HK1 and HK2) are correlated with the tricuspid annular plane systolic excursion (TAPSE).
Data used for the correlation analysis were obtained from animals that had both echocardiographic and mRNA analysis. Correlations were determined using Pearson correlation test.

PFKm gene expression is negatively correlated with the Fulton index (r = -0.5961, p<0.001), relating this gene with the RVH (Figure 29A). We also found a positive correlation between PFKm and TAPSE (r = 0.6377, p<0.01) (Figure 29B), what reinforces the previous correlation.

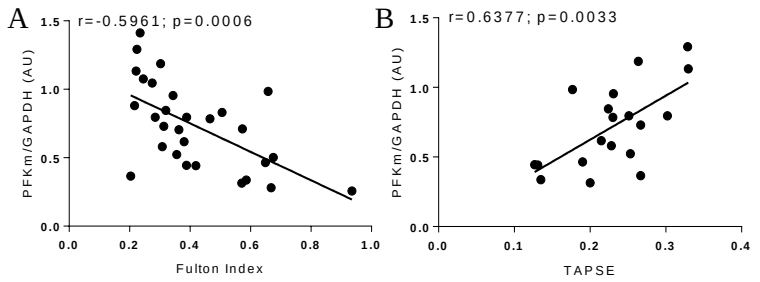

Figure 29 Phosphofructokinase muscle type (PFKm) mRNA expression is correlated with both Fulton index and the tricuspid annular plane systolic excursion (TAPSE).
Data used for the correlation analysis were obtained from animals that had both echocardiographic and mRNA analysis. Correlations were determined using Pearson correlation test.

The PKm gene expression is positively correlated with Fulton index (r = 0.5666, p<0.01) (Figure 30A), which may reveal the involvement of this gene in the development of disturbances in glucose metabolism that may trigger RVH. Concerning to the correlation between PKm and TAPSE, it is negative (r = -0.5527, p<0.05) (Figure 30B). The correlation between PKm and CO is also negative (r = -0.475, p<0.05) (Figure 30C), which is in agreement with the other correlations obtained for this gene.

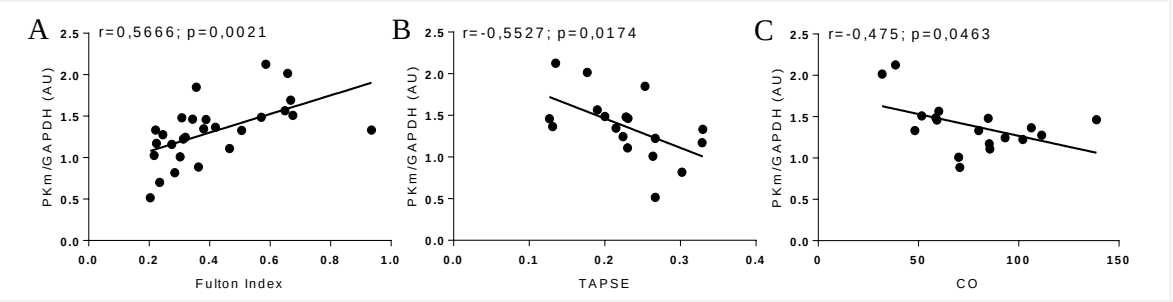

Figure 30 The increased mRNA expression of pyruvate kinase muscle type (PKm) is correlated with Fulton index, tricuspid annular plane systolic excursion (TAPSE) and cardiac output (CO).
Data used for the correlation analysis were obtained from animals that had both echocardiographic and mRNA analysis. Correlations were determined using Pearson correlation test.

Despite the absence of changes in LDH mRNA expression in the RV of animals with MCT-induced PAH, LDHb mRNA expression is positively correlated with TAPSE ($r = 0.5628$, $p<0.05$) (Figure 31A). Relatively to the correlation between LDHd and Fulton Index, this is negative ($r = -0.3878$, $p<0.05$) (Figure 31B). On the other hand, the correlation between LDHd and TAPSE is positive and strong ($r = 0.6756$, $p<0.01$) (Figure 31C).

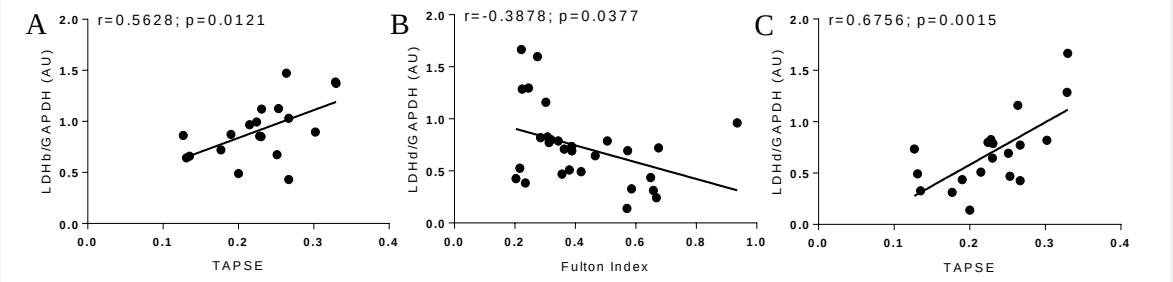

Figure 31 Lactate dehydrogenase b (LDHb) mRNA expression is correlated with tricuspid annular plane systolic excursion (TAPSE), while LDHd is correlated with both Fulton index and TAPSE.
Data used for the correlation analysis were obtained from animals that had both echocardiographic and mRNA analysis. Correlations were determined using Pearson correlation test.

Although there were no differences in mRNA expression between experimental groups, PDHb is correlated with CO and their correlation is positive ($r = 0.463$, $p<0.05$) (Figure 32).

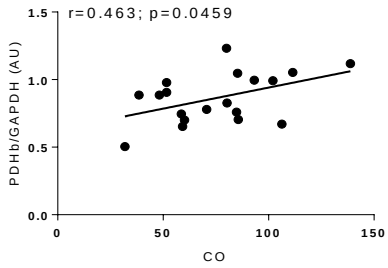

Figure 32 Pyruvate dehydrogenase β (PDHβ) mRNA expression is correlated with cardiac output (CO).
Data used for the correlation analysis were obtained from animals that had both echocardiographic and mRNA analysis. Correlations were determined using Pearson correlation test.

Despite there were no changes in the IRS1 mRNA expression in the RV between experimental groups, its gene expression is negatively correlated with Fulton index ($r = -0.4743$, $p<0.01$) (Figure 33A), which may reveal the involvement of this gene in disturbances in glucose transport and metabolism that may trigger RVH. The correlation between IRS1 and CO is positive ($r = 0.5401$, $p<0.05$) (Figure 33B).

The correlation between IRS2 and TAPSE is negative ($r = -0.5384$, $p<0.05$) (Figure 33C).

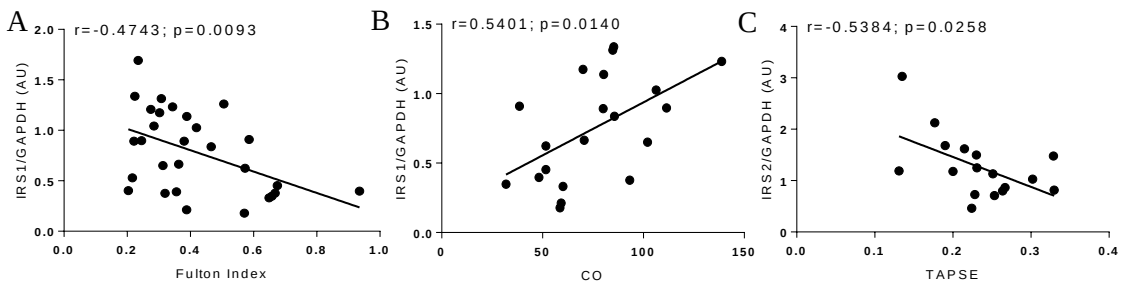

Figure 33 The insulin receptor 1 (IRS1) mRNA expression is correlated with both Fulton index and cardiac output (CO), while mRNA expression of IRS2 is correlated with tricuspid annular plane systolic excursion (TAPSE).
Data used for the correlation analysis were obtained from animals that had both echocardiographic and mRNA analysis. Correlations were determined using Pearson correlation test.

We also verified that PGC-1α mRNA expression displays a positive correlation with CO (r = 0.4923, p<0.05) (Figure 34).

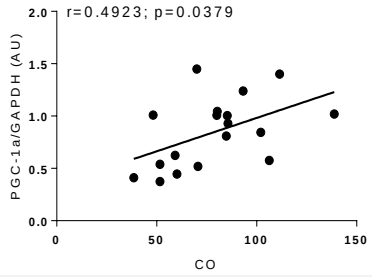

Figure 34 Peroxisome proliferator-activated receptor gamma coactivator 1α (PGC-1α) mRNA expression is correlated with cardiac output (CO).
Data used for the correlation analysis were obtained from animals that had both echocardiographic and mRNA analysis. Correlations were determined using Pearson correlation test.

d. Correlation of RV markers of disease gene expression, BNP and ET-1, with morphometric and echocardiographic parameters

The presented results only refer to the variables that presented significant correlations with each other.

BNP expression is strongly correlated with morphometric and echocardiographic parameters. There was a strong positive correlation with Fulton index (r = 0.6308, p<0.001) (Figure 35A), evidencing its role in RVH. The BNP and TAPSE exhibited a negative correlation (r = -0.6719, p<0.01) (Figure 35B), that also reflect the involvement of these two variables in RVD. Furthermore, the correlation between BNP and CO is negative (r = -0.5479, p<0.05) (Figure 35C).

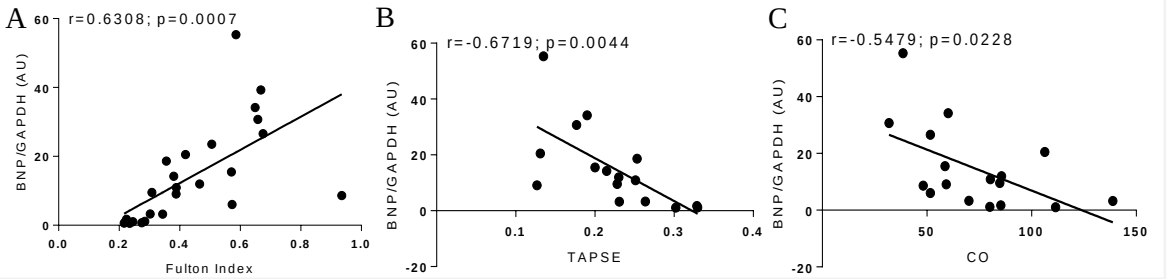

Figure 35 The increased mRNA expression of brain natriuretic peptide (BNP) is correlated with Fulton index, tricuspid annular plane systolic excursion (TAPSE) and cardiac output (CO).
Data used for the correlation analysis were obtained from animals that had both echocardiographic and mRNA analysis. Correlations were determined using Pearson correlation test.

Ultimately, ET-1 mRNA also was found to be related with Fulton index and their correlation is positive ($r = 0.4972$, $p<0.01$) (Figure 36).

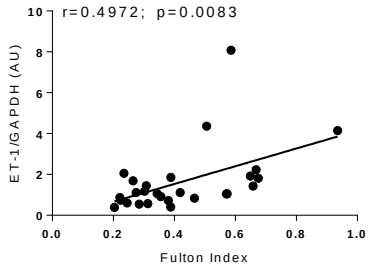

Figure 36 The increased levels of endothelin-1 (ET-1) are correlated with Fulton index.
Data used for the correlation analysis were obtained from animals that had both echocardiographic and mRNA analysis. Correlations were determined using Pearson correlation test.

2. Metabolic Changes in the Development of Pulmonary Arterial Hypertension in Hypoxia/Sugen model

a. Morphometric characterization of Hypoxia/Sugen model

The chronic hypoxia exposure resulted in a decrease of BW in H/S animals, in comparison with N animals (N: 401±12,78g; H/S: 328±11,49g) (Figure 37A). The indicator for RVH, Fulton index, was significantly increased in H/S group in comparison with H and N animal group (Figure 37B). The Lung/TL ratio was also increased in hypoxia animal group, being evidenced and significant in H group (Figure 37C). The RV weight of H/S animals presented a sharp increase in relation to H animals, meaning that RV was significantly dilated and remodelled in this animal group (Figure 37D).

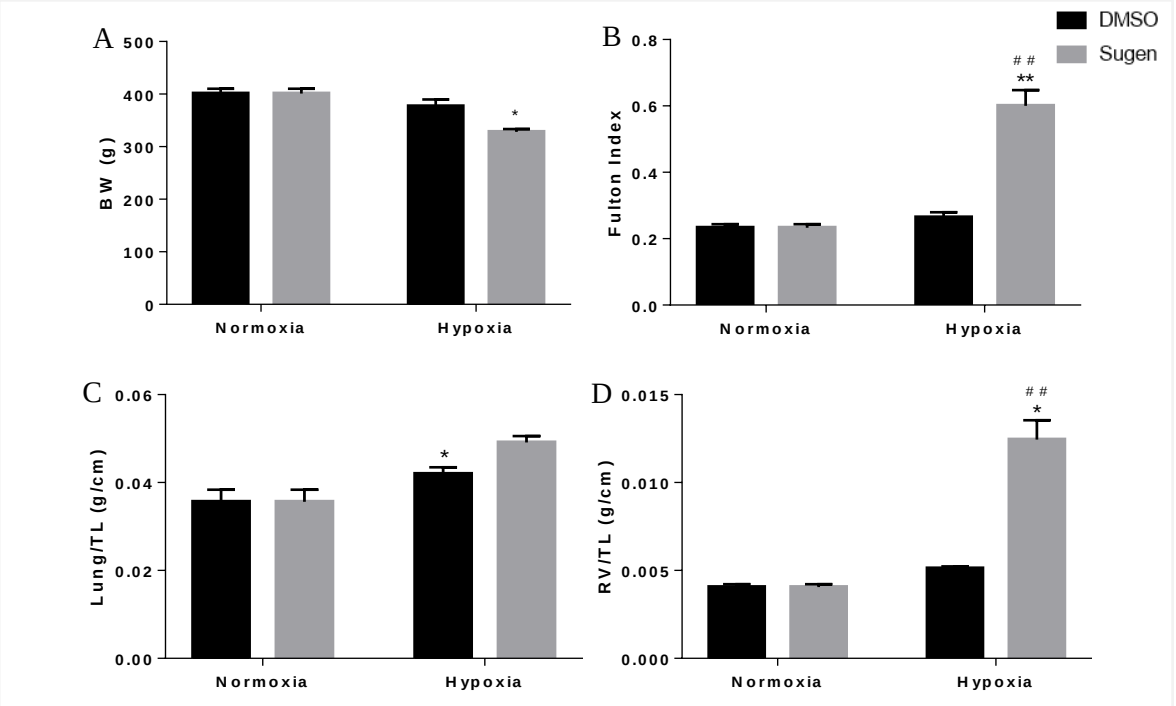

Figure 37 The hypoxia/Sugen5416 animal model reproduced the morphometric conditions verified in MCT-induced PAH. BW: body weight; TL: tibial length; RV: right ventricle.
Bars represent mean ± SEM of 2 rats per each normoxia group, 3 rats per hypoxia group and 4 rats per hypoxia/Sugen5416 group for the morphometric data. *P<0.05 vs. N+BSA; **P<0.01 vs. N+BSA; ##P<0.01 vs. H+BSA. Two-way ANOVA analysis of variance with Tukey's posttest was used for all the parameters presented.

b. mRNA expression in gastrocnemius muscle

The differences between the groups in study are notorious in what concerns molecular alterations. The mRNA levels of GLUT1 in gastrocnemius muscle are

significantly decreased in hypoxia-induced PAH animals when compared to the H/S-induced PAH group (Figure 38A). However, the GLUT4 mRNA expression was not altered between the different animal groups (Figure 38B). No significant differences were found on the mRNA expression of HIF-1α (Figure 38C) and PGC-1α (Figure 38D) between the different groups.

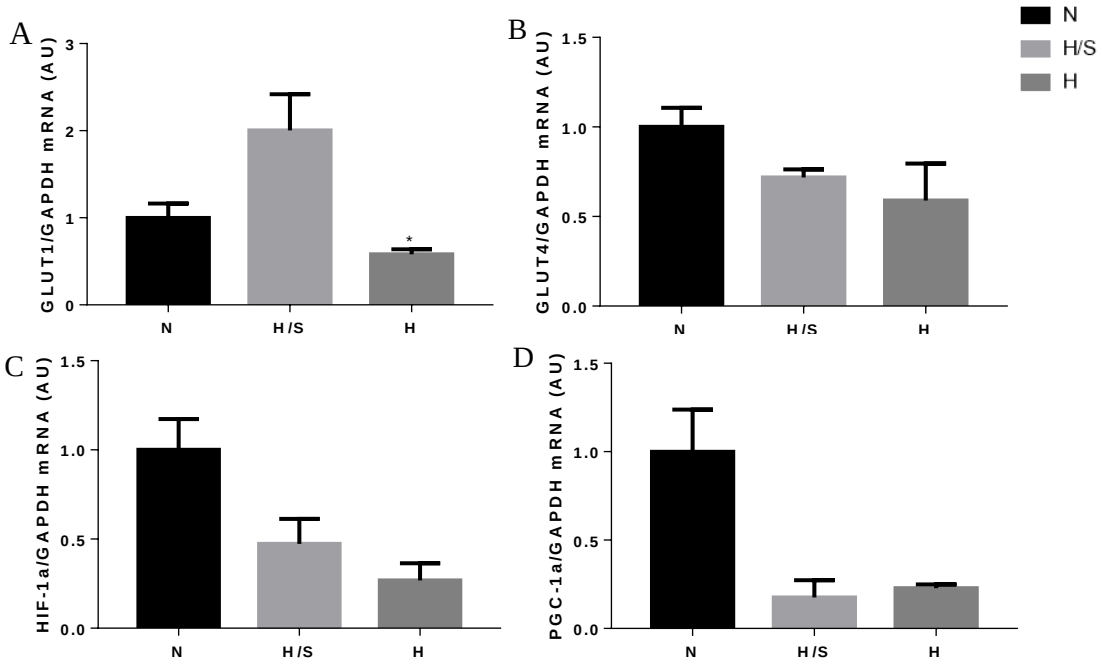

Figure 38 Glucose transporter 1 (GLUT1) presented altered mRNA expression in gastrocnemius muscle in hypoxia/Sugen model. N: normoxia group; H/S: hypoxia/Sugen5416 group; H: hypoxia group; GAPDH: glyceraldehyde 3-phosphate dehydrogenase; HIF-1α: hypoxia inducible factor 1α; PGC-1α: peroxisome proliferator-activated receptor gamma coactivator 1α.
Bars represent mean ± SEM of 4 rats per normoxia group, 3 rats per hypoxia group and 4 rats per hypoxia/Sugen5416 group. *P<0.05 vs. H/S. One-way ANOVA nonparametric analysis of variance with Tukey's posttest was used for all the parameters presented.

c. mRNA expression in lung

In the lung were not detected differences in GLUT1 mRNA expression between the hypoxia-induced PAH and N animal group (Figure 39A), as well as no differences in GLUT4 mRNA expression were found between the three different groups (Figure 39B). However, it occurred a significant increase in HIF-1α in H/S-induced PAH animals when compared with the N group (Figure 39C), and PGC-1α followed a similar pattern of expression and significantly increased in H/S when compared to N group (Figure 39D).

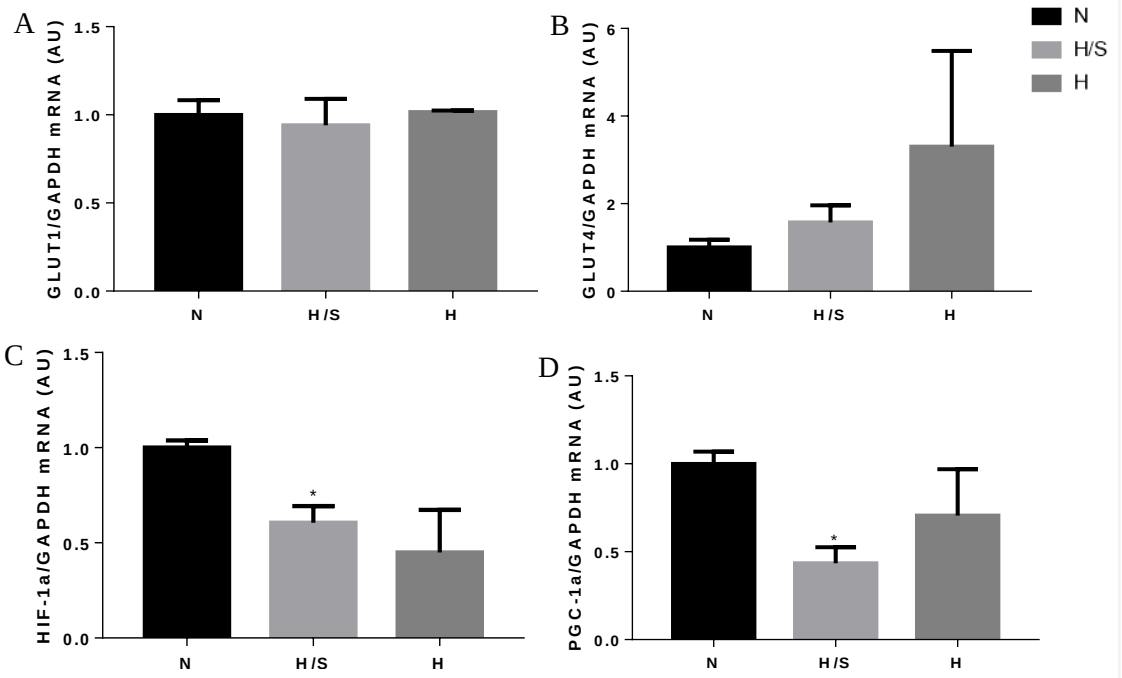

Figure 39 Hypoxia inducible factor 1α (HIF-1α) and peroxisome proliferator-activated receptor gamma coactivator 1α (PGC-1α) presented altered mRNA expression in lungs from the animals of hypoxia/Sugen5416 model. N: normoxia group; H/S: hypoxia/Sugen5416 group; H: hypoxia group; GLUT: glucose transporter.
Bars represent mean ± SEM of 4 rats per normoxia group, 3 rats per hypoxia group and 4 rats per hypoxia/Sugen5416 group. *P<0.05 vs. N. One-way ANOVA nonparametric analysis of variance with Tukey's posttest was used for all the parameters presented.

d. mRNA expression in RV

In the same way as it occurred in MCT model, the RV is the tissue where most of the metabolic alterations were detected. The GLUT1 mRNA expression is significantly increased in H/S animal group when compared to N group, while the hypoxia-induced PAH group displayed GLUT1 levels considerably lower when comparing to hypoxia/Sugen-induced PAH animal group (Figure 40A). Relatively to GLUT4 mRNA expression, it was significantly decreased in H/S animals when compared to N animals (Figure 40B). In the same way as it was occurred in the other analysed tissues, HIF-1α (Figure 40C) and PGC-1α (Figure 40D) followed a similar pattern of expression and exhibited significantly decrease in hypoxia/Sugen-induced PAH animals when compared with the N group.

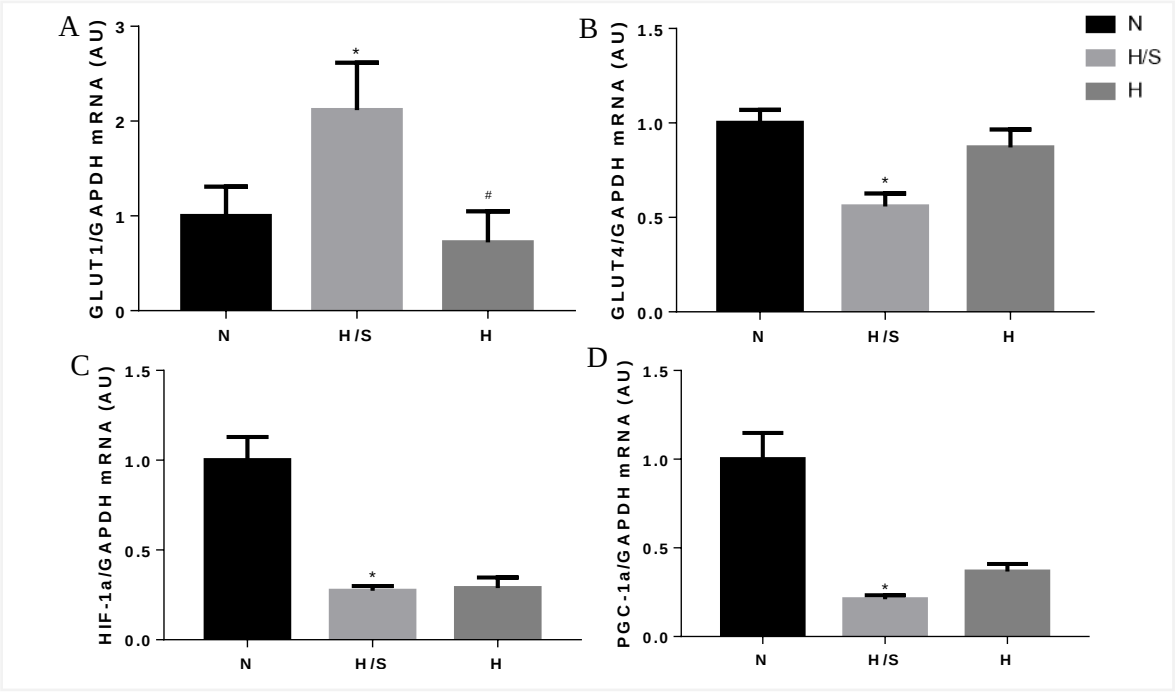

Figure 40 The mRNA expression changes are evident in RV from rats of hypoxia model. N: normoxia group; HS: hypoxia/Sugen 5416 group; H: hypoxia group; GAPDH: glyceraldehyde 3-phosphate dehydrogenase; GLUT: glucose transporter; HIF-1α: hypoxia inducible factor 1α; PGC-1α: peroxisome proliferator-activated receptor gamma coactivator 1α.
Bars represent mean ± SEM of 4 rats per control group, 3 rats per hypoxia group and 4 rats per hypoxia/Sugen5416 group. *P<0.05 vs. N; #P<0.05 vs. H/S. One-way ANOVA nonparametric analysis of variance with Tukey's posttest was used for all the parameters presented.

2.1. Metabolic Changes in the Development of Pulmonary Arterial Hypertension in Hypoxia/Sugen model - Effects of the treatment with Neuregulin-1

a. Oral glucose tolerance test

As in MCT model, in chronic hypoxia model fasting plasma glucose presented similar values between two animal groups in study, H/S+BSA and H/S+rhNRG1 group, without variations between groups (Figure 41A). However, when comparing H/S+BSA with H/S+rhNRG1 animal group, the first one presented significant greater blood glucose concentrations for time points between 15 and 120 min (Figure 41B). Unlike what occurred in the MCT model, there is also a tendency for higher postprandial glucose concentrations in rhNRG1 treated animal group when compared with H/S+BSA animals, as AUC demonstrates with statistical significance (Figures 41B and 41C).

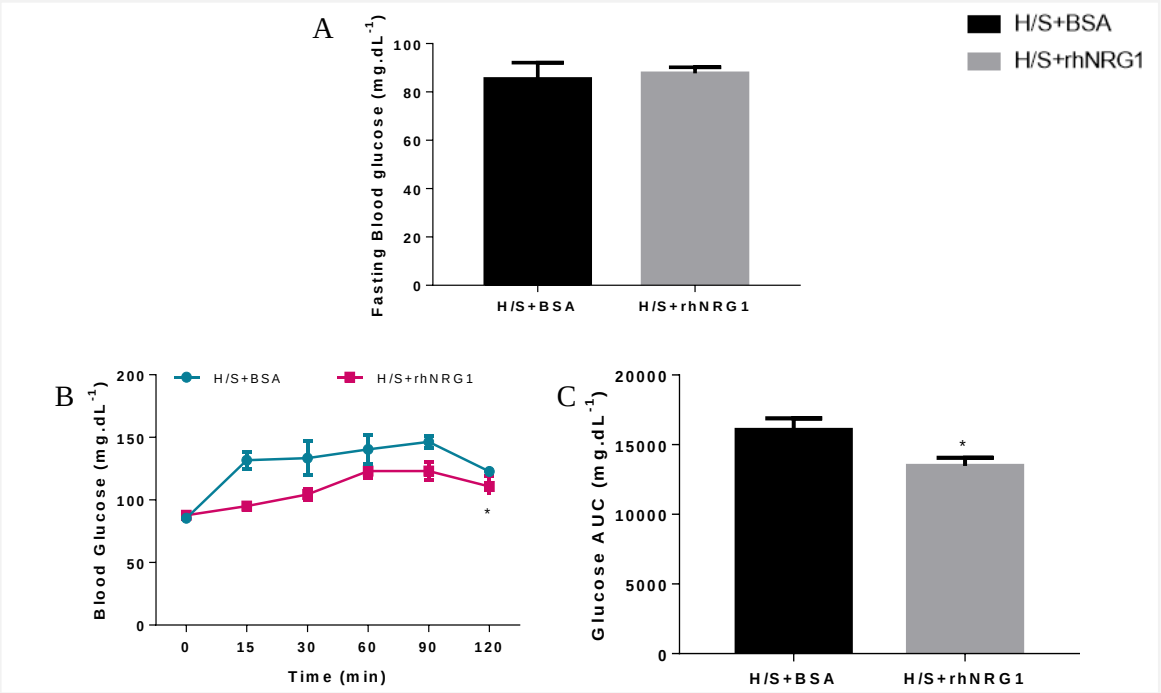

Figure 41 rhNRG1 attenuated whole-body glucose tolerance in hypoxia animals. H/S+BSA: hypoxia/Sugen5416 animals with bovine serum albumin (BSA) group; H/S+rhNRG1: hypoxia/Sugen5416 animals treated with recombinant human neuregulin-1 (rhNRG1).
Bars represent mean ± SEM of 5 rats per H/S+BSA group and 5 rats per H/S+rhNRG1 group for the OGTT. *p<0.05 vs H/S+BSA.

b. mRNA expression in RV from hypoxia rhNRG1 treated animals

Contrary to what was verified in the mRNA analysis of the RV of the MCT model and was expected, GLUT1 mRNA expression in RV is significantly increased in H/S+rhNRG1 treated animal group when compared to H/S+BSA group (Figure 42A). Relatively to GLUT4 mRNA expression, it was significantly decreased in H/S+rhNRG1 animals when compared to H/S+BSA animals (Figure 42B) and, once again, occurred a discrepancy between hypoxia and the MCT model, but also with what was expected in the animals treated with rhNRG1. The levels of NRG1 mRNA expression on RV were also decreased in H/S+rhNRG1 animal group comparing to H/S+BSA animals (Figure 42C).

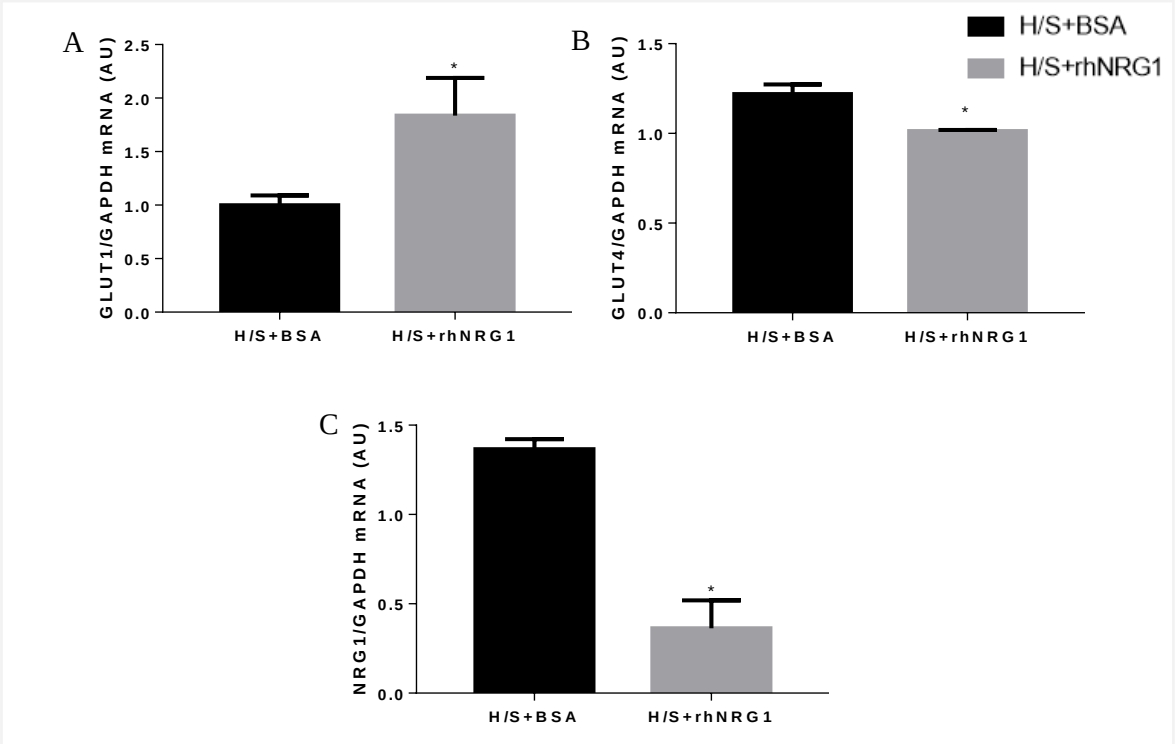

Figure 42 The mRNA expression was altered by rhNRG1 treatment in hypoxia/ Sugen 5416 animal model of pulmonary arterial hypertension (PAH). H/S+BSA: hypoxia/Sugen5416 animals with bovine serum albumin (BSA) group; H/S+rhNRG1: hypoxia/Sugen5416 animals treated with recombinant human neuregulin-1 (rhNRG1); GAPDH: glyceraldehyde 3-phosphate dehydrogenase; GLUT: glucose transporter; HIF-1α: hypoxia inducible factor 1α; PGC-1α: peroxisome proliferator-activated receptor gamma coactivator 1α.
Bars represent mean ± SEM of 5 rats per H/S+BSA group and 5 rats per H/S+rhNRG1 group. *P<0.05 vs. H/S+BSA. One-way ANOVA nonparametric analysis of variance with Tukey's posttest was used for all the parameters presented.

Discussion

This study provided data on the pathophysiological alterations and molecular changes on glucose metabolism resultant from the development of PAH, as well as the effects of the treatment with NRG1. The study was conducted in two well characterized rat models of PH: the MCT and the chronic hypoxia models.

1. Metabolic changes in the development of PAH in monocrotaline model and effects of the treatment with rhNRG1

a. MCT-induced PAH markers and glucose transporters expression vary according to the disease state

The RV is the main prognostic determinant in PAH.[37,38] Despite the continuum remodelling in RV as the disease progresses, it is normal to proceed to the differentiation of two patterns of ventricular remodelling and hypertrophy based on morphometric, echocardiographic and molecular characteristics. In our study, we defined a RVEF of 35% to differentiate this two patterns: the animals with adaptive remodelling/hypertrophy that displayed CRV function, with normal to mildly decreased RVEF, above 35%, in comparison to healthy animals, and the ones with maladaptive remodelling hypertrophy, who displayed DRV function, with RVEF below 35% and sharply decreased comparing with healthy animals.[27] The decrease in RVEF in DRV animal group may also be associated with an increase in RV wall stress and in RV diameter.[278,282] These findings are in accordance with the information provided in a study in MCT-induced PAH that characterized the RV function in rats, where the animal groups were divided according two different doses of MCT injection, a lower dose of 30mg/kg of BW (MCT30) and a higher dose of 80 mg/kg of BW (MCT80). The authors concluded that the animal group with the lower dose of MCT displayed a compensatory RVH and a lesser reduction in RVEF in comparison with the animal group treated with the higher dose of MCT, whose RVEF was significantly decreased comparing with control and MCT30 group, being RVH more evident MCT80 group.[282]

The metabolic switch from mitochondrial OXPHOS to glycolysis that characterizes PAH is defined in the compensated phase of RVH.[35,39] The increase in HIF-1α expression and activity in DRV in relation to CRV phase, which was also documented by other authors,

is related with the development and establishment of an hypoxic environment and hypertrophy of the RV, and triggers for itself an increase in GLUT1 mRNA expression to increase glucose uptake[35,42,173], and the HIF-1α activation and increased expression is an evidence for the metabolic switch from mitochondria-based GO to a glycolytic phenotype, the Warburg effect.[35,147] In fact, we verified an increment in HIF-1α mRNA expression in DRV group in relation to both control and CRV groups, what reinforces the development of hypoxia conditions and RVH in the animals of this group, which are characteristics of PAH development.

The transition from CRV to DRV is also marked by variations of indicators of cardiac function, ET-1 and BNP, that are related with overload and hypertrophy.[86,279] We identified an increase in circulating vasoconstrictors as ET-1 and observed an increase in the mRNA expression of this gene DRV group. A study that analysed RV from both MCT-induced PAH rats and human samples, identified an increase in ET-1 production in the samples from hypertrophied RV, and discovered that this may be implicated in the maintaining of cardiomyocyte survival due to its inotropic effects. The same study also proposed that the modulation of ET-1 receptors is responsible for a decrease in RV afterload by the reversal of PA obstruction and remodelling[101], what evidenced the role of ET-1 in RVH development. Furthermore, the levels of BNP also accompanied the molecular alterations identified at the RV level, contributing to an increased myocardial stress and injury in this group[86] as it was previously described in the analysis of the RVEF. Since cardiac BNP mRNA expression is markedly upregulated in response to RVH or overload[32], this contributed to the establishment of the disease phenotype and confirmed the role of MCT in the development of PAH characteristics. In addition, the studies mentioned above support, in part, our findings and is in accordance with the morphological analysis that we performed, and which indicates for the presence of hypertrophy in RV from the DRV group.

The regulation of intracellular and extracellular levels of glucose depends on levels of expression of GLUT proteins, that are variable as the disease progresses[153,179] and the increase in glucose uptake and utilization that follows cardiac hypertrophy may occur as a cardioprotective mechanism.[211] In RVH, the increase in glucose uptake for glycolysis is achieved with the compensated expression and activity of GLUTs, as the GLUT1, in order to maintain the energy supply, accompanied by an increase in PDH phosphorylation.[39,44,192]

The expression of GLUT1, which is expressed in foetal heart and whose expression is re-induced in the adult heart in some pathophysiological states[180,211], and GLUT4, as it is the major isoform of insulin-dependent GLUT in human heart[182] were assessed. In our study and as expected, GLUT1 presented increased expression in both MCT groups being more evidenced in DRV group, which can be explained by the development of RVH.[212] Based on the results obtained, we could verify that there is an increase in GLUT1 mRNA expression as the cardiac hypertrophy develops and the RV progresses from a compensated to a decompensated state. This may occur due the less efficient ATP production by glycolysis, as it triggers lactate production rather than pyruvate, and does not fuels Krebs' cycle, giving rise to the metabolic switch, the Warburg effect.[192,212] In its turn, the decrease in GLUT4 expression levels was also related with the development of cardiac hypertrophy and with the transition to the decompensated state[215], as we verified. Still, a study in RV MCT-induced remodelling documented an increase in GLUT4 mRNA expression[183], however, it is known that the expression levels of this transporter fluctuate according with the disease state and severity.[215]

b. GLUT1 and GLUT4 expression is correlated with cardiac markers of disease

The reactivation of components of the foetal gene package during RV remodelling and hypertrophy[42], provides useful information to establish some comparisons between the GLUTs and markers of disease. The obtained results showed a negative correlation between GLUT1 mRNA expression and RVEF, as expected according with the literature information, that reports a downregulation of GLUT1 after birth.[153] However, the GLUT4 correlation with RVEF is positive, indicating proportionality between them, once both have decreased activity in animals of the DRV group, but also due to the fact that the hypertrophied heart acts as the foetal heart. In addition to GLUT4 expression, the values of RVEF are also lower in hypertrophied right heart[283], which also contributes to the positive correlation between them.

We also found that GLUT1 gene expression is positively correlated with the expression of HIF-1α, what is in accordance with the information that the increased expression of HIF-1α transcriptionally upregulates GLUT1 and glucose uptake in situations

of RVH.[284] Furthermore, as cancer cells exhibit the same metabolic pattern of PAH characterized by high rates of glucose consumption and glycolysis, and once hypoxia plays a crucial role in the cancer cells proliferation, the expression of GLUT1 has revealed to be regulated by hypoxia conditions in a HIF-1α-dependent manner[285], explaining the similar pattern of expression that we obtained.

The correlation between GLUT4 expression and cardiac functional markers, ET-1 and BNP was also established. Both correlations were negative, since the decrease in GLUT4 expression is accompanied by increased expression of ET-1 and BNP due the development of RVH and overload.

c. Treatment with rhNRG1 modulated the morphophysiological changes in monocrotaline-induced PAH

Although we found a significant decrease in the BW of the animals due to MCT-induced PAH consistent with other works[183,282], the treatment with rhNRG1 did not attenuated this decrease in BW observed in the MCT animal group.

According with Fulton *et al.,* (1952) *"ventricular hypertrophy is estimated by weighing the heart as a whole and by measuring the thickness of the ventricular walls*".[286] The rhNRG1 treatment attenuated RV hypertrophy induced by MCT, as shown by the decreased Fulton index and the RV/TL ratio in MCT-induced PAH rhNRG1 treated animals. Due to the persistent increase on afterload caused by the progression of the disease and RVH, the wall stress increases at the same time and the RV becomes thicker due the accumulation of muscle mass[287], which leads to an increase in its weight. rhNRG1 treatment also attenuated the increased weight of lungs due to the development of marked pulmonary oedema in MCT-induced PH, a side effect of MCT. The previous findings are also in agreement with other investigations on MCT-induced PAH animals from our group, were the treatment with rhNRG1 displayed beneficial effects at structural level, namely in the reduction of the hypertrophy and dilatation of RV.[99]

The information provided by the PAVTI and PAAT/PAET echocardiographic parameters, allowed us to verify that the rhNRG1 treatment ameliorated the alterations on

PA blood flow induced by MCT, through the recovery of the pulmonary circulation on those animals by attenuating vascular remodelling.[99] A decrease in both parameters due to MCT-induced PAH was also verified in other two works of our group in the same animal model and is indicative of PA dysfunction.[99,288] Furthermore, the PAAT/PAET ratio is related with RV dilatation and hypertrophy, taking lower values as the degree of hypertrophy progresses[275,289], allowing us to say that the animals from MCT-induced PAH group developed RVH and that the MCT administration had the desired effects. Beyond being associated to the disease severity, the reduction of PAAT may be related with the decrease in capacitance and an increase in impedance of the pulmonary vascular bed, that causes a deceleration of blood flux at early systole.[275,289] Moreover, the increased stiffness of PA may also be a cause for short PAAT.[275] The inner RV diameter (RVIDd), assessed to verify ventricular dysfunction[270], was also increased MCT animals and attenuated by NRG1, which is in line with earlier findings of the role of NRG1 in restoring RV function.[99]

Concerning to TAPSE, a marker for systolic RV function[281,290] related with the RV contractility capacity[249], it was also decreased in MCT group constituting an evidence for RV decompensation. However, the effects of rhNRG1 did not attenuated this decrease. Usually, the decrease in the displacement of the tricuspid ring towards the apex of the RV during systole, occurs as a consequence of RVH, once in this state the radial forces increasingly contribute to maintain RVEF and to wall stress, what may be an explanation for the decrease in TAPSE.[269] Furthermore, the elliptical deformation of the tricuspid valve supporting structures due to RVH that occurs in PAH, predispose the patients to tricuspid valve leaflet tenting that triggers tricuspid regurgitation.[291] The reflux of blood by the tricuspid valve at each systole is a condition that affects about 60% of patients with severe symptomatic idiopathic PAH, which is also associated with adverse RV remodelling and worst outcome of the disease.[291,292]

So, the treatment with rhNRG1 attenuated the severity of this disease, as it evidenced from the beneficial effects of rhNRG1 on PA and RV remodelling and in overall cardiac function. Beneficial effects of rhNRG1 were evident both at the functional and at the structural level. An experiment that evaluated the expression of NRG receptors ErbB2 and ErbB4 revealed that in failing human heart myocardium the expression of this receptors is downregulated due to their reduced phosphorylation.[261] These findings may constitute a

reason for the phenotype observed in the animals treated with rhNRG1, once it is known that the signalling cascades as the MAPK or PI3K/Akt pathways activation depends on NRG1/ErbB system and its activation by phosphorilation.[241,242,244]

d. rhNRG1 regulated systemic glucose concentration in MCT-induced PAH

The suppression of mitochondrial GO and the subsequent increase in glycolysis, due to hypoxia conditions in PAH, constitutes an hallmark of the increased glucose metabolism in cases of cardiac hypertrophy and in remodelled RV, being also associated with the impairment of RV function.[147,178,192]

The OGTT allowed the acquisition of essential data to evaluate the systemic glucose metabolism and the detection of glucose intolerance in healthy and diseased animals. The fasting blood glucose analysis was performed to evaluate if the all animals are in the same conditions and were fasted at the beginning of the test. As no differences were found between MCT-induced PAH animals and non-diseased control animals, it means that all of them are in the same conditions at the beginning of the test. If differences were detected in this parameter, as an increase of fasting blood glucose in MCT animal group, we would be dealing with hyperinsulinemia and impaired glucose metabolism.[178]

After the oral glucose load, glucose values increased in all animals from all the experimental groups. However, the metabolization of glucose administered was slower in MCT-induced PAH animals compared with MTC rhNRG1-treated group, as expected. Furthermore, blood glucose concentrations did not fall to baseline levels after the 120 minutes as it was supposed, pointing to an the presence of a insulin resistant phenotype[293] in both MCT-induced PAH groups. Based on these results, we can conclude that in our study, the MCT animals demonstrated insulin resistance and that rhNRG1 treatment reduced insulin resistance in MCT animals, but not for CTRL group values.

Glucose response in each group was given by the area under the curve (AUC) obtained from the postprandial glucose test, which represents an index of whole glucose excursion after glucose loading that allows the acquisition of glycaemic index.[294] From this analysis we obtained that the AUC in the MCT-induced PAH group was significantly increased in comparison with the control individuals, indicating the existence of insulin

resistance in this animal group. However, the treatment with rhNRG1 influenced the whole-body glucose metabolism and the MCT animals treated with rhNRG1 demonstrated a significant improvement in glucose tolerance following oral glucose loading, what turns our study consistent results are consistent with studies showing improved glucose uptake in animals treated with NRG1. Although the studies that correlate insulin resistance with PAH are scarce, our findings are in accordance with a recent study from Heresi *et al.*, that evaluated the glucose tolerance and the insulin resistance in humans with IPAH, and concluded that the individuals with IPAH had a higher rate of impaired glucose tolerance.[178] In an *in vivo* model of diabetes/dyslipidaemia in mice, the acute treatment with NRG1 also improved glucose tolerance in fasted mice, and in conditions of glucose intolerance the NRG1 markedly reduced the glycaemic response, reducing the AUC.[295] Furthermore, an *in vitro* study that evaluated the effects of the treatment with NRG1 in glucose tolerance in adult and old rats, revealed that the treatment with NRG1 improved the glucose tolerance in both groups[256], demonstrating the same effects of NRG1 in glucose metabolism as ours. This effects of NRG1 may be due to his role on the modulation of glucose uptake, as NRGs may induce the GLUTs translocation to plasma membrane in muscle cells, especially GLUT4, exerting a role similar to insulin.[241,242] At least, in a study in a model of breast cancer on L6E9 muscle cells in rats, the treatment with NRG1 induced the translocation of GLUT4 to the plasma membrane via the ErbB3/PI3K-dependent signalling pathway to the same extent as insulin, what increased the glucose uptake. In the same study samples of soleus muscle were incubated in the absence or presence of NRG and/or insulin, and NRG treatment significantly increased glucose uptake due to effects on glucose transport by modulation of GLUTs.[249]

mRNA levels of IRS 1 and 2 are also related with insulin resistance. While we did not detected differences in their expression in RV, their expression in the soleus muscle has followed a different pattern. In the soleus muscle from MCT non-treated group, we found decreased IRS1 and IRS2 mRNA expression in comparison with control group. As the IRS1 and IRS2 play a role in the mediation of insulin action in peripheral tissues[230] these results are in agreement with the OGTT results for MCT non-treated group.

According with the literature, the IRS1 and IRS2 downregulation may be related with insulin resistance mechanisms. For example, in skeletal muscle, an increase in aldosterone

concentration has the ability to downregulate IRS1 and 2, once it targets pancreatic β-cells insulin producers, downregulating insulin production, that will decrease the phosphorylation of IRS and interfere the PI3K/Akt signalling pathway. This inactivation of PI3K/Akt signalling culminates in a decrease in NO and can interfere with the muscle contractility. So, insulin resistance is responsible for impairing the input of glucose into the cell as well as the sensitivity of IRS/PI3K/NO signalling pathway.[115] In soleus muscle from MCT rhNRG1-treated group animals, IRS1 mRNA expression remained decrease in comparison with the CTRL group, so, in our study the treatment did not demonstrated modulation of the expression of this gene. However, a study that evaluated IRS1 expression in L6E9 and C2C12 myocytes, revealed that the cells treated with NRG demonstrated an increased expression of IRS1 due to its increased insulin-stimulated phosphorylation, what promoted the IRS1 binding to the p85 subunit of PI3K Ser473-PKB phosphorylation at a submaximal insulin concentration, and the continuity of the signalling pathway.[136] Furthermore, a study in transgenic Ren2 rat revealed that in situations of insulin resistance, the decreased phosphorylation of IRS1 in muscle cells will decrease the Akt activation and phosphorylation, what may be related with the decreased GLUT4 expression, once they are not recruited due to insulin resistance, what results in glucose uptake impairment.[296] Thus, based the findings from other studies, the treatment with rhNRG1 on MCT-induced PAH animals could have modulated the IRS1 expression by the regulation of PI3K/Akt pathway, however, we did not verified this in our study.

e. rhNRG1 is involved in the regulation glycolytic pathway genes expression

In PAH, the RV is characterized by abnormal energy metabolism.[37,38] The Warburg effect concerns the cessation of mitochondrial OXPHOS, supplying catabolic needs of hyperproliferative cells with an alternative glucose metabolism, the glycolysis.[53,139] The accelerated glucose metabolism under aerobic conditions is one of the hallmarks of cells from RV and maybe skeletal muscle in PAH situations.[177,297] In PAH, the underlying metabolic derangements originated evolve from the progress of this disease to the end-stages[4], encompassing not only the RV but other tissues of the organism, such as pulmonary arteries, LV or skeletal muscle.[39] However, glycolytic metabolism mechanism in RV in PAH is not clear and is still unknown. Once that little is known about the details of the molecular

mechanism of PAH development, we evaluated the mRNA expression of several genes to relevant to the glycolytic pathway, aiming to identify metabolic shifts, like the enhanced glycolysis and glucose uptake that follows the suppression of mitochondrial GO. The evaluation was performed in four different tissues: RV, soleus muscle, gastrocnemius muscle and lung. Information about the mRNA gene expression analysis of the gastrocnemius muscle and lung are not shown once no significant data were obtained. Furthermore, we also studied the effects of the treatment with rhNRG1 in the expression of each gene analysed to assess if there is any modulation by this treatment.

-rhNRG1 modulates glycolytic pathway genes expression in soleus muscle in PAH

In PAH, the elevated glycolysis is required to provide sufficient amounts of metabolic intermediates to support anabolic processes of the cells.[297] We evaluated the expression of the glycolytic genes in soleus muscle, and the biggest part of them did not demonstrated alterations between the different experimental groups.

Surprisingly and contrary to expectations face to the alterations on RV, in soleus muscle we did not detect any differences in mRNA expression of HIF-1α, GLUT1 and GLUT4 between the animal groups in study. The transcription factor HIF-1 is the main inductor of glycolysis under low oxygen conditions, acting through the upregulation of genes that encode GLUTs.[298,299] The levels of HIF-1α are similar between all animal groups in study, what means that the hypoxia conditions were not as much severe in this tissue, once HIF-1α expression only increase during exposure to hypoxia.[298] However, it is know that the HIF-1α can be stabilized in many cell types during systemic hypoxia.[341] One example of this stabilization in hypoxia was detected by two studies in cultured cell lines, HeLa, SiHa, Sk-Hep-1, HT1080 and Hep3B in one study, and line cells from hepatocarcionoma. Both investigations showed an interaction between Sirt1 and HIF-1α proteins that modulate their gene expression, in what the first one binds to the second one, deacetylating it, what diminishes the accumulation of HIF-1α and decreases the expression of its target genes, as GLUT1. This allow us to say that Sirt1 activation is necessary for the accumulation of HIF-1α in hypoxia conditions.[300,301] Though, we also analysed Sirt1 in soleus muscle tissue and we do not detect significant alterations in its mRNA expression.

Glycolysis is a multi-regulated pathway, composed by three rate-liming steps catalysed by HK1 and HK2, PFKm and PKm, which act sequentially throughout the metabolic process.[302] Of these four enzymes analysed, only the HK2, which is mainly found in skeletal muscle[190], displayed a decreased expression in the MCT-induced PAH group treated with rhNRG1, to values similar to those in CTRL group. In a study in humans with type 2 diabetes mellitus and insulin resistance, the analysis of mRNA expression of HK2 in skeletal muscle from basal and insulin-stimulated states revealed a decrease in its expression.[191] The literature reported that the NRG1 is responsible for inducing the activation of Ras/Raf/MEK/MAPK and PI3K signalling cascades.[172,241] A study described the involvement of these pathways in the regulation of HK2 expression in embryonic fibroblasts, were the oncogenic Ras expression significantly increased HK2 expression through the activation of PI3K and MAPK signalling, and the deletion of HK2 after the expression of oncogenic Ras reversed oncogenic transformation.[297] The investigators concluded that HK2 is required for oncogenic KRas-driven lung tumorigenesis.[297] The same study investigated the effects of HK2 in a mouse model for breast cancer were induced by activated oncogenic driver ErbB2/Neu, and the HK2 expression is significantly elevated in the tumour tissues and non-expressed in the control. When they deleted HK2, a regression in tumour development occurred, they conclude that HK2 is required for the oncogenic ErbB2-driven mammary gland tumorigenesis in vivo.[297] In our study, these findings may be a clue on how the HK2 and rhNRG1 interact and how this interaction could be beneficial to ameliorate PAH.

From the different LDH isoforms of the enzyme responsible for the conversion of pyruvate into lactate, only LDHb mRNA expression has demonstrated alterations between groups. Although no changes were detected in LDHb expression in MCT-induced PAH non-treated animal group, we observed that the treatment with rhNRG1 attenuated the expression of LDHb in MCT-induced PAH animals in comparison with CTRL group, what implies an increase in pyruvate. This attenuation in LDHb mRNA expression by rhNRG1 evidences one of the interactions of this treatment with the Warburg effect, once in this metabolic shift, the pyruvate is catalysed into lactate by LDH, and then lactate is transported to extracellular ambient, rising the acidity of the medium and favouring the abnormal proliferation of cells. Once the rhNRG1 decreases lactate production, the pyruvate is transported to the mitochondria, were it may be catalysed into acetyl-CoA by PDH and enter to the TCA cycle

to complete oxidization to CO_2, H_2O, and ATP.[78,147] In a study with muscle-specific transgenic mouse lines and primary skeletal myotubes in culture, the investigators discovered that beyond being involved in lactate homeostasis in the skeletal muscle, LDHb is a GO biomarker regulated by the PGC-1α, being negatively correlated with pH, that increases due to lactate accumulation, and associated to a reduced muscle performance. In the same study, the investigators suggest that LDHb is a regulator of mitochondrial function who acts downstream of the PGC-1α/nuclear receptor regulatory pathway. However, its functional significance in skeletal muscle physiology remains unclear.[303] This decrease in LDHb will reflect in a disadvantage to Warburg effect and, consequently, to the PAH phenotype cells: first, once that lactate concentrations will decrease, this triggers a decrease in NAD^+, co-factor produced by LDH, which is necessary for glycolysis to occur; second, the decreased lactate production, will normalize the acidity values of the cellular environment, constituting a disadvantage for PAH proliferating cells.[207] However, in PAH-associated with RVH, the metabolic switch towards aerobic glycolysis is mediated by the increased expression and activity of PDK, what results in the inhibition of PDH and the formation of acetyl-CoA feed TCA cycle, leading to the accumulation of pyruvate in the inside of the cell.[224] Moreover, in initial stages of PAH, where RVH is not established, the treatment with rhNRG1 may improve the glucose metabolism by the modulation of Warburg effect.

The remaining analysed genes did not show differences between the experimental groups in our study, however, another study in MCT-induced PAH, demonstrated differences in mRNA expression of Sirt1, PGC-1α, NRF1 and Tfam in gastrocnemius muscle from MCT animals with compensated and decompensated RV function.[104] One explanation for this difference may reside in the time of response of MCT to the disease development, once these modifications were observed after 4 weeks of treatment with MCT, while our study only had the duration of 3 weeks.

-rhNRG1 is responsible for the modulation of some glycolytic pathway genes expression in RV

When cells are subjected to hypoxia conditions as the ones observed in PAH, they must undergo metabolic adaptations to survive. Indeed, part of this adaptation involves upregulation of genes that encode the enzymes required for anaerobic glycolysis.[304]

In the present study, the RV GLUT1 mRNA expression was significantly increased in MCT animals and was attenuated by the treatment with rhNRG1, as explained above. The data about mRNA expression of GLUT1 that we obtained are consistent with the literature, that explains that GLUT1 mRNA increases in PAH due to pressure overload and hypertrophy[103,135], that we also verified in MCT-induced PAH animals. Furthermore, the HIF-1α activation favours glycolysis through the increase in GLUT1 transcription.[192] Piao *et al.*, (2013) detected an increased mRNA expression of GLUT1 in MCT-RVH induced group of rats[224], which makes our data consistent with those from other authors. Furthermore, in two different studies with a model for RVH without PAH, that was achieved through the PAB characterized by a metabolic shift from GO to FAO and glycolysis, an increased expression of GLUT1 was also found, what was consistent with the elevated rates of glycolysis measured in RVH.[160,212] In another model of MCT-induced PAH, the results were concordant with the ones from the PAB study; it was discovered that the increased glycolysis in the RV of MCT group, that was achieved by FDG uptake, was accompanied by the increased levels of GLUT1 mRNA expression.[212] This allow us to say that our MCT-group displayed elevated levels of GLUT1 to respond to the high glucose demands necessary for glycolysis in cells. The attenuation of GLUT1 expression by rhNRG1 treatment was due the inhibition of PI3K/Akt signalling pathway, once PI3K/Akt is involved in the promotion of cellular glucose uptake by GLUT1[305], what plays effects on the reduction of glucose uptake, cell growth and proliferation. Furthermore, NRG1 effects on glucose uptake were assessed in an *in vitro* study, were the glucose uptake was completely abolished in situations of PI3K inhibition.[253] In contrast, the PI3K inhibition may also trigger insulin resistance and glucose intolerance.[254] This increase in GLUT1 expression in RV is necessary for increase glucose transport into the cytosol to support the less energetically efficient glycolytic metabolism of RVH. Furthermore, the increase in glycolysis will produce more lactate that

will reduces RV contractility[160], what was also proven by the reduction of TAPSE in MCT-induced PAH groups.

We found a decreased GLUT4 mRNA expression in MCT-induced PAH animals that was attenuated and increased by rhNRG1. During the adaptation to the high demand of glucose, as it occurs in the initial stages of PAH, the GLUT4 expression increases[183], however, there is a tendency to a decrease in its expression as the disease progresses to cardiac hypertrophy and to HF.[215] This decrease in GLUT4 is also associated with a decrease in the contractility capacity of the cardiomyocytes, which will translate into changes in TAPSE.[249] In a model of transverse aortic constriction in mice, to describe metabolic alterations due to pressure overload in cardiac metabolism, the investigators reported the existence of reduced GLUT4 in plasma membrane due to reduced Akt phosphorylation, which is induced by PI3K and performed by PDK, what reduces the levels of GLUT4. It demonstrates that the glucose uptake due to GLUT4 translocation was a downstream effect of the PI3K/Akt pathway.[306] The decrease in GLUT4 mRNA expression may also be a predictor for severity of whole-body insulin resistance.[307] Beyond insulin, NRGs are also responsible for inducing the translocation of GLUTs to plasma membrane in muscle cells, potentiating glucose transport and myogenesis.[241,242] This is a reason for the increase in mRNA expression levels of GLUT4 in MCT-induced PAH treated with rhNRG1 group. In an *in vitro* study with L6E9 rat skeletal muscle cell line, the mRNA analysis revealed that in the cellular group treated with NRG the abundance of GLUT4 significantly increased in the plasma membrane, what is consistent with the fact that NRG induces GLUT4 translocation.[249] As GLUT4 depends on insulin or other stimuli from to be activated and translocated from the storage vesicles to the cell membrane through PI3K[153], the treatment with rhNRG1 can act as an intermediary for the activation and translocation of GLUT4, increasing its expression in RV cardiac muscle in order to normalize glucose uptake and metabolism.

The induction and activation of HIF-1α is associated with the development of cardiac hypertrophy.[173] Contrary to what has been observed in soleus muscle, in RV of MCT-induced PAH group we found increased mRNA expression of HIF-1α. Its involvement in the development of PAH was also supported by a study in mice that lack HIF-1α, as they have not developed hypertrophy because they were resistant to hypoxia-induced PH.[308] In a

study with transgenic mice for HIF-1α overexpression, the transgenic group demonstrated an increased rate of anaerobic glycolysis[309], what is correlated with PAH development. The HIF-1α expression was also evaluated in a PAB model to mimic chronic progressive RV pressure overload, such as that which develops in human PAH, and was also increased when compared with non-diseased controls, what demonstrates an uniformity of HIF-1α in both models.[310] Indeed, the increased HIF-1α expression could be an indicator for the increased glucose uptake, once HIF-1α induces the expression of GLUT1, and also for the metabolic switch characteristic of PAH, once it is reported that HIF-1α inhibits PDK and GO.[192] An *in vitro* study developed in C2C12 myocytes in which HIF-1α is knocked down by short-hairpin RNA, revealed that the knockdown of this gene in the skeletal muscle cells resulted in abolition of insulin-stimulated glucose uptake due to the impaired translocation of GLUT4 to the plasma membrane, maybe as a consequence of the reduced phosphorylation of the Akt substrate. From this study, the authors concluded that the HIF-1α is also a key element for GLUT4-mediated glucose uptake in the skeletal muscle cells and may be a target to improve impaired glucose metabolism.[311]

HKs are crucial glycolytic enzymes that play an important role in survival pathways[312], and several reports demonstrated the protective effects of an increased expression of HK, such as the improved resistance of cardiomyocytes against ischemic injury and apoptosis.[313] Insulin is responsible for the activation of HKS in isolated rat hearts[314] and the HIF-1α activation favours glycolysis through the increase in HKs transcription.[192] In comparison with the CTRL group, we found increased HK1 and HK2 mRNA expression in both MCT-induced PAH groups. The MCT-induced PAH rhNRG1 treated group also displayed increased expression of HK2 in relation to MCT-induced PAH group. Our analysis is, in part, coherent with other studies, in what they found that both HK1 and HK2 mRNA expression were increased in an MCT model.[224] Furthermore, in a study with a model of PAB, was also evidenced an increased expression of HK1, being this increase highlighted as one of the indications for RVH.[160] In an MCT-induced PH model in rats, the increased expression of HK1 was also reported in the MCT animal group.[38] As previously mentioned, the elevated mRNA expression of HK2 is related with some cancers, and a study in human cancer lung cell line A549 demonstrated that their expression is dependent of HIF-1 mechanisms, relating increased expression of HK2.[315] A study in cardiomyocytes demonstrated that the increase in HK2 occurs due to the association of the

Akt with the mitochondria, that posteriorly recruits and phosphorylates HK2, activating it. Then, the activated HK2 displays kinase activity and protects cardiomyocytes against apoptotic Bcl-2 proteins, such as Bax and Bak.[313] Furthermore, the HKs are speed-limiting enzymes of the glycolytic pathway, and its expression can induce a downstream cascade amplification reaction, providing more ATP to remodel myocardial cells, being this a reason to have increased RV expression oh HKs in cases of hypertrophy.[38,160] So, the increased expression of HKs may be a mechanism for the maintenance of remodelled cells in the RV, that was not attenuated by NRG1.

The PFKm is one of the primary regulators of glycolytic rate. In contrast with soleus muscle, in RV of MCT-induced PAH group there was a decrease in PFKm mRNA expression and no changes in its expression were evidenced by rhNRG1. A study in hypoxia/Sugen5416 model demonstrated an increased mRNA expression of PFKm in RV.[173] However, in a knockout model for PFKm gene, the decreased levels of PFKm trigger an increase in glucose-6-phosphate and in glycogen storage, and in young mice, the knockout of this gene lead to the development of cardiac hypertrophy and enlargement.[316] A study in mice with transgenic HIF-1α to analyse its influence if overexpression of this gene, showed that the increase in HIF-1α mRNA expression is accompanied by an increased expression of PFK in transgenic mice, as the cellular metabolism changed dramatically in response to hypoxia to increase anaerobic glycolysis.[309] So, our evaluation of mRNA expression of PFKm demonstrates some disparity between the expression of PFKm and the other glycolytic pathway genes, since all others point to an increase in glycolysis in MCT animals.

PKm is responsible for catalyse the final and irreversible step of glycolysis: the dephosphorylation of phosphoenolpyruvate into pyruvate.[182,207,298] The mRNA expression of PKm was also altered in the RV analysis and rhNRG1 accentuated the increase in its expression observed in MCT-induced PAH group. In both MCT groups, the increase in PKm expression will lead to an increase in pyruvate production, that may be converted into lactate and favour the exacerbated cellular proliferation.

The mRNA expression of the glycolysis implicated genes analysed in RV that displayed significant differences between experimental groups, have in common the fact that they are related to the development of RV hypertrophy in MCT-induced PAH group. As

BNP overexpression at cardiac level is markedly upregulated in response to ventricular hypertrophy or overload, is expected that it is upregulated in PAH.[32]

Although we have found no alterations in the RV mRNA expression of the other genes involved in glucose metabolism, there are studies that refer the existence of changes in its expression in situations of RVH. We do not find differences in ET-1 mRNA expression maybe due to the great standard deviation associated with the MCT group.

In an MCT rat model for the study of PH induced RV failure, the mRNA expression of LDHa was found to be significantly increased in MCT animals. A study in MCT-induced PH in male Wistar rats, demonstrated differences in mRNA expression of Sirt1, PGC-1α, a transcriptional coregulator and a master regulator of mitochondria[153,163], and Tfam in RV form MCT animals with compensated and decompensated RV function.[104] However, the duration of the protocol of this study was 4 weeks, while in our study sample collection was performed at the end of the third week after MCT administration. This might be a reason for the different results, as the disease progression stage induced by MCT may be variable depending on several factors.

Two different models, an MCT-induced PH and a PAB model revealed that the RV reliance on glycolysis is evidenced by the increased expression of GLUT1 and HK1.[160,212] So, as we obtained the same results in our study, we may relate the results with the other genes which are altered and infer that our MCT-induced PAH group switched their glucose metabolism towards glycolysis, as expected. However, we were not able to confirm if the RV of the animals in study had significant impairment of mitochondrial metabolism, especially the animals of the MCT-induced PAH group, once we did not verify alterations in both PDHα1 or PDHβ expression. The inhibition of PDHα1 or PDHβ activity is characteristic of Warburg effect and one of the causes for mitochondrial impairment in PAH, switching cell metabolism toward glycolysis.[317]

-Glycolytic pathway genes mRNA expression in RV is related with morphophysiological changes resulting from the development of PAH in monocrotaline model

Our data demonstrated a significant correlation between the RV hypertrophy indicator, Fulton index, and genes as GLUT1[103,135], GLUT4[215], HIF-1α[173,308], PFKm[316], PKm[318], LDHd[317], IRS1[319], BNP[32,201,257] and also ET-1[86], as both are indicators of hypertrophy, which is in line with the literature analysed. These data confirmed that increased RV glucose uptake and metabolism are related to the impairment of RV and with RVH, as we previously demonstrated in the analysis of mRNA expression and in the morphophysiological evaluation performed.

Moreover, our data showed that there is a significant correlation between TAPSE and gene expression of genes as GLUT1[160], GLUT4[249], HIF-1α, HK1, HK2, PFKm, PKm, LDHb, LDHd, IRS2 and BNP. These data confirm that in RV, the glycolysis is related with RV function during hypertrophy and that all of them might contributed to a decrease TAPSE values, what is reflected in alterations on the contractile cappacity of the RV in PAH.

The CO also displayed a correlation with GLUT1, GLUT4[283], HIF-1α[35,39,42], PKm, PDHβ, PGC-1α and BNP[277]. These data confirm that as the disease progresses, CO gradually decreases as long as the RVH transits from cRVH to dRVH.[44,236]

RV mRNA expression also shown that there are genes whose expression is correlated with each other, such as the GLUT1 and GLUT4[153,183], the GLUT1 and HIF-1α[304], and GLUT4 and HIF-1α[311], as we mentioned above during analysis of gene expression.

2. Characterization of the chronic hypoxia model

As explained before, in our study we performed the evaluation of morphological characteristics of the MCT model. A similar methodology was performed in a hypoxia model for PH, in order to investigate the existence of differences in the development of the disease between the two experimental models. Thus, in the same way that we did in MCT model, we started the model evaluation by its morphometric characterization.

As previously mentioned in materials and methods section, some animals were treated with Sugen5416 and exposed to hypoxia. Due to Sugen5416, an antiproliferative treatment, H/S rats develop progressive pulmonary vascular angio-obliterative lesions, PH and RV dysfunction, that may culminate in HF.[92,290] As the hypoxia model is more specific for PH development, the treatment with Sugen5416 in hypoxia model induced the development of a severe and sustained form of PAH and reproduce with greater degree of similarity the model of MCT-induced PAH.[320,321]

a. Progression of PAH in chronic hypoxia/Sugen5416

The morphological analysis revealed that at the end of the experimental protocol, the BW of the H/S animals was decreased, similarly to wat occurred in MCT animals, and as it is characteristic of PAH. There are experiments in this animal model that revealed a decrease in BW in H/S group[310], while that in others the decrease is so smooth and without statistical significance to infer that the combination of Sugen5416 with hypoxia exerts effects on BW reduction in the same way as MCT.[322] Through this evaluation, we also can conclude that the hypoxia treatment severity is lower than hypoxia/Sugen5416, once the loss of BW is one of the consequences of the disease development.

The RV hypertrophy was evident in H/S animal group by the increased Fulton index. The same results were achieved by other studies in hypoxia/Sugen5416 models[320,322–324], relating the development of PH and hypertrophy with Sugen5416, as it was suggested by the literature.[92,290,325] The RV/TL index, also proportional to the hypertrophy degree, has demonstrated to be coherent with Fulton index data for the increased hypertrophy development in H/S animal group. Once again, through this analysis, we can perceive a clear difference in the development of hypertrophy caused by chronic hypoxia, which is very similar to the control animals. The verified alterations reflect that chronic hypoxia and hypoxia/Sugen methods lead to development of PAH with different pathogenicity levels, being chronic hypoxia-induced PAH less severe than hypoxia/Sugen-induced PAH, as it was previously described by other study. [288]

In MCT model, Lung/TL ratio was also evaluated to infer adverse changes in lungs triggered by the MCT administration.[270,326] However, the analysis of this parameter in H

group revealed that the animal exposed to hypoxia developed pulmonary oedema, which was reflected in the increase in lung weight of this animal groups.

Therefore, our results confirmed that hypoxia/Sugen5416 model is also able to reproduce RV functional changes that are generated in PAH development.

b. GLUT1 mRNA expression is altered in gastrocnemius muscle from chronic hypoxia/Sugen5416 animals

In normal situations, the prolonged exposure to hypoxia is related with an enhancement of transcription of GLUT1 and GLUT4 in the skeletal muscle.[327] During the analysis performed in gastrocnemius muscle, we only found alterations in GLUT1 expression, that surprisingly was decreased in H group. The only difference between the results of mRNA analysis in skeletal muscle of this model and MCT model, was the decreased expression of GLUT1 in hypoxia model. It may suggest that maybe the skeletal muscle is not the primary tissue to develop the glycolytic switch in PAH, once the glucose uptake was not increased, otherwise we would have obtained different expression values for GLUTs.

c. HIF-1α and PGC-1α mRNA expression is decreased in lung from chronic hypoxia/Sugen5416 animals

A study in a model of PAH in mice induced by hypoxia/Sugen5416 revealed that after 3 weeks of hypoxia exposure, the lungs from H/S and H animals demonstrated significantly higher FDG uptake than in N group, being this increase more significant in the animals of H/S group and indicative of increased glycolysis.[321] Hence, we performed the analysis of some target genes involved in glycolysis, and it doesn't revealed altered expression of GLUT1 and GLUT4, what means that is unlikely to have increased glucose metabolism in the lung, once one of the glycolysis characteristics is the increased in glucose uptake to support the energetic demands.

We found a decrease in both pulmonary HIF-1α and PGC-1α mRNA expression in the H/S animal group. Despite the exact role of HIF-1α in lung injury is not well stablished, it is known that it is an important mediator of the hypoxic response in animal cells and plays

a central role in controlling the glycolysis pathway in hypoxia conditions.[328] So, as the other genes analysed point to the absence of glycolytic metabolism, this decreased mRNA expression of HIF-1α may have occurred by the same reason. We did not find any publication showing variations in these two genes expression in hypoxia models. However, increased PGC-1α expression is reported in tissues with high energy demands, and its expression is increased in conditions of higher energy requirements.[172] Thus, as we were able to verify through the GLUTs mRNA expression in lungs, the glucose uptake did not increased in any animal group and the glucose metabolism did not switched toward glycolysis, what may be a reason for a decrease in PGC-1α expression.

d. Glycolysis is impaired in RV from hypoxia/Sugen5416 animals

The rate-limiting step for glucose metabolism relies on its transport into the cardiomyocytes through specific carrier-mediated transporters, the GLUT1 and GLUT4. In parallel with the increased PVR due to PAH development, RV myocytes also develop a mitochondrial metabolic phenotype similar to that observed in lung samples. Faced with this, we performed GLUT1 and GLUT4 analysis in RV in the animals from chronic hypoxia model. While the mRNA expression of GLUT1 was increased in the H/S group, the GLUT4 expression was decreased. In a study in a model of chronic hypoxia, an increase in GLUT1 mRNA expression was also found in both 2 and 14 days after hypoxia exposure, and GLUT4 mRNA expression seemed not to be influenced by hypoxia.[329] Our results demonstrated a variation in GLUT1 and GLUT4 very similar to the occurred in the RV hypertrophied in MCT-induced PAH model and are, in part, concordant with the study mentioned. Thus, these alterations may suggest an increase in glycolysis in RV, in the same way that occurs in MCT-induced PAH model.

During the exposure to chronic hypoxia, the HIF-1α expression contributes to de development of PH.[299] However, in our study the HIF-1α demonstrated a decreased mRNA expression in RV from H/S animals. The HIF-1α expression was evaluated in a PAB model to mimic chronic progressive RV pressure overload, such as that which develops in human PAH and compared with a model of chronic hypoxia/Sugen5416, and it was found that HIF-

1α mRNA expression was increased in both conditions, but with more magnitude in the RV from chronic H/S animals.[310]

It is known that mitochondria plays a critical role in energy metabolism and responds to hypoxia damage stimulus.[232] PGC-1α, which is abundantly expressed in heart tissue, plays a critical role in the control of the expression of genes involved in the mitochondrial ATP-generating pathway in the heart. Furthermore, in a chronic hypoxia model developed in H9c2 cell line and in cultured primary cardiac myocytes to study Tetralogy of Fallot, which is also characterized by RVH, the hypoxia conditions significantly induced the expression of PGC-1α, being this increase accompanied by an improvement in mitochondrial biogenesis in the cultured cardiac myocytes.[330] However, it was documented that in situations of cardiac hypertrophy and HF, the mitochondria response is based on the downregulation of genes involved in mitochondria biogenesis and oxidative metabolism, and PGC-1α is one of those genes.[153,163] Moreover, in our study we found that PGC-1α mRNA expression was decreased in the RV from H/S group in comparison with N group. This decreased mRNA expression suggests the existence of decrease in FAO under hypoxia/Sugen5416 conditions, evidencing the metabolic switch towards glycolysis in RV of the animals in this group.

Furthermore, a study in rats with severe PH also clarified the metabolic switch characteristic of PAH by using glucose analogue FDG and 14-(R,S)-[^{18}F]fluoro-6-thia-heptadecanoic acid (^{18}F-FTHA), glucose and FA analogues metabolism, respectively. It revealed that a significant decrease in ^{18}F-FTHA uptake was accompanied by an increase in FDG uptake in the RV, what supports the metabolic switch towards glycolysis in RV cardiomyocytes[325], as we also demonstrated in MCT and hypoxia/Sugen5416 animal models.

e. rhNRG1 regulated plasma glucose concentration in hypoxia/Sugen5416 animals

An additional work was performed to evaluate the effects of the treatment with rhNRG1 in glucose metabolism in chronic hypoxia/Sugen5416 animal model, having been defined two groups of animals were defined: H/S+BSA and H/S+rhNRG1. To evaluate the differences in systemic glucose metabolism and detect glucose intolerance between the two groups, we performed an OGTT. The fasting blood glucose analysis, that was performed to

evaluate if all the animals are the same conditions and were fasted at the beginning of the test, did not revealed differences between the two groups, as expected.

After the oral glucose load, glucose values increased in both animal groups. However, the metabolization of glucose administered was slower in H/S+BSA group, in the same way that it has occurred in MCT-induced PAH rats non-treated with rhNRG1. Furthermore, the blood glucose concentrations of H/S+rhNRG1 group were significantly lower when compared to the H/S+BSA group, what means that the animals that received the treatment of rhNRG1 displayed improved glucose metabolism, in the same way it has occurred in MCT model. Additionally, blood glucose concentrations did not fall to baseline levels after the 120 minutes, meaning that the animals may have developed insulin resistance.[293] Based on these findings, we can suggest that the H/S+BSA animals developed insulin resistance that was attenuated by rhNRG1 treatment, as we verified in the H/S+rhNRG1 group, similarly to what we found in the MCT model.

The analysis of the AUC allowed us to infer the response to glucose load in each group[294] and the data revealed that in H/S+rhNRG1 group the response to glucose was better in comparison with H/S+BSA group, that displayed higher values for glucose AUC. These data demonstrate that the H/S+rhNRG1 animals have a higher glucose tolerance which is consistent with studies showing improved glucose uptake in animals treated with NRG1.[256]

f. rhNRG1 treatment effects in RV GLUTs expression in hypoxia/Sugen model

The treatment of H/S animals with rhNRG1 did not modulated the RV expression of GLUT1 and GLUT4 as it was previously demonstrated in MCT model. The GLUT1 maintained it high expression in the H/S+rhNRG1 animal group in comparison with the H/S+BSA group, while the GLUT4 followed the inverse pattern of expression in the same groups, and its decrease was no attenuated by the effects of the treatment with rhNRG1.

However, when we examined the mRNA expression of rhNRG1 in the RV, it also displayed lower values of expression in H/S+rhNRG1 treated animals in comparison with H/S+BSA group. Similar results were verified in other study of our group in an MCT-induced PAH model, where was also found a significant decrease in NRG1 expression in

the diseased animal group treated with rhNRG1.[99] The increased expression of NRG1 in RV from H/S+BSA animals may be associated with poorer RV function as a consequence of the increase in afterload and myocardial stress.[99] A decrease in mRNA expression of rhNRG1 in the treated group may occur due to a mechanism of negative feedback related to the rhNRG1 exogenous administration.

3. Limitations

During the development of this work we faced some limitations. Some of them were proper of the models used and are described previously, as the development of pathological changes in lungs as pulmonary oedema, that we identified through the morphological analysis in both models used. Another limitation was the number of animals in each experimental group, which can be countered by an increase in the number of animals for each group.

During the molecular analysis performed, although the primers used were specifically designed for this animal model, some primers did not work properly. The Tfam primer did not work and for this reason, no data regarding Tfam expression are documented.

Conclusion

In the present study, we observed that RV GLUT1 and GLUT4 mRNA expression is altered in PAH and was similar between the MCT and hypoxia/Sugen5416 animal models, being this related with the development of RVH. However, the treatment with rhNRG1 only attenuated GLUTs expression toward normal values in MCT-induced PAH model. The expression of GLUT1 and GLUT4 is correlated with cardiac markers of disease, while the glycolytic pathway genes are correlated with the morphophysiological changes resulting from the development of PAH in MCT model.

Little is known about the details of the molecular mechanism of PAH development and how the expression of some genes relevant to the glycolytic pathway are related with this pathophysiology. From the analysis of some glycolytic pathway genes, we conclude that beyond GLUTs, several genes are related, not only with the Warburg effect, but also with the disease progression. We also found that the treatment with rhNRG1 attenuated the changes in some glycolytic pathway genes, resulting in an improvement in glucose metabolism.

The glucose tolerance evaluation revealed that the animals with PAH from both models are insulin resistant, and the treatment with rhNRG1 regulated systemic glucose concentration in both animal models.

Besides, as our study was performed in two animal models, we conclude that MCT-induced PAH and hypoxia/Sugen5416-induced PAH induced similar changes on RV, both at the morphophysiological and at the metabolic level.

We can conclude that NRG1 pathway may represent a potential therapeutic target in PAH mainly in the reduction of insulin resistance associated with this disease.

Bibliographic references

1. World Health Organization. Cardiovascular diseases (CVDs). *WHO* (2017). Available at: http://www.who.int/mediacentre/factsheets/fs317/en/. (Accessed: 15th February 2018)
2. Handler, C. & Coghlan, G. *Pulmonary Hypertension*. *A Textbook of Cardiovascular Medicine* (Oxford University Press Inc., 2012).
3. Guignabert, C. *et al.* New molecular targets of pulmonary vascular remodeling in pulmonary arterial hypertension: Importance of endothelial communication. *Chest* **147,** 529–537 (2015).
4. Chan, S. Y. & Rubin, L. J. Metabolic dysfunction in pulmonary hypertension: from basic science to clinical practice. *Eur. Respir. Rev.* **26,** 170094 (2017).
5. Barst, R. J. *Pulmonary Arterial Hypertension: Diagnosis and Evidence-Based Treatment*. (British Library Cataloguing, 2008). doi:10.1019/200530071
6. Montani, D. *et al.* Pulmonary arterial hypertension. *Orphanet J. Rare Dis.* **8,** 97 (2013).
7. Kirson, N. Y., Birnbaum, H. G., Ivanova, J. I. & Williamson, T. Prevalence of pulmonary arterial hypertension and chronic thromboembolic pulmonary hypertension in the United States. *Curr. Med. Res. Opin.* **27,** 1763–1768 (2011).
8. Yafawi, R. El, Knauft, M., Stokem, K., Palminteri, J. & Wirth, J. in *Encyclopedia of Cardiovascular Research and Medicine* (eds. Sawyer, D. & Vasan, R.) 181–194 (Elsevier Inc., 2017). doi:10.1097/MJT.0b013e31820e828c
9. McLaughlin, V. V., Shah, S. J., Souza, R. & Humbert, M. Management of pulmonary arterial hypertension. *J. Am. Coll. Cardiol.* **65,** 1976–1997 (2015).
10. Handler, C. & Coghlan, G. *Pulmonary Arterial Hypertension - the facts*. (Oxford University Press Inc., 2010).
11. Hoeper, M. M. *et al.* A global view of pulmonary hypertension. *Lancet Respir. Med.* **4,** 306–322 (2016).
12. Habib, G. *et al.* Pulmonary Arterial Hypertension in France Results from a National Registry. *Am. J. Respir. Crit. Care Med.* **173,** 1023–1030 (2006).
13. Prins, K. W. & Thenappan, T. WHO Group I Pulmonary Hypertension: Epidemiology and Pathophysiology. *Cardiol. Clin.* **34,** 363–374 (2016).
14. Mcgoon, M. D. *et al.* Pulmonary Arterial Hypertension: Epidemiology and Registries. *J. Am. Coll. Cardiol.* **62,** D51–D59 (2013).
15. Ling, Y. *et al.* Changing Demographics, Epidemiology, and Survival of Incident Pulmonary Arterial Hypertension. *Am. J. Respir. Crit. Care Med.* **186,** 790–796 (2012).
16. Mclaughlin, V. V & Suissa, S. Prognosis of Pulmonary Arterial Hypertension. *Circulation*

122, 106–108 (2010).

17. Thenappan, T., Ormiston, M. L., Ryan, J. J. & Archer, S. L. Pulmonary arterial hypertension: pathogenesis and clinical management. *Br. Med. J.* **360,** (2018).
18. Marques-Alves, P., Baptista, R., Da Silva, A. M., Pêgo, M. & Castro, G. Real-world, long-term survival of incident patients with pulmonary arterial hypertension. *Rev. Port. Pneumol. (English Ed.* **23,** 124–131 (2017).
19. Benza, R. L. *et al.* An Evaluation of Long-term Survival From Time of Diagnosis in Pulmonary Arterial Hypertension From the REVEAL Registry. *Chest* **142,** 448–456 (2012).
20. Genetic and Rare Diseases Information Center (GARD). Pulmonary arterial hypertension. Available at: https://rarediseases.info.nih.gov/diseases/7501/pulmonary-arterial-hypertension. (Accessed: 17th August 2018)
21. Peacock, A. J. & Barberà, J. A. *Therapeutic Strategies in Pulmonary Arterial Hypertension*. (Atlas Medical Publishing Ltd, 2009).
22. McCollister, D. H. *et al.* Depressive Symptoms in Pulmonary Arterial Hypertension: Prevalence and Association With Functional Status. *Psychosomatics* **51,** 339–339.e8 (2010).
23. Badesch, D. B. *et al.* Pulmonary arterial hypertension: Baseline characteristics from the REVEAL registry. *Chest* **137,** 376–387 (2010).
24. Xu, M. *et al.* Role for Functional SOD2 Polymorphism in Pulmonary Arterial Hypertension in a Chinese Population. *Environ. Res. Public Heal.* **14,** 266 (2017).
25. Pezzuto, B. *et al.* Circulating biomarkers in pulmonary arterial hypertension: Update and future direction. *J. Hear. Lung Transplant.* **34,** 282–305 (2015).
26. Santos-Ribeiro, D. *et al.* Pulmonary arterial hypertension: Basic knowledge for clinicians. *Arch. Cardiovasc. Dis.* **109,** 550–561 (2016).
27. Vonk-Noordegraaf, A. *et al.* Right heart adaptation to pulmonary arterial hypertension: Physiology and pathobiology. *J. Am. Coll. Cardiol.* **62,** 22–33 (2013).
28. Pavandeep Kaur Ghataorhe. Metabolic phenotype analysis in patients with pulmonary hypertension Doctor of Philosophy Pavandeep Kaur Ghataorhe. (Imperial College London Hammersmith, 2016).
29. Liu, N., Parry, S., Xiao, Y., Zhou, S. & Liu, Q. Molecular targets of the Warburg effect and inflammatory cytokines in the pathogenesis of pulmonary artery hypertension. *Clin. Chim. Acta* **466,** 98–104 (2017).
30. Thompson, A. A. R. & Lawrie, A. Targeting Vascular Remodeling to Treat Pulmonary Arterial Hypertension. *Trends Mol. Med.* **23,** 31–45 (2017).
31. Xiao, Y. *et al.* PDGF Promotes the Warburg Effect in Pulmonary Arterial Smooth Muscle Cells via Activation of the PI3K/AKT/mTOR/HIF-1α Signaling Pathway. *Cell. Physiol.*

Biochem. 1603–1613 (2017). doi:10.1159/000479401

32. Casserly, B. & Klinger, J. R. Brain natriuretic peptide in pulmonary arterial hypertension: biomarker and potential therapeutic agent. *Drug Des. Devel. Ther.* **3,** 269–87 (2009).
33. Brittain, E. *et al.* Fatty Acid Metabolic Defects and Right Ventricular Lipotoxicity in Human Pulmonary Arterial Hypertension. *Circulation* **133,** 1936–44 (2016).
34. Groot, A. L. G. *et al.* in *The Right Ventricle in Health and Disease* (eds. Voelkel, N. F. & Schranz, D.) 3–18 (Humana Press, 2015). doi:10.1007/978-1-4939-1065-6_1
35. Sutendra, G. *et al.* A metabolic remodeling in right ventricular hypertrophy is associated with decreased angiogenesis and a transition from a compensated to a decompensated state in pulmonary hypertension. *J. Mol. Med.* **91,** 1315–1327 (2013).
36. Galiè, N. *et al.* 2015 ESC/ERS Guidelines for the diagnosis and treatment of pulmonary hypertension. *Eur. Respir. J.* **46,** 903–975 (2015).
37. Gomez-Arroyo, J. *et al.* Metabolic Gene Remodeling and Mitochondrial Dysfunction in Failing Right Ventricular Hypertrophy due to Pulmonary Arterial Hypertension. *Circ Hear. Fail* **6,** 136–144 (2013).
38. Zhang, W. *et al.* Up-regulation of hexokinase1 in the right ventricle of monocrotaline induced pulmonary hypertension. *Respir. Res.* **15,** 4–9 (2014).
39. Paulin, R. & Michelakis, E. D. The Metabolic Theory of Pulmonary Arterial Hypertension. *Circ. Res.* **115,** 148–164 (2014).
40. Naeije, R. & Manes, A. The right ventricle in pulmonary arterial hypertension. *Eur. Respir. Rev.* **23,** 476–487 (2014).
41. Guimaron, S. *et al.* Current Knowledge and Recent Advances of Right Ventricular Molecular Biology and Metabolism from Congenital Heart Disease to Chronic Pulmonary Hypertension. *Biomed Res. Int.* **2018,** 1–10 (2018).
42. Ryan, J. J. *et al.* Right Ventricular Adaptation and Failure in Pulmonary Arterial Hypertension. *Can. J. Cardiol.* **31,** 391–406 (2015).
43. Maria, M. V. Di & Abman, S. H. in *The Right Ventricle in Health and Disease* (eds. Voelkel, N. F. & Schranz, D.) 41–56 (Humana Press, 2015).
44. Fessel, J. P. & Oldham, W. M. in *Pulmonary Hypertension: Basic Science to Clinical Medicine* (eds. Zamanian, B. A. M., T., R. & Waxman, A. B.) 135–145 (Springer, 2016).
45. Grinnan, D., Farr, G., Fox, A. & Sweeney, L. The Role of Hyperglycemia and Insulin Resistance in the Development and Progression of Pulmonary Arterial Hypertension. *J. Diabetes Res.* **2016,** (2016).
46. Rose-Jones, L. J. & McLaughlin, V. V. Pulmonary Hypertension: Types and Treatments. *Curr. Cardiol. Rev.* **11,** 73–79 (2015).

47. Simonneau, G. *et al.* Updated clinical classification of pulmonary hypertension. *J. Am. Coll. Cardiol.* **62,** 34–41 (2013).
48. Price, L., Bouillon, K., Wort, S. J. & Humbert, M. in *Pulmonary Vascular Disorders* (eds. Humbert, M., Souza, R. & Simonneau, G.) **41,** 76–84 (Karger, 2012).
49. Marshall, J. D., Bazan, I., Zhang, Y., Fares, W. H. & Lee, P. J. Mitochondrial dysfunction and pulmonary hypertension: Cause, Effect or Both. *Am. J. Physiol. Cell. Mol. Physiol.* **314,** L782–L796 (2018).
50. Groth, A. *et al.* Inflammatory cytokines in pulmonary hypertension. *Respir. Res.* **15,** 1–9 (2014).
51. Orriols, M., Catalina, M. & Puerto, G. BMP type II receptor as a therapeutic target in pulmonary arterial hypertension. *Cell. Mol. Life Sci.* **74,** 2979–2995 (2017).
52. Feher, A. & Sinusas, A. J. Assessment of right ventricular metabolism: An emerging tool for monitoring pulmonary artery hypertension. *J. Nucl. Cardiol.* **24,** 1990–1993 (2017).
53. Chester, A. H., Yacoub, M. H. & Moncada, S. Nitric oxide and pulmonary arterial hypertension. *Glob. Cardiol. Sci. Pract.* **14,** 1–16 (2017).
54. Maron, B. A. & Leopold, J. A. The role of the renin-angiotensin-aldosterone system in the pathobiology of pulmonary arterial hypertension (2013 Grover Conference series). *Pulm. Circ.* **4,** 200–210 (2014).
55. Rabinovitch, M. *et al.* Inflammation and Immunity in the Pathogenesis of Pulmonary Arterial Hypertension. *Circ. Res.* **115,** 165–175 (2015).
56. Stacher, E. *et al.* Modern age pathology of pulmonary arterial hypertension. *Am. J. Respir. Crit. Care Med.* **186,** 261–272 (2012).
57. Thompson, A. A. R. & Lawrie, A. Targeting Vascular Remodeling to Treat Pulmonary Arterial Hypertension. *Trends Mol. Med.* **xx,** 1–15 (2016).
58. Jonigk, D. *et al.* Plexiform Lesions in Pulmonary Arterial Hypertension Composition , Architecture , and Microenvironment. *Am. J. Pathol.* **179,** 167–179 (2011).
59. Archer, S. L., Fang, Y.-H., Ryan, J. J. & Piao, L. Metabolism and Bioenergetics in the Right Ventricle and Pulmonary Vasculature in Pulmonary Hypertension. *Pulm. Circ.* **3,** 144–152 (2013).
60. Bensley, J. G., Stacy, V. K., De Matteo, R., Harding, R. & Black, M. J. Cardiac remodelling as a result of pre-term birth: Implications for future cardiovascular disease. *Eur. Heart J.* **31,** 2058–2066 (2010).
61. Le, B., Sutherland, M. R. & Black, M. J. Maladaptive structural remodelling of the heart following preterm birth. *Curr. Opin. Physiol.* **1,** 89–94 (2018).
62. Ryan, J. J. & Archer, S. L. Emerging Concepts in the Molecular Basis of Pulmonary Aterial

Hypertension. *Circulation* **131,** 1691–1702 (2015).

63. Han, Y. & Singh, J. Right Ventricular Metabolism : A Brief Review. *Adv. Pulm. Hypertens.* **13,** 185–187 (2015).
64. Rajabi, M., Kassiotis, Æ. C. & Razeghi, Æ. P. Return to the fetal gene program protects the stressed heart: a strong hypothesis. *Heart Fail. Rev.* **12,** 331–343 (2007).
65. Zhou, G., Chen, T. & Usha Raj, J. MicroRNAs in pulmonary arterial hypertension. *Am. J. Respir. Cell Mol. Biol.* **52,** 139–151 (2015).
66. Kazimierczyk, R. & Kami, K. The role of platelets in the development and progression of pulmonary arterial hypertension. *Adv. Med. Sci.* **63,** 312–316 (2018).
67. Soubrier, F. *et al.* Genetics and Genomics of Pulmonary Arterial Hypertension. *J. Am. Coll. Cardiol.* **62,** D13–D21 (2013).
68. Freund-Michel, V., Khoyrattee, N., Savineau, J. P., Muller, B. & Guibert, C. Mitochondria: Roles in pulmonary hypertension. *Int. J. Biochem. Cell Biol.* **55,** 93–97 (2014).
69. Talati, M. & Hemnes, A. Fatty acid metabolism in pulmonary arterial hypertension: role in right ventricular dysfunction and hypertrophy. *Pulm. Circ.* **5,** 269–278 (2015).
70. Chester, A. H. & Yacoub, M. H. The role of endothelin-1 in pulmonary arterial hypertension. *Glob. Cardiol. Sci. Pract.* **29,** 62–78 (2014).
71. Sandoo, A., Veldhuijzen van Zanten, J. J. C. S., Metsios, G. S., Carroll, D. & Kitas, G. D. The Endothelium and Its Role in Regulating Vascular Tone. *Open Cardiovasc. Med. J.* **4,** 302–312 (2010).
72. Goldenberg, N. M. & Kuebler, W. M. Endothelial cell regulation of pulmonary vascular tone, inflammation, and coagulation. *Compr. Physiol.* **5,** 531–559 (2015).
73. Davies, R. J. & Morrell, N. W. Molecular mechanisms of pulmonary arterial hypertension: Role of mutations in the bone morphogenetic protein type II receptor. *Chest* **134,** 1271–1277 (2008).
74. Liang, O. D. *et al.* Endothelial to haematopoietic transition contributes to pulmonary arterial hypertension. *Cardiovasc. Res.* **113,** 1560–1573 (2017).
75. Lai, Y.-C., Potoka, K. C., Champion, H. C., Mora, A. L. & Gladwin, M. T. Pulmonary Arterial Hypertension: The Clinical Syndrome. *Circ. Res.* **115,** 115–130 (2014).
76. Schermuly, R. T., Ghofrani, H. A., Wilkins, M. R. & Grimminger, F. Mechanisms of disease: Pulmonary arterial hypertension. *Nat. Rev. Cardiol.* **8,** 443–455 (2011).
77. Hansmann, G. *et al.* Pulmonary Arterial Hypertension Is Linked to Insulin Resistance and Reversed by Peroxisome Proliferator-Activated Receptor-γ Activation. *Circulation* **115,** 1275–1284 (2007).
78. Leopold, J. A. & Maron, B. A. Molecular Mechanisms of Pulmonary Vascular Remodeling

in Pulmonary Arterial Hypertension. *Int. J. Mol. Sci.* **17,** 1–14 (2016).

79. Tuder, R. M. *et al.* Relevant issues in the pathology and pathobiology of pulmonary hypertension. *J. Am. Coll. Cardiol.* **62,** (2013).
80. Eelen, G. *et al.* Endothelial Cell Metabolism. *Physiol Rev* **98,** 3–58 (2018).
81. Kalidasan Thambiayya. Endothelial dysfunction in pulmonary arterial hypertension (PAH) | The FASEB Journal. *FASEB J.* **29,** (2015).
82. Budhiraja, R., Tuder, R. M. & Hassoun, P. M. Endothelial Dysfunction in Pulmonary Hypertension. *Circulation* **109,** 159–165 (2004).
83. Comhair, S. A. A. *et al.* Human primary lung endothelial cells in culture. *Am. J. Respir. Cell Mol. Biol.* **46,** 723–730 (2012).
84. Morrell, N. W. *et al.* Cellular and Molecular Basis of Pulmonary Arterial Hypertension. *J. Am. Coll. Cardiol.* **54,** S21–S31 (2009).
85. Clavé, M. M. & Lopes, A. A. in *Endothelium and Cardiovascular Diseases: Vascular Biology and Clinical Syndromes* (eds. Luz, P. L. Da, Libby, P., Chagas, A. C. P. & Laurindo, F. R. M.) 439–451 (Elsevier Inc., 2018). doi:10.1016/B978-0-12-812348-5.00029-5
86. McMahon, T. J. & Bryan, N. S. Biomarkers in Pulmonary Vascular Disease: Gauging Response to Therapy. *Am. J. Cardiol.* **120,** S89–S95 (2017).
87. Archer, S. L., Weir, E. K. & Wilkins, M. R. Basic Science for Clinicians Basic Science of Pulmonary Arterial Hypertension for Clinicians New Concepts and Experimental Therapies. *Circulation* **121,** 2045–2066 (2010).
88. Jung, C. *et al.* Arginase Inhibition Reverses Monocrotaline-Induced Pulmonary Hypertension. *Int. J. Mol. Sci.* **18,** 1–13 (2017).
89. Klinger, J. R. & Kadowitz, P. J. The Nitric Oxide Pathway in Pulmonary Vascular Disease. *Am. J. Cardiol.* **120,** S71–S79 (2017).
90. Pluchart, H., Khouri, C., Blaise, S., Roustit, M. & Cracowski, J. Targeting the Prostacyclin Pathway : Beyond Pulmonary Arterial Hypertension. *Trends Pharmacol. Sci.* **38,** 512–523 (2017).
91. Perros, F. *et al.* Nebivolol for improving endothelial dysfunction, pulmonary vascular remodeling, and right heart function in pulmonary hypertension. *J. Am. Coll. Cardiol.* **65,** 668–680 (2015).
92. Bogaard, H. J. *et al.* Adrenergic receptor blockade reverses right heart remodeling and dysfunction in pulmonary hypertensive rats. *Am. J. Respir. Crit. Care Med.* **182,** 652–660 (2010).
93. Russi, A. E. & Brown, M. A. Adrenergic signaling in heart failure and cardiovascular aging.

Maturitas **93,** 255–269 (2016).

94. Zhang, W. *et al.* β-Adrenergic Receptor-PI3K Signaling Crosstalk in Mouse Heart: Elucidation of Immediate Downstream Signaling Cascades. *PLoS One* **6,** e26581 (2011).
95. Ngala, R. A. *et al.* Metabolic responses to BRL37344 and clenbuterol in soleus muscle and C2C12 cells via different atypical pharmacologies and β2-adrenoceptor mechanisms. *Br. J. Pharmacol.* **155,** 395–406 (2008).
96. Oudit, G. Y. *et al.* Phosphoinositide 3-Kinase γ-Deficient Mice Are Protected From Isoproterenol-Induced Heart Failure. *Circulation* **108,** 2147–2152 (2003).
97. Ciccarelli, M., Santulli, G., Pascale, V., Trimarco, B. & Iaccarino, G. Adrenergic receptors and metabolism: role in development of cardiovascular disease. *Front. Physiol.* **4,** 1–5 (2013).
98. Pentassuglia, L. & Sawyer, D. B. The Role of Neuregulin 1β/ErbB signaling in the heart. *Exp. Cell Res.* **315,** 627–637 (2009).
99. Mendes-Ferreira, P. *et al.* Neuregulin-1 improves right ventricular function and attenuates experimental pulmonary arterial hypertension. *Cardiovasc. Res.* **109,** 44–54 (2016).
100. Galiè, N., Manes, A. & Branzi, A. The endothelin system in pulmonary arterial hypertension. *Cardiovasc. Res.* **61,** 227–237 (2004).
101. Nagendran, J. *et al.* Endothelin axis is upregulated in human and rat right ventricular hypertrophy. *Circ. Res.* **112,** 347–354 (2013).
102. Modulation, M. *et al.* Neuregulins Regulate Cardiac Parasympathetic Activity - Muscarinic Modulation of β-Adrenergic Activity in Myocytes From Mice With Neuregulin-1 Gene Deletion. *Circulation* **110,** 713–717 (2004).
103. Liu, J. *et al.* Fibroblast growth factor 21 attenuates hypoxia-induced pulmonary hypertension by upregulating PPARγ expression and suppressing inflammatory cytokine levels. *Biochem. Biophys. Res. Commun.* **6,** 4–10 (2018).
104. Enache, I., Jamal, A. C., Fabrice, B., Geny, B. & Charloux, A. Skeletal muscle mitochondrial dysfunction precedes right ventricular impairment in experimental pulmonary hypertension. *Mol. Cell. Biochem.* **373,** 161–170 (2013).
105. Batt, J., Ahmed, S. S., Correa, J., Bain, A. & Granton, J. Skeletal Muscle Dysfunction in Idiopathic Pulmonary Arterial Hypertension. *Am. J. Respir. Cell Mol. Biol.* **50,** 74–86 (2014).
106. Bernocchi, P. *et al.* Skeletal muscle abnormalities in rats with experimentally induced heart hypertrophy and failure. *BasicRespiratory Cardiol.* **98,** 114–123 (2003).
107. Mainguy, V. *et al.* Peripheral muscle dysfunction in idiopathic pulmonary arterial hypertension. *Thorax* **65,** 113–118 (2010).

108. Ranchoux, B. *et al.* Endothelial dysfunction in pulmonary arterial hypertension: an evolving landscape (2017 Grover Conference Series). *Pulm. Circ.* **8,** 1–17 (2018).
109. Chat, S. *et al.* Endothelial-to-Mesenchymal Transition in Pulmonary Hypertension. *Circulation* **131,** 1006–1018 (2015).
110. Prins, K. W. *et al.* Interleukin-6 is Independently Associated with Right Ventricular Function in Pulmonary Arterial Hypertension. *J. Hear. Lung Transplant.* **37,** (2018).
111. Sutendra, G. & Michelakis, E. D. The metabolic basis of pulmonary arterial hypertension. *Cell Metab.* **19,** 558–573 (2014).
112. Li, C. *et al. Targeting the RhoA-ROCK pathway to regulate T-cell homeostasis in hypoxia-induced pulmonary arterial hypertension*. *Pulmonary Pharmacology & Therapeutics* (Elsevier Ltd, 2018). doi:10.1016/j.pupt.2018.04.004
113. Wilson, J. L. *et al.* Unraveling endothelin-1 induced hypercontractility of human pulmonary artery smooth muscle cells from patients with pulmonary arterial hypertension. *PLoS One* **13,** e0195780 (2018).
114. Savai, R. *et al.* Pro-proliferative and inflammatory signaling converge on FoxO1 transcription factor in pulmonary hypertension. *Nat. Med.* **20,** 1289–1300 (2014).
115. Bruder-Nascimento, T., Da Silva, M. A. B. & Tostes, R. C. The involvement of aldosterone on vascular insulin resistance: Implications in obesity and type 2 diabetes. *Diabetol. Metab. Syndr.* **6,** 1–8 (2014).
116. Man, F. S. De *et al.* Dysregulated Renin – Angiotensin – Aldosterone System Contributes to Pulmonary Arterial Hypertension. *Am. J. Respir. Crit. Care Med.* **186,** 780–789 (2012).
117. Jaisser, F. & Farman, N. Emerging Roles of the Mineralocorticoid Receptor in Pathology: Toward New Paradigms in Clinical Pharmacology. *Pharmacol. Rev.* **68,** 49–75 (2016).
118. Maron, B. A. *et al.* Effectiveness of Spironolactone Plus Ambrisentan for Treatment of Pulmonary Arterial Hypertension (from the [ARIES] Study 1 and 2 Trials). *Am. J. Cardiol.* **112,** 720–725 (2013).
119. Garg, R. & Adler, G. K. Role of mineralocorticoid receptor in insulin resistance. *Curr. Opin. Endocrinol. Diabetes Obes.* **19,** 168–175 (2012).
120. Duarte, J. D., Hanson, R. L. & Machado, R. F. Pharmacologic treatments for pulmonary hypertension: Exploring pharmacogenomics. *Future Cardiol.* **9,** 335–349 (2013).
121. Lan, N. S. H., Massam, B. D., Kulkarni, S. S. & Lang, C. C. Pulmonary Arterial Hypertension: Pathophysiology and Treatment. *Diseases* **6,** 1–22 (2018).
122. Varol, E., Uysal, B. A. & Ozaydin, M. Platelet Indices in Patients With Pulmonary Arterial Hypertension. *Clin. Appl. Thromb.* **17,** E171–E174 (2011).
123. Mustafa, M. *et al.* Enhanced hemostatic indices in patients with pulmonary arterial

hypertension: An observational study. *Thromb. Res.* **126,** 280–282 (2010).

124. Soon, E. *et al.* Elevated levels of inflammatory cytokines predict survival in idiopathic and familial pulmonary arterial hypertension. *Circulation* **122,** 920–927 (2010).
125. Rabinovitch, M. Molecular pathogenesis of pulmonary arterial hypertension. *J. Clin. Invest.* **122,** 4306–4313 (2012).
126. Mathew, R. Pulmonary hypertension and metabolic syndrome: Possible connection, PPARγ and Caveolin-1. *World J. Cardiol.* **6,** 692–705 (2014).
127. Steiner, M. K. *et al.* IL-6 Overexpression Induces Pulmonary Hypertension. *Circ. Res.* **104,** 236–244 (2009).
128. Savale, L. *et al.* Impact of interleukin-6 on hypoxia-induced pulmonary hypertension and lung inflammation in mice. *Respir. Res.* **10,** 1–13 (2009).
129. Huertas, A. *et al.* Leptin and regulatory T-lymphocytes in idiopathic pulmonary arterial hypertension ´. *Eur. Respir. J.* **40,** 895–904 (2012).
130. Price, L. C. *et al.* Inflammation in Pulmonary Arterial Hypertension. *Chest* **141,** 210–221 (2012).
131. Kendall, R. T., Feghali-bostwick, C. A. & Rauch, B. H. Fibroblasts in fibrosis: novel roles and mediators. *Front. Pharmacol.* **5,** (2014).
132. Baum, J. & Duffy, H. S. Fibroblasts and Myofibroblasts: What are we talking about ? *J. Cardiovasular Pharmacol.* **57,** 376–379 (2011).
133. Pollard, T. D., Earnshaw, W. C., Lippincott-Schwartz, J. & Johnson, G. T. in *Cell Biology* 491–504 (Elsevier, 2017). doi:10.1016/B978-0-323-34126-4.00028-1
134. Shao, D., Park, J. E. S. & Wort, S. J. The role of endothelin-1 in the pathogenesis of pulmonary arterial hypertension. *Pharmacol. Res.* **63,** 504–511 (2011).
135. Widyantoro, B., Emoto, N. & Nakayama, K. Endothelial Cell – Derived Endothelin-1 Promotes Cardiac Fibrosis in Diabetic Hearts Through Stimulation of. *Circulation* **121,** 2407–2418 (2010).
136. Shimizu, M. *et al.* Collagen remodelling in myocardia of patients with diabetes. *J. Clin. Pathol.* **46,** 32–36 (1993).
137. Meuse, A. J., Perreault, C. L. & Morgan, J. P. in *Cellular and molecular alterations in the failing human heart* (eds. Hasenfuss, G., Holubarsch, C., Just, H. & Alpert, N. R.) 291–301 (Steinkopff, 1992).
138. Travers, J. G., Kamal, F. A., Robbins, J., Yutzey, K. E. & Burns, C. Cardiac Fibrosis: The Fibroblast Awakens. *Circ. Res.* **118,** 1021–1040 (2016).
139. Rain, S. *et al.* Right Ventricular Myocardial Stiffness in Experimental Pulmonary Arterial Hypertension - Relative Contribution of Fibrosis and Myofibril Stiffness. *Circ Hear. Fail* **9,**

1–9 (2016).

140. Zhao, Y. D. *et al.* Metabolic heterogeneity of idiopathic pulmonary fibrosis: a metabolomic study. *BMJ Open Respir. Res.* **4,** 1–10 (2017).
141. Ghofrani, H. A. *et al.* Sildenafil for treatment of lung fibrosis and pulmonary hypertension: a randomised controlled trial. *Lancet (London, England)* **360,** 895–900 (2002).
142. Jimenez, S. A. & Piera-velazquez, S. Endothelial to mesenchymal transition (EndoMT) in the pathogenesis of systemic sclerosis-associated pulmonary fibrosis and pulmonary arterial hypertension. Myth or reality? *Matrix Biol.* (2016). doi:10.1016/j.matbio.2016.01.012
143. Sung, Y. K. & Chung, L. Connective Tissue Disease-Associated Pulmonary Arterial Hypertension. *Rheum. Dis. Clin. NA* **41,** 295–313 (2015).
144. Kalluri, R. & Weinberg, R. A. The basics of epithelial-mesenchymal transition. *J. Clin. Invest.* **119,** 1420–1428 (2010).
145. Gong, H., Lyu, X., Wang, Q., Hu, M. & Zhang, X. Endothelial to mesenchymal transition in the cardiovascular system. *Life Sci.* **184,** 95–102 (2017).
146. Talati, M. & Hemnes, A. Fatty acid metabolism in pulmonary arterial hypertension : role in right ventricular dysfunction and hypertrophy. **5,** 269–278 (2015).
147. Peng, H. *et al.* The Warburg effect: A new story in pulmonary arterial hypertension. *Clin. Chim. Acta* **461,** 53–58 (2016).
148. Cellsignal.Com. Warburg Effect. *Cell Signal. Tech.* 2014 (2014).
149. Long, M. *et al.* Metabolic Dysfunction in Pulmonary Arterial Hypertension. **8,** 444–454 (2016).
150. Fessel, J. P. *et al.* Metabolomic Analysis of Bone Morphogenetic Protein Receptor Type 2 Mutations in Human Pulmonary Endothelium Reveals Widespread Metabolic Reprogramming. *Pulm. Circ.* **2,** 201–213 (2012).
151. Zhao, Y. *et al.* Metabolomic heterogeneity of pulmonary arterial hypertension. *PLoS One* **9,** (2014).
152. Bertrand, L., Horman, S., Beauloye, C. & Vanoverschelde, J. L. Insulin signalling in the heart. *Cardiovasc. Res.* **79,** 238–248 (2008).
153. Shao, D. & Tian, R. Glucose Transporters in Cardiac Metabolism and Hypertrophy. *Comprehensive Physiology* **6,** 331–351 (2016).
154. Lopaschuk, G. D. & Ussher, J. R. Evolving Concepts of Myocardial Energy Metabolism: More Than Just Fats and Carbohydrates. *Circ. Res.* **119,** 1173–1176 (2016).
155. Ohira, H. *et al.* Shifts in myocardial fatty acid and glucose metabolism in pulmonary arterial hypertension: a potential mechanism for a maladaptive right ventricular response. *Eur. Hear. J. - Cardiovasc. Imaging* **17,** 1424–1431 (2016).

156. Nagaya, N. *et al.* Impaired Regional Fatty Acid Uptake and Systolic Dysfunction in Hypertrophied Right Ventricle. *J. Nucl. Med.* **39,** 1998 (1998).
157. Stanley, W. C., Recchia, F. A. & Lopaschuk, G. D. Myocardial Substrate Metabolism in the Normal and Failing Heart. *Physiol Rev* **85,** 1093–1129 (2005).
158. Graham, B. B., Robinson, J. C. & Tuder, R. M. Fatty Acid Metabolism, Bone Morphogenetic Protein Receptor Type 2, and the Right Ventricle. *Am. J. Respir. Crit. Care Med.* **194,** 655–656 (2016).
159. Rich, S. Right Ventricular Adaptation and Maladaptation in Chronic Pulmonary Arterial Hypertension. *Cardiol. Clin.* **30,** 257–269 (2012).
160. Fang, Y.-H. *et al.* Therapeutic inhibition of fatty acid oxidation in right ventricular hypertrophy: exploiting Randle's cycle. *J. Mol. Med.* **90,** 31–43 (2012).
161. Ware, B. *et al.* Chronic heart failure selectively induces regional heterogeneity of insulin-responsive glucose transporters Bruce. *AJP Regul. Integr. Comp. Physiol.* **301,** R1300–R1306 (2011).
162. García-Rua, V. *et al.* Increased Expression of Fatty-Acid and Calcium Metabolism Genes in Failing Human Heart. *PLoS One* **7,** 1–10 (2012).
163. Lopaschuk, G. D., Ussher, J. R., Folmes, C. D. L., Jaswal, J. S. & Stanley, W. C. Myocardial Fatty Acid Metabolism in Health and Disease. *Physiol Rev* **90,** 207–258 (2010).
164. Sankaralingam, S. & Lopaschuk, G. D. Cardiac energy metabolic alterations in pressure overload – induced left and right heart failure (2013 Grover Conference Series). *Pulm. Circ.* **5,** 15–28 (2015).
165. Doenst, T., Nguyen, T. D. & Abel, E. D. Cardiac Metabolism in Heart Failure: Implications Beyond ATP Production. *Circ. Res.* **113,** 709–724 (2013).
166. Talati, M. H. *et al.* Mechanisms of Lipid Accumulation in the Bone Morphogenetic Protein Receptor Type 2 Mutant Right Ventricle. *Am. J. Respir. Crit. Care Med.* **194,** 719–728 (2016).
167. Longo, N., Frigen, M. & Pasquali, M. CARNITINE TRANSPORT AND FATTY ACID OXIDATION. *Biochim. Biophys. Acta - Mol. Basis Dis.* **1863,** 2422–2435 (2016).
168. Hemnes, A. R. *et al.* Evidence for Right Ventricular Lipotoxicity in Heritable Pulmonary Arterial Hypertension. *Am. J. Respir. Crit. Care Med.* **189,** 325–334 (2014).
169. Yang, J. *et al.* CD36 Deficiency Rescues Lipotoxic Cardiomyopathy. *Circ. Res.* **100,** 1208–1217 (2007).
170. Angin, Y. *et al.* CD36 inhibition prevents lipid accumulation and contractile dysfunction in rat cardiomyocytes. *Biochem. J.* **448,** 43–53 (2012).
171. Sun, W., Liu, Q., Leng, J., Zheng, Y. & Li, J. The role of Pyruvate Dehydrogenase Complex

in cardiovascular diseases. *Life Sci.* **121,** 97–103 (2015).

172. Cantó, C. *et al.* Neuregulins Increase Mitochondrial Oxidative Capacity and Insulin Sensitivity in Skeletal Muscle Cells. *Diabetes* **56,** 2185–2193 (2007).
173. Drake, J. I. *et al.* Molecular Signature of a Right Heart Failure Program in Chronic Severe Pulmonary Hypertension. *Am. J. Respir. Cell Mol. Biol.* **45,** 1239–1247 (2011).
174. Sigma Aldrich. Cancer Metabolism. *BioFiles* **7,** 1–32 (2012).
175. Cottrill, K. A. & Chan, S. Y. Metabolic dysfunction in pulmonary hypertension: the expanding relevance of the Warburg effect. *Eur. J. Clin. Invest.* **43,** 855–865 (2013).
176. D'Alessandro, A. *et al.* Hallmarks of Pulmonary Hypertension: Mesenchymal and Inflammatory Cell Metabolic Reprogramming. *Antioxid. Redox Signal.* **28,** 230–250 (2018).
177. Heiden, M. G. Vander, Cantley, L. C. & Thompson, C. B. Understanding the Warburg Effect: The Metabolic Requirements of Cell Proliferation. *Science* **324,** 1029–1033 (2009).
178. Heresi, G. A. *et al.* Abnormal Glucose Metabolism and High Energy Expenditure in Idiopathic Pulmonary Arterial Hypertension. **14,** 190–199 (2017).
179. Machado, U. F., Schaan, B. D. & Seraphim, P. M. Transportadores de glicose na síndrome metabólica. *Arq. Bras. Endocrinol. Metabol.* **50,** 177–189 (2006).
180. Aerni-Flessner, L., Abi-Jaoude, M., Koenig, A., Payne, M. & Hruz, P. W. GLUT4, GLUT1, and GLUT8 are the dominant GLUT transcripts expressed in the murine left ventricle. *Cardiovasc. Diabetol.* **11,** 1–10 (2012).
181. Karp, G. *Cell and Molecular Biology - Concepts and Experiments*. *Molecular Biology* (John Wiley & Sons, Inc., 2010).
182. Szablewski, L. Glucose transporters in healthy heart and in cardiac disease. *Int. J. Cardiol.* **230,** 70–75 (2017).
183. Broderick, T. L. & King, T. M. Upregulation of GLUT-4 in right ventricle of rats with monocrotaline-induced pulmonary hypertension. *Med. Sci. Monit.* **14,** BR261-4 (2008).
184. Can, M. M. *et al.* Increased right ventricular glucose metabolism in patients with pulmonary arterial hypertension. *Clin Nucl Med* **36,** 743–748 (2011).
185. Marsboom, G. *et al.* Lung 18F-fluorodeoxyglucose positron emission tomography for diagnosis and monitoring of pulmonary arterial hypertension. *Am. J. Respir. Crit. Care Med.* **185,** 670–679 (2012).
186. Zhang, W. H. *et al.* Up-regulation of hexokinase1 in the right ventricle of monocrotaline induced pulmonary hypertension. *Respir. Res.* **15,** 1–6 (2014).
187. Kolwicz, S. C. & Tian, R. Glucose metabolism and cardiac hypertrophy. *Cardiovasc. Res.* **90,** 194–201 (2011).
188. Liang, Q., Donthi, R. V., Kralik, P. M. & Epstein, P. N. Elevated hexokinase increases

cardiac glycolysis in transgenic mice. *Cardiovasc. Res.* **53,** 423–430 (2002).

189. McCommis, K. S., Douglas, D. L., Krenz, M. & Baines, C. P. Cardiac-specific Hexokinase 2 Overexpression Attenuates Hypertrophy by Increasing Pentose Phosphate Pathway Flux. *J. Am. Heart Assoc.* **2,** 1–13 (2013).
190. Calmettes, G. *et al.* Hexokinases and cardioprotection. *J. Mol. Cell. Cardiol.* **78,** 107–127 (2015).
191. Alibegovic, A. C. *et al.* Insulin resistance induced by physical inactivity is associated with multiple transcriptional changes in skeletal muscle in young men. *Am. J. Physiol. Endocrinol. Metab.* **299,** 752–763 (2010).
192. Piao, L., Marsboom, G. & Archer, S. L. Mitochondrial metabolic adaptation in right ventricular hypertrophy and failure. *J. Mol. Med.* **88,** 1011–1020 (2011).
193. Bertero, T. *et al.* Vascular stiffness mechanoactivates YAP/TAZ-dependent glutaminolysis to drive pulmonary hypertension. *J. Clin. Invest.* **126,** 3313–3335 (2016).
194. Burns, J. S. & Manda, G. Metabolic pathways of thewarburg effect in health and disease: Perspectives of choice, chain or chance. *Int. J. Mol. Sci.* **18,** 1–28 (2017).
195. Asosingh, K. & Erzurum, S. Mechanisms of right heart disease in pulmonary hypertension (2017 Grover Conference Series). *Pulm. Circ.* **8,** 1–6 (2018).
196. Sutendra, G. *et al.* Pyruvate dehydrogenase inhibition by the inflammatory cytokine TNFα contributes to the pathogenesis of pulmonary arterial hypertension. *J. Mol. Med.* **89,** 771–783 (2011).
197. Altin, S. E. & Schulze, P. C. Metabolism of the right ventricle and the response to hypertrophy and failure. *Prog. Cardiovasc. Dis.* **55,** 229–233 (2012).
198. Ryan, J. J. & Archer, S. L. The Right Ventricle in Pulmonary Arterial Hypertension: Disorders of Metabolism, Angiogenesis and Adrenergic Signaling in Right Ventricular Failure. *Circ. Res.* **115,** 176–188 (2014).
199. Piao, L. *et al.* FOXO1-mediated upregulation of pyruvate dehydrogenase kinase-4 (PDK4) decreases glucose oxidation and impairs right ventricular function in pulmonary hypertension : therapeutic benefits of dichloroacetate. *J. Mol. Med.* **91,** 333–346 (2013).
200. Ferriero, R. *et al.* Phenylbutyrate Therapy for Pyruvate Dehydrogenase Complex Deficiency and Lactic Acidosis. *Sci. Transl. Med.* **5,** (2013).
201. Fan, J. *et al.* Tyr-301 Phosphorylation Inhibits Pyruvate Dehydrogenase by Blocking Substrate Binding and Promotes the Warburg. *J. Biolo* **289,** 26533–26541 (2014).
202. Sun, X. *et al.* Reversal of right ventricular remodeling by dichloroacetate is related to inhibition of mitochondria-dependent apoptosis. *Hypertens. Res.* **39,** 1–10 (2016).
203. PDHA1 Gene. *GeneCards*® (2018). Available at: https://www.genecards.org/cgi-

bin/carddisp.pl?gene=PDHA1&keywords=PDHA2. (Accessed: 29th September 2018)

204. PDHA2 Gene. *GeneCards*® (2018). Available at: https://www.genecards.org/cgi-bin/carddisp.pl?gene=PDHA2&keywords=PDHA2. (Accessed: 29th September 2018)
205. PDHB Gene. *GeneCards*® (2018). Available at: https://www.genecards.org/cgi-bin/carddisp.pl?gene=PDHB&keywords=PDHb. (Accessed: 29th September 2018)
206. Valvona, C. J., Fillmore, H. L., Nunn, P. B. & Pilkington, G. J. The Regulation and Function of Lactate Dehydrogenase A: Therapeutic Potential in Brain Tumor. *Brain Pathol.* **26,** 3–17 (2015).
207. Gray, L. R., Tompkins, S. C. & Taylor, E. B. Regulation of pyruvate metabolism and human disease. *Cell. Mol. Life Sci.* **71,** 2577–2604 (2014).
208. Li, L. *et al.* Platelet-Derived Growth Factor-B (PDGF-B) Induced by Hypoxia Promotes the Survival of Pulmonary Arterial Endothelial Cells through the PI3K / Akt / Stat3 Pathway. *Cell Physiol Biochem* **35,** 441–451 (2015).
209. Dromparis, P. & Sutendra, G. The role of mitochondria in pulmonary vascular remodeling. 1003–1010 (2010). doi:10.1007/s00109-010-0670-x
210. Raghavan, A. *et al.* Hypoxia-Induced Pulmonary Arterial Smooth Muscle Cell Proliferation Is Controlled by Forkhead Box M1. *Respir. Cell Mol. Biol.* **46,** 431–436 (2012).
211. Pereira, R. O. *et al.* GLUT1 Deficiency in Cardiomyocytes Does not Accelerate the Transition from Compensated Hypertrophy to Heart Failure. *J. Mol. Cell. Cardiol.* **72,** 95–103 (2014).
212. Piao, L. *et al.* The inhibition of pyruvate dehydrogenase kinase improves impaired cardiac function and electrical remodeling in two models of right ventricular hypertrophy: resuscitating the hibernating right ventricle. *J. Mol. Med.* **88,** 47–60 (2010).
213. Sertié, R. A. L., Sertié, A. L., Giannocco, G., Poyares, L. L. & Nunes, M. T. Acute growth hormone administration increases myoglobin expression and Glut4 translocation in rat cardiac muscle cells. *Metabolism.* **63,** 1499–1502 (2014).
214. Huang, S. & Czech, M. P. The GLUT4 Glucose Transporter. *Cell Metab.* **5,** 237–252 (2007).
215. De Leon, E. B. *et al.* Neuromuscular electrical stimulation improves GLUT-4 and morphological characteristics of skeletal muscle in rats with heart failure. *Acta Physiol.* **201,** 265–273 (2011).
216. Archer, S. L. *et al.* Epigenetic Attenuation of Mitochondrial Superoxide Dismutase 2 (SOD2) in Pulmonary Arterial Hypertension: a basis for excessive cell proliferation and a new therapeutic target. *Circulation* **121,** 2661–2671 (2011).
217. Garnier, A., Fadel, E., Lemaire, C. & Veksler, V. Sirtuin 1 regulates pulmonary artery

smooth muscle cell proliferation: role in pulmonary arterial hypertension. *J. Hypertens.* **36,** 1164–1177 (2018).

218. Michan, S. & Sinclair, D. Sirtuins in mammals: insights into their biological function. *Biochem. J.* **404,** 1–13 (2007).
219. Houtkooper, R. H., Pirinen, E. & Auwerx, J. Sirtuins as regulators of metabolism and healthspan. *Nat. Rev. Mol. Cell Biol.* **13,** 225–238 (2016).
220. Tanno, M., Kuno, A. & Horio, Y. Emerging beneficial roles of sirtuins in heart failure. *BasicRespiratory Cardiol.* **107,** (2012).
221. Malenfant, S., Potus, F., Fournier, F. & Breuils-bonnet, S. Skeletal muscle proteomic signature and metabolic impairment in pulmonary hypertension. *J. Mol. Med.* **93,** 573–584 (2015).
222. Guignabert, C. *et al.* Pathogenesis of pulmonary arterial hypertension: Lessons from cancer. *Eur. Respir. Rev.* **22,** 543–551 (2013).
223. Boucherat, O. *et al.* The cancer theory of pulmonary arterial hypertension. *Pulm. Circ.* **7,** 285–299 (2017).
224. Piao, L. *et al.* Cardiac glutaminolysis: a maladaptive cancer metabolism pathway in the right ventricle in pulmonary hypertension. *J. Mol. Med.* **91,** 1185–1197 (2013).
225. Cikach, F. S. *et al.* Breath Analysis in Pulmonary Arterial Hypertension. *Chest* **145,** 551–558 (2014).
226. National Institute of Diabetes and Digestive and Kidney Diseases (NIDDK). Prediabetes & Insulin Resistance. (2009). Available at: https://www.niddk.nih.gov/health-information/diabetes/overview/what-is-diabetes/prediabetes-insulin-resistance. (Accessed: 8th May 2018)
227. Zamanian, R. T. *et al.* Insulin resistance in pulmonary arterial hypertension. *Eur. Respir. J.* **33,** 318–324 (2009).
228. Martins, A. R. *et al.* Mechanisms underlying skeletal muscle insulin resistance induced by fatty acids: importance of the mitochondrial function. *Lipids Health Dis.* **11,** 1–11 (2012).
229. Kubota, T., Kubota, N. & Kadowaki, T. The role of endothelial insulin signaling in the regulation of glucose metabolism. *Rev. Endocr. Metab. Disord.* **14,** 207–216 (2013).
230. Kido, Y. *et al.* Tissue-specific insulin resistance in mice with mutations in the insulin receptor , IRS-1 , and Find the latest version : the insulin receptor , IRS-1 , and IRS-2. *J. Clin. Invest.* **105,** 199–205 (2000).
231. Fujita, T. Insulin resistance and salt-sensitive hypertension in metabolic syndrome. *Nephrol. Dial. Transplant.* **22,** 3102–3107 (2007).
232. Rao, J., Li, J., Liu, Y. & Lu, P. The key role of PGC-1a in mitochondrial biogenesis and the

proliferation of pulmonary artery vascular smooth muscle cells at an early stage of hypoxic exposure. *Mol. Cell. Biochem.* **367,** 9–18 (2012).

233. NRF1 Gene. *GeneCards*® (2018). Available at: https://www.genecards.org/cgi-bin/carddisp.pl?gene=NRF1&keywords=NRF1. (Accessed: 29th September 2018)
234. Yoshinaga, K. *et al.* in *Perspectives on Nuclear Medicine for Molecular Diagnosis and Integrated Therapy* (eds. Kuge, Y., Shiga, T. & Tamaki, N.) 193–207 (Springer, 2016).
235. Marra, A. M. *et al.* Biomarkers in Pulmonary Hypertension. *Heart Fail. Clin.* **14,** 393–402 (2018).
236. Frump, A. L., Perez, V. D. J., Lahm, T., City, Q. & Physiology, I. The emerging role of angiogenesis in adaptive and maladaptive right ventricular remodeling in pulmonary hypertension. *Am. J. Physiol. Cell. Mol. Physiol.* **314,** L443–L460 (2017).
237. Rawat, D. K. *et al.* Increased Reactive Oxygen Species, Metabolic Maladaptation, and Autophagy Contribute to Pulmonary Arterial Hypertension–Induced Ventricular Hypertrophy and Diastolic Heart Failure. *Hypertension* **64,** 1266–1274 (2014).
238. Potus, F. *et al.* Role for DNA Damage Signaling in Pulmonary Arterial Hypertension. *Circulation* **129,** 786–797 (2014).
239. Paulin, R. *et al.* A miR-208-Mef2 axis drives the decompensation of right ventricular function in pulmonary hypertension. *Circ. Res.* **116,** 56–69 (2015).
240. Potus, F. *et al.* Downregulation of miR-126 Contributes to the Failing Right Ventricle in Pulmonary Arterial Hypertension. *Circulation* **132,** 932–943 (2015).
241. Cantó, C. *et al.* Neuregulin Signaling on Glucose Transport in Muscle Cells. *J. Biol. Chem.* **279,** 12260–12268 (2004).
242. Mendes-Ferreira, P., De Keulenaer, G. W., Leite-Moreira, A. F. & Brás-Silva, C. Therapeutic potential of neuregulin-1 in cardiovascular disease. *Drug Discov. Today* **18,** 836–842 (2013).
243. Falls, D. L. in *The EGF Receptor Family* (ed. Carpenter, G.) 15–31 (Elsevier, 2014).
244. Odiete, O., Hill, M. F. & Sawyer, D. B. Neuregulin in Cardiovascular Development and Disease. *Circ. Res.* **111,** 1376–1385 (2012).
245. Rupert, C. E. & Coulombe, K. L. K. The roles of neuregulin-1 in cardiac development, homeostasis, and disease. *Biomark. Insights* **2015,** 1–9 (2015).
246. Lemmens, K., Segers, V. F. M., Demolder, M. & Keulenaer, G. W. De. Role of Neuregulin-1/ErbB2 Signaling in Endothelium-Cardiomyocyte Cross-talk. *J. Biol. Chem.* **281,** 19469–19477 (2006).
247. Galindo, C., Ryzhov, S. & Sawyer, D. B. Neuregulin as a Heart Failure Therapy and Mediator of Reverse Remodeling. *Curr. Heart Fail. Rep.* **11,** 40–49 (2014).

248. Lee, K.-F. *et al.* Requirement for neuregulin receptor erbB2 in neural and cardiac development. *Nature* **378,** 394–398 (1995).
249. Suárez, E. *et al.* A Novel Role of Neuregulin in Skeletal Muscle. *J. Biol. Chem.* **276,** 18257–18264 (2001).
250. Miller, T. A. *et al.* Palmitate alters neuregulin signaling and biology in cardiac myocytes. *Biochem. Biophys. Res. Commun.* **379,** 32–37 (2010).
251. Liu, F. *et al.* Heterozygous knockout of neuregulin-1 gene in mice exacerbates doxorubicin-induced heart failure. *Am. J. Physiol. Circ. Physiol.* **289,** 660–666 (2005).
252. Bersell, K., Arab, S., Haring, B. & Ku, B. Neuregulin10/ErbB4 Signaling Induces Cardiomyocyte Proliferation and Repair of Heart Injury. *Cell* **138,** 257–270 (2009).
253. Cote, G. M., Miller, T. A., Lebrasseur, N. K., Kuramochi, Y. & Sawyer, D. B. Neuregulin-1α and β isoform expression in cardiac microvascular endothelial cells and function in cardiac myocytes in vitro. *Exp. Cell Res.* **311,** 135–146 (2005).
254. Brachmann, S. M., Ueki, K., Engelman, J. A., Kahn, R. C. & Cantley, L. C. Phosphoinositide 3-Kinase Catalytic Subunit Deletion and Regulatory Subunit Deletion Have Opposite Effects on Insulin Sensitivity in Mice. *Mol. Cell. Biol.* **25,** 1596–1607 (2005).
255. Carver, R. S., Sliwkowski, M. X., Sitaric, S. & Russell, W. E. Insulin Regulates Heregulin Binding and ErbB3 Expression in Rat Hepatocytes. *J. Biol. Chem.* **271,** 13491–13496 (1996).
256. Caillaud, K. *et al.* Neuregulin 1 improves glucose tolerance in adult and old rats. *Diabetes Metab.* **42,** 96–104 (2015).
257. Carver, R. S., Mathew, P. M. & Russell, W. E. Hepatic Expression of ErbB3 Is Repressed by Insulin in a Pathway Sensitive to PI-3 Kinase Inhibitors. *Endocrinology* **138,** 5195–5201 (1997).
258. Wang, F. *et al.* Pharmacological postconditioning with Neuregulin-1 mimics the cardioprotective effects of ischaemic postconditioning via ErbB4-dependent activation of reperfusion injury salvage kinase pathway. *Mol. Med.* **24,** 1–12 (2018).
259. Clement, C. M. *et al.* Neuregulin-1 Attenuates Neointimal Formation following Vascular Injury and Inhibits the Proliferation of Vascular Smooth Muscle Cells. *J. Vasc. Res.* **44,** 303–312 (2007).
260. Gomez-Arroyo, J. *et al.* Metabolic gene remodeling and mitochondrial dysfunction in failing right ventricular hypertrophy secondary to pulmonary arterial hypertension. *Circ Hear. Fail* **6,** 136–144 (2013).
261. Rohrbach, S., Niemann, B., Silber, R.-E. & Holtz, J. Neuregulin receptors erbB2 and erbB4

in failing human myocardium - Depressed expression and attenuated activation. *Basic Respir. Cardiol.* **100,** 240–249 (2005).

262. Weisbroth, S. H. *et al. Laboratory Animal Medicine*. **I,** (Elsevier Inc, 2015).
263. Worp, H. B. Van Der *et al.* Can Animal Models of Disease Reliably Inform Human Studies? *PLoS Med.* **7,** (2010).
264. Naeije, R. & Dewachter, L. Modèles animaux d ' hypertension artérielle pulmonaire. *Rev. Mal. Respir.* **24,** 481–496 (2007).
265. Davidson, M. K., Lindsey, J. R. & Davis, J. K. Requirements and selection of an animal model. *Isr. J. Med. Sci.* **23,** 551–5 (1987).
266. Maarman, G., Lecour, S., Butrous, G., Thienemann, F. & Sliwa, K. A comprehensive review: the evolution of animal models in pulmonary hypertension research; are we there yet ? *Pulm. Circ.* **3,** 739–756 (2013).
267. Sztuka, K. & Jasińska-stroschein, M. Animal models of pulmonary arterial hypertension: A Systematic Review and Meta-Analysis of data from 6126 animals. *Pharmacol. Res.* **125,** 201–214 (2017).
268. Stenmark, K. R., Meyrick, B., Galie, N., Mooi, W. J. & Mcmurtry, I. F. Animal models of pulmonary arterial hypertension: the hope for etiological discovery and pharmacological cure. *Am. J. Physiol. Cell. Mol. Physiol.* **297,** L1013–L1032 (2009).
269. Vitali, S. H. *et al.* The Sugen 5416/hypoxia mouse model of pulmonary hypertension revisited: long-term follow-up. *Pulm. Circ.* **4,** 619–629 (2014).
270. Gomez-arroyo, J. G. *et al.* The monocrotaline model of pulmonary hypertension in perspective. *Am. J. Physiol. Cell. Mol. Physiol.* **302,** L363–L369 (2011).
271. Carlos Bueno-Beti, Sassi, Y., Hajjar, R. J. & Hadri, L. in *Experimental Models of Cardiovascular Diseases* (ed. Ishikawa, K.) 233–241 (Humana Press, 2018).
272. Colvin, K. L. & Yeager, M. E. Animal Models of Pulmonary Hypertension: Matching Disease Mechanisms to Etiology of the Human Disease. *J. Pulm. Respir. Med.* **4,** (2014).
273. Plestina, R. & Stoner, H. B. Pulmonary oedema in rats given monocrotaline pyrrole. *J. Pathol.* **106,** 235–249 (1972).
274. Bueno-Beti, C., Hadri, L., Hajjar, R. J. & Sassi, Y. in *Experimental Models of Cardiovascular Diseases* (ed. Ishikawa, K.) 243–252 (Humana Press, 2018).
275. Koskenvuo, J. W. *et al.* A comparison of echocardiography to invasive measurement in the evaluation of pulmonary arterial hypertension in a rat model. *Int. J. Cardiovasc. Imaging* **26,** 509–518 (2010).
276. Urboniene, D., Haber, I., Fang, Y. H., Thenappan, T. & Archer, S. L. Validation of high-resolution echocardiography and magnetic resonance imaging vs. high-fidelity

catheterization in experimental pulmonary hypertension. *Am. J. Physiol. Cell. Mol. Physiol.* **299,** L401-12 (2010).

277. Yin, F. C. P., Spurgeon, H. A., Rakusan, K., Weisfeldt, M. L. & Lakatta, E. G. Use of tibial length to quantify cardiac hypertrophy: application in the aging rat. *Am. J. Physiol. Circ. Physiol.* **243,** H941–H947 (1982).
278. Kawut, S. M. *et al.* Determinants of Right Ventricular Ejection Fraction in Pulmonary Arterial Hypertension. *Chest* **135,** 752–759 (2010).
279. Kuc, R. E. *et al.* Modulation of endothelin receptors in the failing right ventricle of the heart and vasculature of the lung in human pulmonary arterial hypertension. *Life Sci.* **118,** 391–396 (2014).
280. Hemnes, A. R. *et al.* Testosterone negatively regulates right ventricular load stress responses in mice. *Pulm. Circ.* **2,** (2012).
281. Dayeh, N. R. *et al.* Echocardiographic validation of pulmonary hypertension due to heart failure with reduced ejection fraction in mice. *Nature* **8,** 1–11 (2018).
282. Hessel, M. H. M. *et al.* Characterization of right ventricular function after monocrotaline-induced pulmonary hypertension in the intact rat. *Am. J. Hear. Circ. Physiol.* **291,** 2424–2430 (2006).
283. Hamill, N. *et al.* Fetal cardiac ventricular volume, cardiac output, and ejection fraction determined with four-dimensional ultrasound using Spatio-Temporal Image Correlation (STIC) and Virtual Organ Computed-aided AnaLysis (VOCAL™). *Am. J. Obstet. Gynecol.* **205,** 16.e1-76.e10 (2011).
284. Tuder, R. M., Davis, L. A. & Graham, B. B. Targeting energetic metabolism: A new frontier in the pathogenesis and treatment of pulmonary hypertension. *Am. J. Respir. Crit. Care Med.* **185,** 260–266 (2012).
285. Sadlecki, P. *et al.* The Role of Hypoxia-Inducible Factor-1α, Glucose Transporter-1, (GLUT-1) and Carbon Anhydrase IX in Endometrial Cancer Patients. *Biomed Res. Int.* **2014,** (2014).
286. Fulton, R. M., Hutchinson, E. C. & Jones, A. M. Ventricular weight in cardiac hypertrophy. *Br. Heart J.* **14,** 413–420 (1952).
287. Foschi, M. *et al.* The Dark Side of the Moon: The Right Ventricle. *J. Cardiovasc. Dev. Dis.* **4,** (2017).
288. Adão, R. *et al.* Urocortin-2 improves right ventricular function and attenuates pulmonary arterial hypertension. *Cardiovasc. Res.* **114,** 1165–1177 (2018).
289. Jones, J. E. *et al.* Serial noninvasive assessment of progressive pulmonary hypertension in a rat model. *Am. J. Physiol. - Hear. Circ. Physiol.* **283,** H364–H371 (2002).

290. Mertens, L. L. & Friedberg, M. K. Imaging the right ventricle-current state of the art. *Nat. Rev. Cardiol.* **7,** 551–563 (2010).
291. Chen, L., Larsen, C. M., Le, R. J. & Connolly, H. M. The Prognostic Significance of Tricuspid Valve Regurgitation in Pulmonary Arterial Hypertension. *Clin. Respir. J.* **12,** 1572–1580 (2018).
292. Medvedofsky, D. *et al.* Tricuspid regurgitation progression and regression in pulmonary arterial hypertension: implications for right ventricular and tricuspid valve apparatus geometry and patients outcome. *Eur. Hear. J. - Cardiovasc. Imaging* **18,** 86–94 (2017).
293. American Diabetes Association. Postprandial blood glucose. *Diabetes Care* **24,** 775–778 (2001).
294. Sakaguchi, K. *et al.* Glucose area under the curve during oral glucose tolerance test as an index of glucose intolerance. *Diabetol. Int.* **7,** 53–58 (2016).
295. Ennequin, G. *et al.* Neuregulin 1 improves glucose tolerance in db/db mice. *PLoS One* **10,** 7–9 (2015).
296. Lastra, G. *et al.* Low-dose spironolactone reduces reactive oxygen species generation and improves insulin-stimulated glucose transport in skeletal muscle in the TG(mRen2)27 rat. *Am. J. Physiol. Endocrinol. Metab.* **295,** E110–E116 (2008).
297. Patra, K. C. *et al.* Hexokinase 2 Is Required for Tumor Initiation and Maintenance and Its Systemic Deletion Is Therapeutic in Mouse Models of Cancer. *Cancer Cell* **24,** 1–16 (2013).
298. Wallace, D. C. Mitochondria and cancer. *Nat. Rev. Cancer* **12,** 685–698 (2012).
299. Ball, M. K. *et al.* Regulation of Hypoxia-induced Pulmonary Hypertension by Vascular Smooth Muscle Hypoxia-Inducible Factor-1α. *Am. J. Respir. Crit. Care Med.* **189,** 314–324 (2014).
300. Joo, H. *et al.* SIRT1 deacetylates and stabilizes hypoxia-inducible factor-1α (HIF-1α) via direct interactions during hypoxia. *Biochem. Biophys. Res. Commun.* **462,** 294–300 (2015).
301. Laemmle, A. *et al.* Inhibition of SIRT1 Impairs the Accumulation and Transcriptional Activity of HIF-1α Protein under Hypoxic Conditions. *PLoS One* **7,** e33433 (2012).
302. Ausina, P., Da, D., Majerowicz, D., Zancan, P. & Sola-penna, M. Insulin specifically regulates expression of liver and muscle phosphofructokinase isoforms. *Biomed. Pharmacother.* **103,** 228–233 (2018).
303. Liang, X. *et al.* Exercise Inducible Lactate Dehydrogenase B Regulates Mitochondrial Function in Skeletal Muscle. *J. Biol. Chem.* **291,** 25306–25318 (2016).
304. Chen, C., Pore, N., Behrooz, A., Ismail-beigi, F. & Maity, A. Regulation of glut1 mRNA by Hypoxia-inducible Factor-1. *J. Biol. Chem.* **276,** 9519–9525 (2001).

305. Milam, B. M., Strouch, M., Pelling, J. C. & Bentrem, D. J. Apigenin Inhibits the GLUT-1 Glucose Transporter and the Phosphoinositide 3-Kinase / Akt Pathway in Human Pancreatic Cancer Cells. *Pancreas* **37,** 426–431 (2008).
306. Zhabyeyev, P. *et al.* Pressure-overload-induced heart failure induces a selective reduction in glucose oxidation at physiological afterload. *Cardiovasc. Res.* **97,** 676–685 (2013).
307. Doehner, W. *et al.* Reduced glucose transporter GLUT4 in skeletal muscle predicts insulin resistance in non-diabetic chronic heart failure patients independently of body composition. *Int. J. Cardiol.* **138,** 19–24 (2010).
308. Yu, A. Y. *et al.* Impaired physiological responses to chronic hypoxia in mice partially deficient for hypoxia-inducible factor 1α. *J. Clin. Invest.* **103,** 691–696 (1999).
309. Hölscher, M. *et al.* Unfavourable consequences of chronic cardiac HIF-1α stabilization. *Cardiovasc. Res.* **94,** 77–86 (2012).
310. Bogaard, H. J. *et al.* Chronic pulmonary artery pressure elevation is insufficient to explain right heart failure. *Circulation* **120,** 1951–1960 (2009).
311. Sakagami, H. *et al.* Loss of HIF-1α impairs GLUT4 translocation and glucose uptake by the skeletal muscle cells. *Am. J. Physiol. Endocrinol. Metab.* **306,** E1065–E1076 (2014).
312. Waskova-Arnostova, P. *et al.* Right-to-left ventricular differences in the expression of mitochondrial hexokinase and phosphorylation of Akt. *Cell. Physiol. Biochem.* **31,** 66–79 (2013).
313. Miyamoto, S., Murphy, A. N. & Brown, J. H. Akt mediates mitochondrial protection in cardiomyocytes through phosphorylation of mitochondrial hexokinase-II. *Cell Death Differ.* **15,** 521–529 (2008).
314. Russell, R. R., Mrus, J. M., Mommessin, J. I. & Taegtmeyer, H. Compartmentation of hexokinase in rat heart: A critical factor for tracer kinetic analysis of myocardial glucose metabolism. *J. Clin. Invest.* **90,** 1973–1977 (1992).
315. Riddle, S. R. *et al.* Hypoxia induces hexokinase II gene expression in human lung cell line A549. *Am. J. Physiol. Cell. Mol. Physiol.* **278,** L407–L416 (200AD).
316. García, M. *et al.* Phosphofructo-1-kinase deficiency leads to a severe cardiac and hematological disorder in addition to skeletal muscle glycogenosis. *PLoS Genet.* **5,** e1000615 (2009).
317. Potus, F. *et al.* Transcriptomic Signature of Right Ventricular Failure in Experimental Pulmonary Arterial Hypertension: Deep Sequencing Demonstrates Mitochondrial, Fibrotic, Inflammatory and Angiogenic Abnormalities. *Int. J. Mol.* **19,** 1–21 (2018).
318. Christofk, H. R., Vander Heiden, M. G., Wu, N., Asara, J. M. & Cantley, L. C. Pyruvate kinase M2 is a phosphotyrosine-binding protein. *Nature* **452,** 181–186 (2008).

319. Riehle, C. & Abel, E. D. Insulin Signaling and Heart Failure. *Circ. Res.* **118,** 1151–1169 (2016).
320. Graham, B. B. *et al.* Severe pulmonary hypertension is associated with altered right ventricle metabolic substrate uptake. *Am. J. Physiol. Cell. Mol. Physiol.* **309,** 435–440 (2015).
321. Izquierdo-garcia, J. L., Arias, T., Rojas, Y. & Garcia-ruiz, V. Metabolic Reprogramming in the Heart and Lung in a Murine Model of Pulmonary Arterial Hypertension. *Front. Cardiovasc. Med.* **5,** (2018).
322. Wang, Z., Schreier, D. A., Hacker, T. A. & Chesler, N. C. Progressive right ventricular functional and structural changes in a mouse model of pulmonary arterial hypertension. *Physiol. Rep.* **1,** 1–11 (2013).
323. Zungu-Edmondson, M., Shults, N. V., Wong, C. M. & Suzuki, Y. J. Modulators of right ventricular apoptosis and contractility in a rat model of pulmonary hypertension. *Cardiovasc. Res.* **110,** 30–39 (2016).
324. De Raaf, M. A. *et al.* SuHx rat model: Partly reversible pulmonary hypertension and progressive intima obstruction. *Eur. Respir. J.* **44,** 160–168 (2014).
325. Ciuclan, L. *et al.* A Novel Murine Model of Severe Pulmonary Arterial Hypertension. *Am. J. Respir. Crit. Care Med.* **184,** 1171–1182 (2011).
326. Reindel, J. F., Ganey, P. E., Slocombe, R. F. & Roth, R. A. Development of Morphologic, Hemodynamic, and Biochemical Changes in Lungs of Rats Given and Biochemical Pyrrole Changes Monocrotaline. *Toxicol. Appl. Pharmacol.* **106,** 179–200 (1990).
327. Gan, Z. Hypoxia in skeletal muscles: from physiology to gene expression. *Exp. Physiol.* **88,** 109–119 (2016).
328. Luo, F. M. *et al.* Hypoxia-inducible transcription factor-1α promotes hypoxia-induced A549 apoptosis via a mechanism that involves the glycolysis pathway. *BMC Cancer* **6,** (2006).
329. William I. Sivitz, Lund, D. D., Yorek, B., Grover-mckay, M. & Schmid, P. G. Pretranslational regulation of two cardiac glucose transporters in rats exposed to hypobaric hypoxia. *Am. J. Physiol.* **263,** E562–E569 (1992).
330. Zhu, L. *et al.* Hypoxia induces PGC-1 α expression and mitochondrial biogenesis in the myocardium of TOF patients. *Nat. Publ. Gr.* **20,** 676–687 (2010).

Appendix

Table 1 Updated classification of pulmonary hypertension and characteristics*

WHO Group	Clinical Group	Origin	Clinical Definition	Hemodynamic Definition
1	Pulmonary arterial hypertension	1.Idiopathic PAH 2.Heritable PAH BMPRII mutations ALK-1, ENG, SMAD9, CAV1, KCNK3 Unknown 3.Drug and toxin induced 4.Associated with: Connective tissue disease HIV infection Portal hypertension Congenital heart diseases Schistosomiasis 5.Pulmonary venoocclusive disease and/or pulmonary capillary hemangiomatosis Idiopathic Heritable EIF2AK4 mutations, other mutations Drugs, toxins and radiation induced Associated with: Connective tissue disease HIV infection 1".Persistent PH of the new-born	Precapillary PH	mPA ≥ 25 mmHg mPAWP < 15 mmHg

2	Pulmonary hypertension due to left heart disease	1.Left ventricular systolic dysfunction 2.Left ventricular diastolic dysfunction 3.Valvular disease 4.Congenital/acquired left heart inflow/outflow tract obstruction and congenital cardiomyopathies 5.Congenital/acquired pulmonary vein stenosis	Postcapillary PH	mPA ≥ 25 mmHg mPAWP > 15 mmHg
			Isolated postcapillary PH	DPG < 7 mmHg and/or PVR ≤ 3Wood units
			Combined postcapillary and precapillary PH	DPG < 7 mmHg and/or PVR ≥ 3Wood units
3	Pulmonary hypertension due to lung diseases or hypoxia	1.Chronic obstructive pulmonary disease 2.Interstitial lung disease 3.Other pulmonary diseases with mixed restrictive and obstructive pattern 4.Sleep-disordered breathing 5.Alveolar hypoventilation disorders 6.Chronic exposure to high altitude 7.Developmental lung diseases	Precapillary PH	mPA ≥ 25 mmHg mPAWP < 15 mmHg
4	Chronic thromboem_ -bolic PH	1.Chronic thromboembolic pulmonary hypertension 2.Other pulmonary artery obstructions Angiosarcoma Other intravascular tumours Arteritis Congenital pulmonary artery stenosis Parasites (hydatidosis)	Precapillary PH	mPA ≥ 25 mmHg mPCWP < 15 mmHg

5	Pulmonary hypertension with unclear multifactorial mechanisms	1.Hematologic disorders: chronic haemolytic anaemia, myeloproliferative disorders, splenectomy 2.Systemic disorders: sarcoidosis, pulmonary histiocytosis, Lymphangioleiomyomatosis 3.Metabolic disorders: glycogen storage disease, Gaucher disease, thyroid disorders 4.Others: tumoral obstruction, fibrosing mediastinitis, chronic renal failure, segmental PH	Precapillary PH	mPA ≥ 25 mmHg mPAWP < 15 mmHg
			Postcapillary PH	mPA ≥ 25 mmHg mPAWP > 15 mmHg
			Isolated postcapillary PH	DPG < 7 mmHg and/or PVR ≤ 3Wood units
			Combined postcapillary and precapillary PH	DPG < 7 mmHg and/or PVR ≥ 3Wood units

*Defined in 5th WSPH, Nice, 2013.

ALK1: activin-like receptor kinase-1; BMPRII: bone morphogenetic protein receptor type 2; CAV1: caveolin-1; DPG: diastolic pulmonary gradient; ENG: endoglin; EIF2AK4: eukaryotic translation initiation factor 2 alpha kinase 4 HIV: human immunodeficiency virus; KCNK3: potassium two pore domain channel subfamily K member 3; mPAP: mean pulmonary artery pressure; mPAWP: mean pulmonary artery wedge pressure; mPCWP: mean pulmonary capillary wedge pressure PAH: pulmonary arterial hypertension; PH: pulmonary hypertension; PVR: pulmonary vascular resistance; SMAD9: mothers against decapentaplegic 9; WHO: World Health Organization.

Based on the tables from Simonneau, G. *et al,*. 2013. "*Updated Clinical Classification of Pulmonary Hypertension"*; Leopold, J. A. & Maron, B. A. 2016. "*Molecular mechanisms of pulmonary vascular remodelling in pulmonary arterial hypertension*"; McLaughlin, V. V., Shah, S. J., Souza, R. & Humbert, M. 2015. "*Management of pulmonary arterial hypertension*" and Galiè, N. *et al,*. 2015. *"ESC/ERS Guidelines for the diagnosis and treatment of pulmonary hypertension"*.

Table 2 Experimental models for pulmonary arterial hypertension

Animal model	Species	Histological features	Advantages	Disadvantages
Monocrotaline	Sheep; dog; rat	Medial hypertrophy muscularization of non-muscular arteries Vascular inflammation	Severe PH RV failure Predictable and reproducible	Toxic stimulus No plexiform lesions
Monocrotaline + pneumonectomy	Rat	Medial hypertrophy Muscularization of non-muscular arteries Neointima formation	Severe PH RV failure Proliferation of endothelial cells	Toxic stimulus Difficult manipulation
BMPRII knockout	Mouse	Increased muscularization	Well-suited to study the genetic factors that contribute to PH	Homozygous knockouts die in utero
Fawn-hooded rat	Rat	Increased muscularization	Well-suited to study the genetic factors that contribute to PH	Presence of systemic hypertension
Overexpression of S100A4	Mouse	Plexiform lesions	Presence of plexiform lesions	Only 5% of S100A4 overexpressing mice develop PH
Chronic Hypoxia + SU5416	Rat	Medial hypertrophy Muscularization of non-muscular arteries Neointima formation Plexiform lesions	Physiological stimulus Proliferation of endothelial cells	Not clear which group it mimics
Schistosomiasis	Mouse	Perivascular inflammation Medial thickening Formation of plexiform-like lesions	Comparable to human schistosomiasis associated with PAH	Not significant PH
Left-to-right shunt	Sheep; pig; dog; rat	Medial hypertrophy Increased VSMC proliferation Intimal proliferation Plexiform lesions can be seen	Imitate the formation of plexiform lesions in human severe PAH	Sophisticated surgical approaches Pathological alterations can appear at a late stage
Closure of the ductus arteriosus	Foetal and new-born lambs	Medial hypertrophy Muscularization of non-muscular arteries Adventitial fibrosis	Relatively large size of the foetal lamb Uterine surgical intervention is well tolerated	Sophisticated surgical approaches Pathological alterations can appear at a late stage

BMPRII: bone morphogenetic protein receptor type II gene; PAH: pulmonary arterial hypertension; PH: pulmonary hypertension; RV: right ventricle; *S100A4*: S100 calcium-binding protein A4 gene; SU5416: vascular endothelial growth factor receptor inhibitor; VSMC: vascular smooth muscle cells.

Based on the table from Santos-Ribeiro, D. *et al.* 2016. *"Pulmonary arterial hypertension: Basic knowledge for clinicians"*.

Table 3 Primers used in the molecular analysis

Oligo name	Sequence (5'→ 3')	Direction	Gene Symbol	Length bp	Tm (ºC)
RnGAPDH_F1	CCA TCA ACG ACC CCT TCA T	forward	GAPDH	19	54,79
RnGAPDH_R1	CTT CCC ATT CTC AGC CTT G	reverse		19	53,19
Rn_Nppb_F1	CTG TCG CCG CTG GGA GGT CAC T	forward	BNP	19	65,73
Rn_Nppb_R1	AGC CAT TTC CTC TGA CTT TTC TC	reverse		23	54,98
Rn_Edn1_F1	GCT GGT GGA GGG AAG AAA AC	forward	ET-1	20	56,10
Rn_Edn1_R1	GTG TAT CAA CTT CTG GTC TCT GTA	reverse		24	53,84
RnHif1a_F1	CAA CTG CCA CCA CTG ATG	forward	HIF-1α	18	53,83
RnHif1a_R1	CCA CTG TAT GCT GAT GCC TTA	reverse		21	54,67
RnPpargc1a_F1	CAG CCA CTC CAC CAA GAA AG	forward	PGC-1α	20	56,05
RnPpargc1a_R1	TCA CCA AAC AGC CGT AGA CT	reverse		20	56,12
rat_GLUT1_P1	GCA GAA GGG CAA CAG GAT AC	forward	GLUT1	20	60,2
rat_GLUT1_P2	TCC TTA TTG CCC AGG TGT TC	reverse		20	59,3
rat_GLUT4_P1	ATA GCC CTT TTC CTT CCC AA	forward	GLUT4	20	58,5
rat_GLUT4_P2	AGG CAC CCT CAC TAC CTT TT	reverse		20	60,6
Rn_Hk1_F1	GTG GAG CCG TCT GAT GTT G	forward	HK1	19	56,03
Rn_Hk1R1	GTG GTG TGC CCT TGT TGT	reverse		18	56,01
Rn_Hk2_F1	CGG AAG GAG ATG GAG AAA GG	forward	HK2	20	54,83
Rn_Hk2_R1	GAG CAC ACG GAA GTT GGT T	reverse		19	55,63
Rn_Ldha_F1	CAG CAA GAG GGA GAG AGC	forward	LDHa	18	55,01
Rn_Ldha_R1	GGT TTG AGA CGA TGA GCA GTT TG	reverse		23	56,38

Rn_Ldhb_F1	TGG GGA AGT CTC TGG CTG	forward	LDHb	18	56,74
Rn_Ldhb_R1	TGG CTG TCA CGG AGT AAT CT	reverse		20	55,69
Rn_Ldhc_F1	GGT CGG AGT TGG AAA TGT GG	forward	LDHc	20	56,07
Rn_Ldhc_R1	GAG TGC TGA GGA AAA GGC T	reverse		19	54,96
Rn_Ldhd_F1	TTG AGG GGG GAG TGT GTG	forward	LDHd	18	57,01
Rn_Ldhd_R1	GCA GGT GGG TAT TGA GAC C	reverse		19	55,66
Rn_Pfkm_F1	GGT TGT GTT CTG GGG ATG C	forward	PFKm	19	56,46
Rn_Pfkm_R1	TGG GGA TTC GGT GCT CAA AA	reverse		20	57,11
Rn_Pkm_F1	TGT GGA GAT GCT GAA GGA GAT	forward	PKm	21	55,61
Rn_Pkm_R1	AGG TCG GTA GAG AAT GGG AT	reverse		20	54,82
Rn_Irs1_F1	GCA GGC ACC ATC TCA ACA ATC	forward	IRS1	21	56,63
Rn_Irs1_R1	GTT TCC CAC CCA CCA TAC T	reverse		19	54,50
Rn_Irs2_F1	ATG CGA ATG TGG TGT GGC T	forward	IRS2	19	57,73
Rn_Irs2_R1	AGA AGA AGT CAG GTG GGG T	reverse		19	55,46
Rn_Nrf1_F1	AGA GAC AGC AGA CAC GGT TG	forward	NRF-1	20	57,12
Rn_Nrf1_R1	TTG GGT TTG GAG GGT GAG AT	reverse		20	56,15
Rn_Tfam_F1	TGG GGC GTG CTA AGA ACA	forward	Tfam	18	56,86
Rn_Tfam_R1	CGG AAT ACA GAT AAG GCT GAC AG	reverse		23	54,98
RnSirt1_F1	GAA CCT CTG CCT CAT CTA CA	forward	SIRT1	20	53,69
RnSirt1_R1	CAT ACT CGC CAC CTA ACC TA	reverse		20	53,45
Rn_Pdha1_F1	ATG GTG ATG GTG CTG CTA	forward	PDHα1	18	55,38
Rn_Pdha1_R1	GTA GTA ATC CGT GCT GGC T	reverse		19	54,43
Rn_Pdha2_F1	CCC ACA GAC CAC ATC ATC AC	forward	PDHα2	20	55,60
Rn_Pdha2_R1	AAA GGA GGC TGT GCT AAA GG	reverse		20	55,07
Rn_Pdhb_F1	TGC TAG AGA ATG AAC TGA TGT ATG G	forward	PDHβ	25	54,37
Rn_Pdhb_R1	GTG ATG TGG GTC CCT TGC	reverse		18	56,24

Protocol 1 – total RNA extraction

1. Add the beads (1.4 mm, 3 small spoons) to 30-40mg of each tissue sample and 500µL of phenol solution (fume hood);
2. Homogenise sample at 6500 rpm for 3 cycles of 30 seconds using a tissue disruptor. Between cycles, incubate samples on ice for 30 seconds;
3.Incubate 5 min on ice after the tissue disruption;
4.Add 100µL of chloroform and mix (fume hood);
5.Incubate for 10 min at room temperature;
6.Centrifuge for 15 min at 4°C 15000rpm;
7.Collect the aqueous phase (upper) to a new Eppendorf with 500µL of isopropanol and mix;
8.Incubate 10 min at room temperature;
9. Centrifuge for 10 min at 4°C, 15000 rpm;
10. Discard supernatant paying attention to the pellet;
11. Wash the pellet with 500µL of ethanol 70%;
12. Centrifuge for 5 min at 4°C, 15000 rpm;
13. Discard supernatant with a pipette;
14. Spin the RNA samples and remove ethanol excess with a pipette;
15. Dry RNA at room temperature by leaving the cap open for 5-10 min;
16. Resuspend RNA with 50 µL of ultrapure H_2O;